

Phosphorylation Bar Codes Induce Distinct Conformations and Functionalities of β -arrestin

by

Kelly Nicole Nobles

Department of Biochemistry
Duke University

Date: _____

Approved:

Robert J. Lefkowitz, Supervisor

Marc G. Caron

Terrence G. Oas

Sudha K. Shenoy

John D. York

Dissertation submitted in partial fulfillment of
the requirements for the degree of Doctor of Philosophy in the Department of
Biochemistry in the Graduate School
of Duke University

2010

ABSTRACT

Phosphorylation Bar Codes Induce Distinct Conformations and Functionalities of β -arrestin

by

Kelly Nicole Nobles

Department of Biochemistry
Duke University

Date: _____

Approved:

Robert J. Lefkowitz, Supervisor

Marc G. Caron

Terrence G. Oas

Sudha K. Shenoy

John D. York

An abstract of a dissertation submitted in partial
fulfillment of the requirements for the degree
of Doctor of Philosophy in the Department of
Biochemistry in the Graduate School
of Duke University

2010

Copyright by
Kelly Nicole Nobles
2010

Abstract

Seven transmembrane spanning receptors (7TMRs), or G-protein coupled receptors (GPCRs), represent the largest and most ubiquitous of the several families of plasma membrane receptors and regulate virtually all known physiological processes in humans. The classical paradigm of signal transduction in response to 7TMR stimulation involves an agonist-induced conformational change of the receptor which leads to interaction with and dissociation of the heterotrimeric G-protein into independent $G\alpha$ and $G\beta\gamma$ signaling subunits. Following their activation, 7TMRs are phosphorylated by G-protein coupled receptor kinases (GRKs) and subsequently recruit β -arrestins. β -arrestins are multifunctional adaptor proteins which not only desensitize G-protein signals, but also facilitate receptor internalization and mediate numerous signaling pathways on their own. As β -arrestins universally interact with members of the 7TMR superfamily, we (1) developed an *in vitro* model system to assess conformational changes that occur in β -arrestins in response to phosphorylation and (2) to map the sites of phosphorylation on the β_2 adrenergic receptor by different GRKs which would determine the conformation(s) assumed by β -arrestin and thereby, in turn, instruct its functional capabilities.

We determined conformational changes in β -arrestin1 *in vitro* using limited tryptic proteolysis and MALDI-TOF MS analysis in the presence of a phosphopeptides derived from the C-terminus of the V_2 vasopressin receptor (V_2Rpp or V_2R4p) or the corresponding unphosphorylated peptide (V_2Rnp). Upon V_2Rpp binding, we show that the previously shielded R^{393} becomes accessible, which indicates release of the C-terminus. Moreover, we have shown that R^{285} becomes more accessible and this residue is located in a region of β -arrestin1

responsible for stabilization of its polar core. These two findings demonstrate “activation” of β -arrestin1. We also show a functional consequence of the release of β -arrestin1’s C-terminus by enhanced clathrin binding. In addition, we have shown marked protection of β -arrestin1’s N-domain in the presence of V₂Rpp; consistent with previous studies suggesting the N-domain is responsible for recognizing phosphates in 7TMRs. Using a differentially phosphorylated V₂R peptide (V₂R4p), we show that β -arrestin1 is able to adopt distinct conformations in response to different phosphorylation patterns. Furthermore, a striking difference is observed in the conformation of V₂Rpp-bound β -arrestin1 when compared to β -arrestin2, namely the flexibility of the inter-domain hinge region. These data represent the first direct evidence that the β -arrestin1 conformation is differentially instructed by phosphorylation patterns and that the “receptor-bound” conformations of β -arrestins1 and 2 are different.

Phosphorylation of 7TMRs by GRKs plays essential roles in regulation of receptor function by promoting interactions of the receptors with β -arrestins. We hypothesized that different GRKs phosphorylate distinct sets of sites thereby establishing a “bar code.” In order to test this hypothesis, we monitored the phosphorylation events of the β 2AR upon stimulation with a classical full agonist, isoproterenol, or a β -arrestin “biased” agonist, carvedilol, in the presence of a full complement of GRKs or when individual GRKs (2 or 6) were depleted by siRNA. We demonstrate that at least thirteen sites on the β 2AR show changes in phosphorylation in response to the agonist isoproterenol. Of these, phosphorylation increased 10 to more than 300 fold in 12 (S261, S262, S345, S346, S355, S356, T360, S364, S396, S401, S407 AND S411) and decreased 50% in one (S246). Depletion of GRK2 or 6 by siRNA indicates that S355, 356 are GRK6 sites whereas the remainder are GRK2 sites. Phosphorylation of GRK2 sites

inhibits that of GRK6 sites. Carvedilol, a β -arrestin biased agonist, promotes phosphorylation of only the GRK6 sites S355, 356. In HEK293 cells, GRK2 phosphorylation is found to be the major positive regulator of receptor internalization; to contribute to receptor desensitization; and to inhibit β -arrestin mediated ERK activation. Phosphorylation of the two GRK6 sites contributes to receptor desensitization and internalization and is required for β -arrestin mediated ERK activation. These data indicate that different ligands promote distinct patterns of receptor phosphorylation which dictate different patterns of β -arrestin mediated function.

Table of Contents

Abstract	iv
List of Figures	x
List of Tables.....	xii
List of Abbreviations	xiii
Acknowledgements	xvii
1. Introduction	1
1.1 Classical Seven Transmembrane Receptor Signaling	1
1.2 Regulation of 7TMR Signaling	8
1.2.1 Regulation of G protein Activity	8
1.2.2 Heterologous Desensitization	9
1.2.3 Homologous Desensitization	11
1.3 β -arrestins: Multifunctional Adaptors	15
1.3.1 β -arrestins and Clathrin-Mediated Endocytosis of 7TMRs	15
1.3.2 Regulation of β -arrestins and 7TMRs by Ubiquitination	17
1.3.3 G protein-Independent Activation of MAP Kinases by β -arrestins	18
1.3.4 β -arrestin Bias	22
1.4 Objectives for this Dissertation	26
2. Materials and Methods.....	28
2.1 Materials and Reagents	28

2.2 DNA Plasmids and Cell Lines.....	29
2.3 Techniques	30
<i>Purification of Recombinant Rat β-arrestin 1</i>	30
<i>Limited Trypsin Proteolysis</i>	31
<i>MALDI-TOF MS Analysis</i>	32
<i>LC/ESI-MS Analysis</i>	33
<i>Clathrin Binding</i>	34
<i>Cell Culture and Transfection</i>	34
<i>SILAC and Small Interfering RNA (siRNA) Silencing of Gene Expression</i>	35
<i>2AR purification and digestion</i>	36
<i>Immobilized Metal Ion Affinity Chromatography (IMAC)</i>	37
<i>LC/MS/MS and Data Analyses</i>	38
<i>Immunoprecipitation and Immunoblotting</i>	39
<i>β2AR Desensitization in GloSensor Cells</i>	39
<i>Internalization Assay</i>	40
<i>ERK Activation Assay</i>	40
<i>BRET Assay</i>	41
<i>Statistical Analysis</i>	41
3. The Active Conformation of β -arrestin1 and its Difference from β -arrestin2	42
3.1 Introduction	42
3.2 Results.....	47

3.3 Discussion	76
4. Distinct GRK Phosphorylation Sites on the β 2AR: A “Bar Code” Which Differentially Encodes β -arrestin Functions	86
4.1 Introduction	86
4.2 Results.....	88
4.3 Discussion	115
5. Future Directions.....	126
References	129
Biography.....	143

List of Figures

Figure 1-1: 7TMR Crystal Structures.....	4
Figure 1-2: Classical 7TMR Signaling.....	6
Figure 1-3: Heterologous and Homologous Desensitization of the β 2AR.....	13
Figure 1-4: β -arrestin Scaffolds the ERK1/2 and JNK3 MAPK Cascades.....	21
Figure 1-5: Mechanism of β -arrestin biased ligands.....	25
Figure 3-1: The Basal Conformation of Bovine β -arrestin1.....	45
Figure 3-2: Sequence Alignment of Recombinant Rat β -arrestin1 and 2.....	50
Figure 3-3: Limited Tryptic Proteolysis Patterns of β -arrestin1.....	52
Figure 3-4: Conformation Changes in β -arrestin1 Require Phosphates.....	55
Figure 3-5: MALDI-TOF Spectra of β -arrestin1 Tryptic Fragments.....	63
Figure 3-6: Enhancement of Clathrin Binding to β -arrestin1 in the Presence of V2Rpp.....	66
Figure 3-7: Model of β -arrestin1 activation in the presence of V2Rpp.....	68
Figure 3-8: Differentially phosphorylated V2R peptides induce distinct β -arrestin1 conformations.....	71
Figure 3-9: Conformational Differences Between β -arrestin1 and 2.....	75
Figure 4-1: Desensitization of the β 2AR After GRK2, 6 or 2+6 siRNA Treatment.....	91
Figure 4-2: The Roles of GRK2 and 6 in β 2AR Internalization and ERK Activation.....	95
Figure 4-3: β -arrestin2 BRET Biosensor.....	99
Figure 4-4: β 2AR Phosphorylation Dictates Distinct β -arrestin Conformations.....	101
Figure 4-5: β 2AR Phosphorylation Analysis by MS-Based Quantitative Proteomics.....	104
Figure 4-6: Dephosphorylation of β 2AR Ser246 by Isoproterenol Stimulation.....	106
Figure 4-7: Quantitative MS Analysis of Stimulated β 2AR Phosphorylation.....	108

Figure 4-8: GRK2 and 6 Phosphorylate Different Sites on the β 2AR..... 111

Figure 4-9: Phosphorylation of S355 and S356 on β 2AR. 114

Figure 4-10: β 2AR Phosphorylation Bar Codes. 117

List of Tables

Table 3-1: Final assignment of limited tryptic proteolytic fragments of β -arrestin1	58
--	----

List of Abbreviations

7TMR	Seven transmembrane receptor
AC	Adenylyl cyclase
ANOVA	Analysis of variance
AR	Adrenergic receptor
ATII	Angiotensin II
AT_{1A}R	Angiotensin II type 1A receptor
ARF6	ADP-ribosylation factor 6
ARNO	ARF nucleotide binding site opener
ATP	Adenosine triphosphate
β₂AR	β ₂ -adrenergic receptor
BSA	bovine serum albumin
cAMP	3'-5' cyclic adenosine monophosphate
DAG	Diacylglycerol
DSP	Dithiobis(succinimidyl)propionate
EDTA	Ethylene diamine tetraacetic acid
ERK	Extracellular signal-related kinases
ESI	Electrospray ionization
FBS	Fetal bovine serum
GAP	GTPase activating protein
Gα	α subunit of heterotrimeric G protein
Gβγ	βγ subunit of heterotrimeric G protein

GDP	Guanosine diphosphate
GEF	Guanine nucleotide exchange factor
GPCR	G protein coupled receptor
G protein	Guanine nucleotide binding protein
GRK	G protein-coupled receptor kinase
GST	Gutathione-S-transferase
GTP	Guanosine triphosphate
HEK	Human embryonic kidney
HRP	Horseradish peroxidase
IB	Immunoblot
ICI	ICI-118,551 a β 2AR inverse agonist
IMAC	Immobilized metal ion affinity chromatography
IP	Immunoprecipitation
IP₃	Inositol 1,4,5-triphosphate
Iso	Isoproterenol
JNK3	Jun N-terminal kinase 3
kDa	kilodalton
LC	Liquid chromatography
LC/MS/MS	Liquid chromatography/tandem mass spectrometry
MALDI-TOF	Matrix-assisted laser desorption ionization-time-of-flight
MAP	Mitogen activated protein
MEF	Mouse embryonic fibroblast

MEK	Mitogen-activated protein/extracellular signal-regulated kinase
MKK	MAP kinase kinase
MKKK	MAP kinase kinase kinase
MS	Mass spectrometry
PAGE	Polyacrylamide gel electrophoresis
PAR	Protease-activated receptor
PBS	Phosphate-buffered saline
PCR	Polymerase chain reaction
PH	Pleckstrin homology
PIP₂	Phosphatidylinositol 4,5-bisphosphate
PKA	Protein Kinase A
PKC	Protein Kinase C
PKD	Protein Kinase D
PLC	Phospholipase C
PMSF	Phenylmethylsulfonyl fluoride
RGS	Regulators of G protein signaling
RNAi	RNA interference
SDS	Sodium dodecyl sulfate
S.E.	Standard error
SEM	Standard error of the mean
SILAC	Stable isotope labeling with amino acids in cell culture
siRNA	Small interfering RNA

TBS	Tris buffered saline
TBST	Tris buffered saline tween
V₂Rnp	Non-phosphorylated V2R-tail peptide
V₂Rpp	V2R tail peptide with eight phosphates
V₂R4p	V2R tail peptide with four phosphates

Acknowledgements

First and foremost, I would like to thank my mentor Dr. Robert J. Lefkowitz for providing me with invaluable knowledge, guidance and unwavering support. I am sincerely grateful for the opportunity to train with such a world-class researcher. I would also like to thank my committee members: Drs. Marc Caron, Terrence Oas, Sudha Shenoy and John York for their generous advice and helpful discussions. A gracious thank you to Dr. Kunhong Xiao without whose help this work would not have been possible. Thank you to all of the Lefkowitz lab members with special thanks to Dr. Seungki Ahn, Darrell Capel, Lucie Langevin, Dr. Arun Shukla and Dr. Erin Whalen. Finally, this thesis would be incomplete without a mention of the support given me by my family. Your continuous love lifted me up when my graduate career seemed interminable.

1. Introduction

1.1 *Classical Seven Transmembrane Receptor Signaling*

All living beings must respond and adapt to ever-changing surroundings in order to maintain homeostasis and this is accomplished by converting extracellular stimuli to intracellular responses. Eukaryotic cells transduce many signals across the plasma membrane by seven transmembrane spanning receptors (7TMRs), also known as G-protein coupled receptors (GPCRs), and these signals must be subsequently amplified and ultimately converted to appropriate physiological responses. 7TMRs represent the largest known family of cell surface receptors encoded by the mammalian genome (>1% of all human genes) and they mediate responses to widely varying stimuli including hormones, neurotransmitters, odorants and light [1]. These receptors regulate virtually all known physiological processes in humans and therefore, not surprisingly, approximately 60% of currently marketed drugs, either directly or indirectly, target 7TMRs, [2]. Despite the fact that there are over 1,000 members in the 7TMR superfamily, these receptors share both a conserved structural motif and a common signal transduction theme involving the generation of second messenger cascades.

7TMRs are integral membrane proteins consisting of seven α -helical membrane spanning regions separated by alternating intracellular and extracellular loop regions [3]. Structural details of 7TMRs at atomic resolution are just beginning to emerge with the structural determination of four 7TMRs and a high resolution structure of rhodopsin; the human beta-2 adrenergic receptor (β 2AR), the human adenosine 2A receptor (A_{2A}) and the avian β 1 adrenergic receptor (β 1AR) (Figure 1-1, upper panel) [4-13]. With the exception of

rhodopsin, these crystal structures were determined in the presence of antagonists or inverse agonists thus rendering only inactive conformations of the receptors. However, specific work with rhodopsin, a light activated 7TMR, has shown that receptor activation alters the orientation of α helices 3 and 6 which unmask G protein binding sites in the 2nd, 3rd and 4th cytoplasmic loops [14, 15]. The only active state 7TMR 3D structure determined is that of opsin, the active state of rhodopsin. Comparison of the opsin structure with rhodopsin shows dramatic structural changes on the cytoplasmic surface of the molecule which renders opsin capable of interacting with heterotrimeric guanine nucleotide binding proteins, or G proteins (Figure 1-1, lower panel) (reviewed in [3]).

Association of G proteins with 7TMRs results in the exchange of the bound GDP molecule for GTP on the $G\alpha$ subunit [16-18]. GTP binding then causes a conformational change in $G\alpha$ and subsequent dissociation of the heterotrimer into two functional, or signaling, units: a GTP-bound $G\alpha$ subunit ($G\alpha$ -GTP) and a $G\beta\gamma$ heterodimer [19, 20]. Both $G\alpha$ -GTP and $G\beta\gamma$ interact with specific effector proteins, such as adenylyl cyclase (AC), to stimulate the generation of second messenger molecules involved in intracellular signaling cascades (Figure 1-2). In this sense, heterotrimeric G proteins are signal transducers that link activated 7TMRs to downstream effectors in a signaling pathway and this signal transduction also promotes amplification since each step is catalytic (i.e. one agonist-occupied 7TMR can activate multiple G proteins leading to amplification at the level of G protein effectors and second messengers).

Figure 1-1: 7TMR Crystal Structures. (A-C) Bovine rhodopsin, avian β 1AR and human A_{2A} adenosine receptors, respectively, are superimposed on the human β 2AR. Color coding for each superposition is indicated below the structures. The degrees of overlap between these structures have an overall similar architecture, but the differences are substantive enough to indicate differences in helical packing. (D) Differences between opsin and rhodopsin illustrating differences between conserved amino acids including those of the ionic lock. Briefly, the ionic lock is broken and new interactions are formed between Arg 135 and Tyr 223, and also between Glu 247 and Lys 231. (E) Complex between a C-terminal peptide of rhodopsin's G protein, transducin, illustrating interactions between the receptor and G protein. One of the major differences between inactive rhodopsin and the active-state opsin is the formation of a cavity between transmembrane helices 3, 5 and 6 which can accommodate transducin. Adapted from B. K. Kobilka et al., *The Structure and Function of GPCRS*. Nature, 2009. **459** p. 356-363.

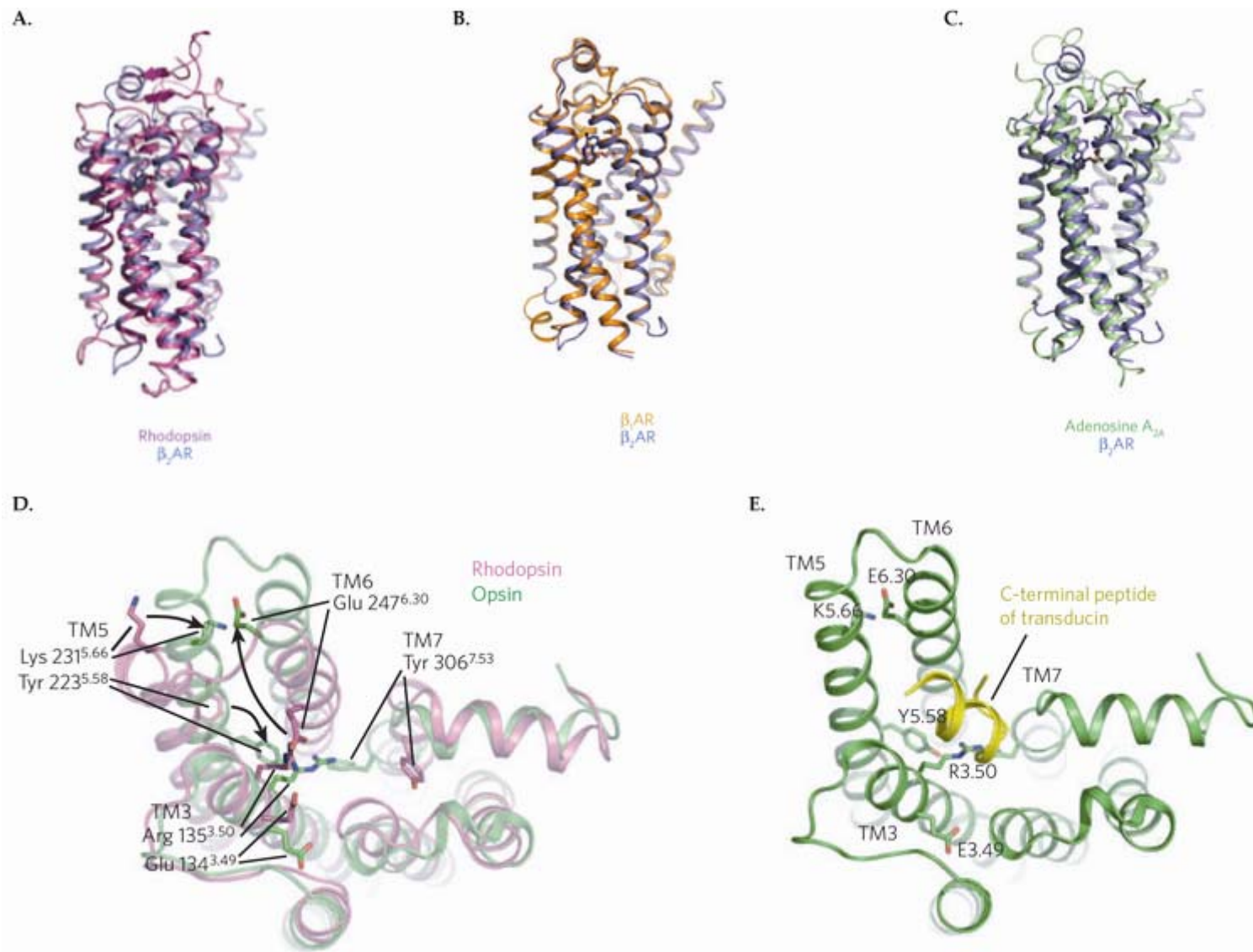


Figure 1-1: 7TMR Crystal Structures.

Figure 1-2: Classical 7TMR Signaling. Activation of a 7TMR (R) by a ligand (L) promotes interaction with a membrane-bound heterotrimeric G protein. Subsequent displacement of GDP with GTP on the $G\alpha$ subunit causes dissociation of the heterotrimer into two signaling subunits: $G\alpha$ -GTP and the $G\beta\gamma$ heterodimer. This nucleotide exchange and dissociation allows activation of effector molecules such as adenylyl cyclase (AC), which converts ATP to the second messenger molecule cAMP. Intracellular proteins, such as PKA, are regulated by second messengers to mediate a host of cellular processes.

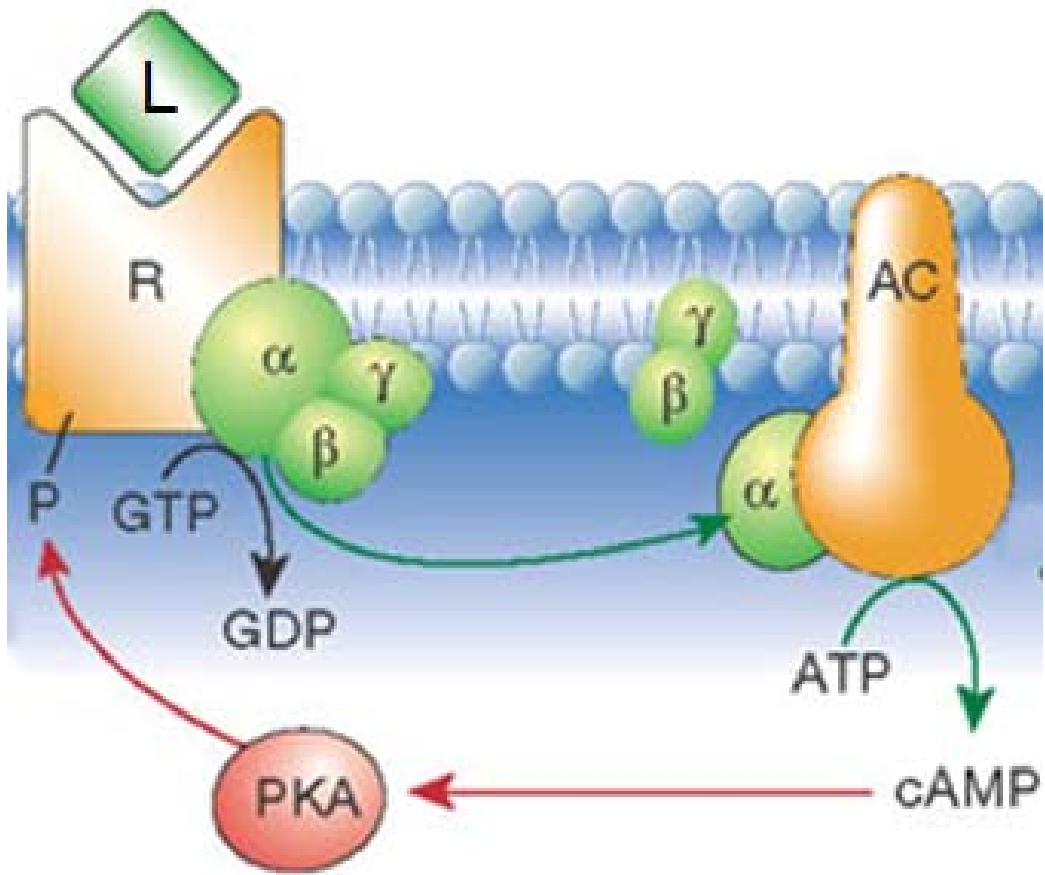


Figure 1-2: Classical 7TMR Signaling.

G-proteins associate with the plasma membrane and this family displays great combinatorial diversity with 21 $G\alpha$, 6 $G\beta$ and 12 $G\gamma$ subunits reported to be expressed in human cells [21]. Based on sequence homology, G proteins are classified by their $G\alpha$ subunit into one of four categories: G_s , $G_{i/o}$, G_q and $G_{12/13}$. Classically, G_s stimulate adenylyl cyclase (AC) isoforms to produce 3'-5' cyclic adenosine monophosphate (cAMP) whereas G_i inhibits AC activity thereby lowering cellular cAMP levels [22]. G_s and G_i activation by 7TMRs leads to activation of cAMP-dependent protein kinase (PKA), which then phosphorylates intracellular proteins to mediate a host of cellular processes. G_q activates phospholipase C (PLC) isoforms resulting in the hydrolysis phosphatidylinositol 4,5-bisphosphate (PIP_2) to produce the second messengers inositol 1,4,5-triphosphate (IP_3) and diacylglycerol (DAG) [23, 24]. Increased DAG concentrations in the plasma membrane and IP_3 -dependent release of Ca^{2+} from the endoplasmic reticulum are necessary for the activation of both protein kinase C (PKC) and protein kinase D (PKD) [25, 26]. The $G_{12/13}$ family is known to associate with and activate the small GTPase protein Rho through a guanine nucleotide exchange factor (p115RhoGEF) [27, 28]. Finally, $G\beta\gamma$ heterodimers also transducer signals through a variety of effectors including, but not limited to, PLC- β_2 , PLC- β_3 , certain AC isoforms and K^+ and Ca^{2+} channels (Reviewed in [29]). 7TMR-mediated stimulation elicits cellular responses not only at the receptor level, but also depends on the available G proteins, modulators of G protein signaling and effector molecules.

The β_2AR , a prototypical G_s coupled 7TMR, responds to the endogenous catecholamines epinephrine and norepinephrine and mediates numerous physiological responses including bronchial relaxation, skeletal muscle blood flow, increased chronotropic and inotropic effects, and uterine relaxation (Reviewed in [30]). Upon stimulation, the dissociated $G\alpha_s$ -GTP activates

adenylyl cyclase which catalyzes the formation of cAMP from ATP. cAMP then binds to and allosterically modulates PKA causing the release of the catalytic subunits of the kinase from the regulatory subunits. The catalytic subunits are then free to phosphorylate intracellular target proteins on serine and threonine residues and these target proteins then mediate many of the aforementioned physiological responses. The β 2AR is but only one example of how activation of a 7TMR and its cognate G proteins leads to intracellular responses. Signaling pathways for processes such as cell growth, cell death, metabolism, membrane ion permeability, nucleic acid transcription, protein translation, and many more can trace their initiation to 7TMR stimulation. Yet, as important as activation of these pathways is for initiating physiological responses, a cell's ability to attenuate or terminate receptor-mediated responses is equally important for maintaining homeostasis.

1.2 Regulation of 7TMR Signaling

Defects in 7TMR signaling have severe consequences which affects receptor-stimulated biological responses in pathological situations (eg. hypertension and heart failure) and also results in undesirable physiological consequences such as uncontrolled cell growth and tumorigenesis, and vascular hypertrophy [31-33]. Termination of signal transduction cascades through G protein inactivation and termination of receptor activation are critical, regulatory mechanisms necessary for proper cellular function.

1.2.1 Regulation of G protein Activity

As mentioned above, 7TMR activation leads to exchange of GDP for GTP on the $G\alpha$ subunit which initiates dissociation of the heterotrimer into its signaling units ($G\alpha$ -GTP and the

G $\beta\gamma$ heterodimer). In this sense, the 7TMR itself acts as a guanine nucleotide exchange factor (GEF). In fact, early studies showed that agonist-dependent increases in intracellular second messenger concentrations are dictated by the phosphorylation state of the guanine nucleotide bound to G α , namely G α -GTP, and that G α -GDP exists only in the inactive heterotrimer form of the G protein [18]. G proteins themselves are members of the GTPase superfamily and it is the intrinsic GTPase activity of the G α subunit that converts the bound GTP to GDP and thus begins the process of its own deactivation by cleaving the terminal phosphate bond. The newly formed G α -GDP then re-associates with free G $\beta\gamma$ subunits to form the inactive complex once again.

In vitro studies with recombinant G α proteins displayed a timing paradox in that the intrinsic GTPase activity of G α is often too slow for termination of G protein signaling seen in physiological settings. The discovery of regulators of G protein signaling (RGS proteins) explained this paradox because they serve as GTPase-activating proteins (GAPs) which accelerate the termination of G protein signaling events. RGS proteins bind directly to G α -GTP and have been shown to accelerate G α catalytic activity 40-fold in recombinant systems [34, 35]. Moreover, 7TMR activation has been shown to increase the expression of various RGS proteins thereby creating a negative feedback loop in which stimulation of a signaling pathway ultimately leads to signal termination by downstream effectors [36, 37].

1.2.2 Heterologous Desensitization

Regulation of signaling at the level of the 7TMRs themselves is termed desensitization and is a physiologically important process that uncouples the receptor from its signaling

cascade(s) despite the continued presence of a ligand. Classically, desensitization has been divided into two categories based on the specificity for agonist-occupied 7TMRs [38, 39]. Heterologous desensitization occurs when stimulation by one agonist leads to a broad pattern of unresponsiveness to further stimulation by a variety of other agonists. This type of desensitization relies on phosphorylation of 7TMRs by the second messenger kinases PKA and PKC.

The β 2AR itself is a substrate for PKA with phosphorylation occurring at consensus sites in both the third intracellular loop and the proximal region of the carboxy terminal tail. Studies have shown, with *in vitro*, reconstituted proteins, that the β 2AR's ability to couple to G_s is diminished after PKA phosphorylation [40]. Thus, heterologous desensitization is a general feedback inhibition mechanism since any 7TMR with a consensus PKA site can be phosphorylated whether it is agonist-occupied or not (Figure 1-3, upper panel). *In vitro* studies have also shown that other kinases, such as PKC, can mediate heterologous desensitization of the β 2AR. Similar to PKA, it has been shown that phosphorylation of the β 2AR by PKC attenuates receptor coupling to G_s and thus it is possible for signals that activate PKC (by increased intracellular Ca^{2+} levels) to affect receptors that initiate entirely separate second messenger cascades [41]. 7TMR signaling through G proteins is amplified at each step since one receptor can activate numerous G proteins and, once an effector molecule is activated, the generation of second messengers such as cAMP can be catalytic. As such, maximal second messenger generation can occur even at low concentrations of agonist when receptor occupancy is low and under these conditions the negative feedback loop of heterologous desensitization may be particularly important.

1.2.3 Homologous Desensitization

Homologous desensitization is a highly conserved two phase process that occurs when a cell's response to a specific agonist decreases. Typically, only the agonist-occupied 7TMR is phosphorylated on key serine and threonine residues located in the third intracellular loop and/or the carboxy terminal tail by G protein coupled receptor kinases (GRKs) [42, 43]. However, GRK phosphorylation of the agonist-occupied receptor alone only attenuates 7TMR signaling by up to 30% [44-46]. In order to achieve substantial homologous desensitization, an additional protein from the arrestin family is required and binds directly to the GRK-phosphorylated receptor (Figure 1-3, lower panel) [47].

Arrestins function by stoichiometrically binding to 7TMRs specifically phosphorylated by the GRKs. General receptor phosphorylation is not sufficient for arrestin binding as demonstrated by the fact that in G protein coupling assays arrestin binding has an approximately 100-fold preference for GRK phosphorylated β 2ARs over those phosphorylated by PKA [48]. In the case of the β 2AR, homologous desensitization blocks the receptors ability to couple to G proteins by 70-80% as opposed to the 30% seen with GRK phosphorylation alone [41, 44]. Arrestin augmentation of GRK-mediated desensitization was not observed with β 2AR phosphorylated by either PKA or PKC. In contrast to heterologous desensitization, the time scale for GRK-mediated desensitization occurs rapidly and is most likely important during high levels of receptor occupancy because the GRKs display a much greater preference for agonist-occupied 7TMRs.

Figure 1-3: Heterologous and Homologous Desensitization of the β 2AR. The upper panel illustrates non-specific heterologous desensitization of β 2AR and another 7TMR species in response to the β 2AR agonist, isoproterenol (Iso). Briefly, activation of the receptor by Iso leads to dissociation of the heterotrimeric G protein freeing $G\alpha_s$ to activate adenylyl cyclases (upper, left panel). AC activation then leads to the production of cAMP which then binds to and activates PKA. Many 7TMRs contain PKA phosphorylation sites and the upper, right panel illustrates phosphorylation of both the agonist-occupied β 2AR and a non-stimulated 7TMR, the histamine H-1 receptor (H1R) and this phosphorylation terminates signaling by both of these receptors. The bottom panel illustrates the selectivity of homologous desensitization for agonist-occupied 7TMRs. Continuing with the β 2AR system, Iso activation leads to specific phosphorylation of the β 2AR by GRK proteins while the H1R remains unmodified. β -arrestin then translocates to the membrane where it preferentially interacts with the agonist-occupied, phosphorylated β 2AR thereby sterically precluding activation of G proteins (lower, right panel).
Figure provided by C.D. Nelson.

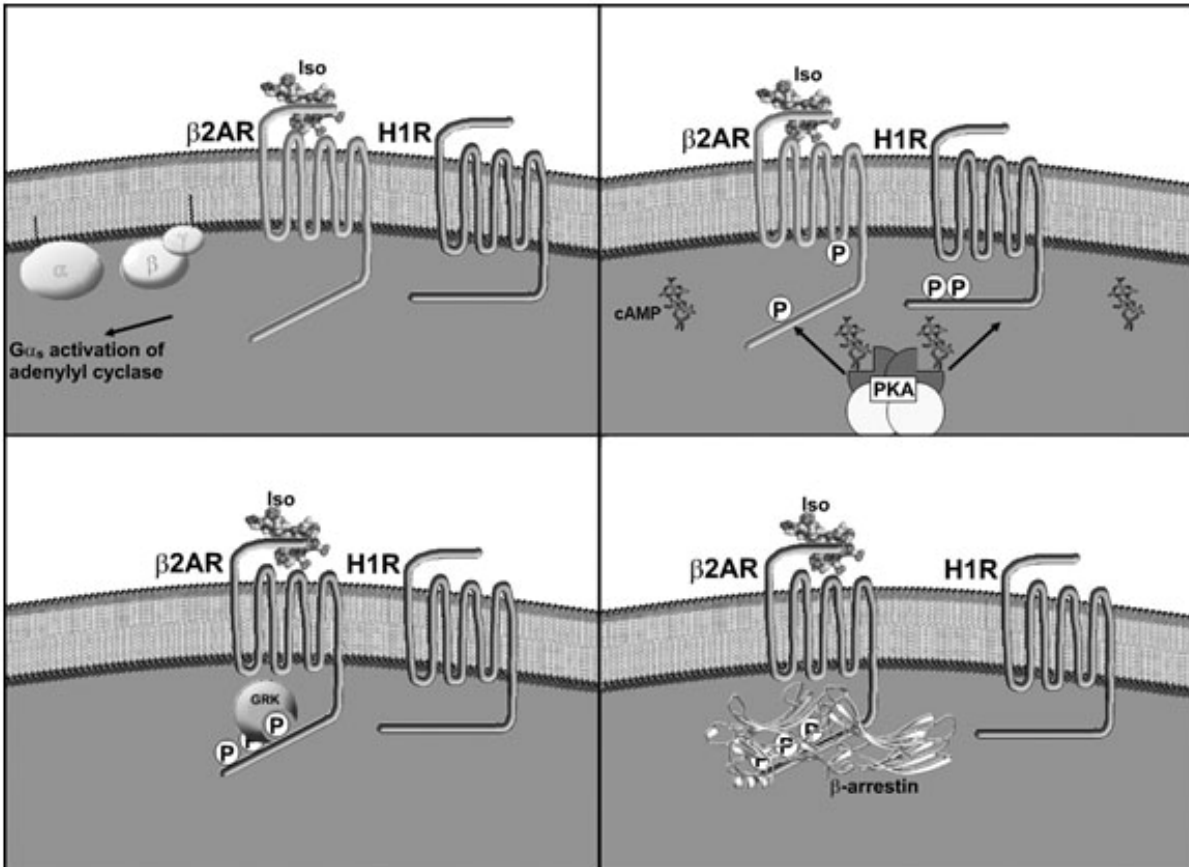


Figure 1-3: Heterologous and Homologous Desensitization of the $\beta 2AR$.

The GRK family consists of seven members: two, rhodopsin kinase (GRK1) and GRK7 are confined to the retina; GRKs 2, 3, 5 and 6 are fairly ubiquitously expressed; and GRK4 shows only very localized expression [49, 50]. The family as a whole shares about 50-90% sequence similarity with a conserved three domain structure: a central catalytic core flanked by an amino terminal domain of approximately 185 amino acids and a carboxy terminal domain of varying length [51]. Given the relative paucity of widely expressed GRKs (2, 3, 5 and 6) relative to the large number of 7TMRs, it is likely that multiple GRKs are capable of desensitizing multiple receptors. However, despite a great deal of previous work with model systems, primarily rhodopsin and β 2AR, relatively little is known outside these systems about the receptor specificity of the GRKs.

As with the GRKs, the expression of two of the four arrestin family members, arrestin1 (visual arrestin) and arrestin 4 (X arrestin), is limited to retinal rods and cones, respectively [52]. Arrestins 2 and 3, (hereafter referred to as β -arrestin 1 and 2, respectively) are ubiquitously expressed and interact with almost all 7TMRs in an activation-dependent manner [52]. The arrestin family members share about 50-85% amino acid homology. Solved crystal structures of the basal state of arrestin1, arrestin4 and β -arrestin1 show a conserved structure among arrestin family members; an elongated, two-domain (N- and C-domain) molecule with these domains connected by a twelve residue linker region [53]. Given the small number of arrestins, it is likely that β -arrestin 1 and 2 are reasonably able to substitute for one another, to some extent, as is evidenced from studies with knockout mice of β -arrestin1 or 2 [54]. The embryonically lethal double knockout mice indicate the importance of β -arrestins for proper

7TMR function. The versatility of the GRKs and β -arrestins is remarkable considering the small number of proteins that regulate the desensitization of a vast number of 7TMRs.

1.3 β -arrestins: Multifunctional Adaptors

Recent evidence shows that β -arrestins, in addition to their role in 7TMR desensitization, also serve as multifunctional adaptors which link 7TMRs to a growing list of endocytic and signaling molecules. Amongst the former group are clathrin, AP2, ARNO and ARF6 [55], while the latter are signaling molecules such as Src and components of several mitogen-activated protein (MAP) kinase cascades (e.g. ERK1, 2, JNK3 and p38) (reviewed in [56]). Recent systems biology techniques coupled with quantitative mass spectrometry-based proteomic approaches have revealed the enormous complexity of β -arrestin-mediated processes and has grown the list of non-receptor partners for β -arrestin at an exponential rate [57, 58].

1.3.1 β -arrestins and Clathrin-Mediated Endocytosis of 7TMRs

Though initially discovered for their role in 7TMR desensitization, later research demonstrated that β -arrestins also play a key role in receptor internalization. In response to agonist stimulation, 7TMRs are sequestered and internalized from the cell surface so that the receptor is unavailable to surface stimulation (reviewed in [59]). Many 7TMRs undergo endocytosis via clathrin-coated pits and β -arrestin serves as the link between the endocytic machinery and receptor. The C-terminus of β -arrestin contains binding sites for both the β 2 adaptin subunit of the AP-2 adaptor complex and clathrin which bring 7TMRs to clathrin coated pits, a process critical for receptor recycling and degradation [60-62]. Mutations in β -arrestin's C-terminus at either the AP-2 or clathrin binding sites ablate 7TMR sequestration but

has no deleterious effects on either β -arrestin translocation to the plasma membrane or binding of GRK-phosphorylated 7TMRs [63].

The internalization of some 7TMRs, such as the β 2AR, also depends on an interaction between β -arrestin and the Src family of non-receptor tyrosine kinases. Once recruited to the receptor, Src phosphorylates dynamin, which is a necessary enzyme for vesicle fission of clathrin-coated pits from the plasma membrane [64-66]. β -arrestins also bind various other proteins implicated in 7TMR internalization such as ARNO (ARF nucleotide binding site opener) which regulates the activity of the small G protein ARF6 (ADP-ribosylation factor 6) [55, 67]. Upon activation, ARF6 is released by β -arrestin and assists in 7TMR endocytosis. After internalization and vesicular acidification, 7TMRs can be de-phosphorylated and recycled back to the plasma membrane (re-sensitization) and/or targeted for proteolytic degradation.

Two patterns of agonist-dependent β -arrestin interaction with 7TMRs have emerged with respect to their endocytic adaptor function [54]. Class A receptors, such as the β 2AR, preferentially interact with β -arrestin2 both transiently and with low-affinity binding. β -arrestin is subsequently released after targeting of the 7TMR to clathrin-coated pits such that the receptor internalizes without the β -arrestin. Conversely, Class B receptors, such as the V2 vasopressin receptor (V2R), bind to either β -arrestin1 or 2 very tightly and do not dissociate from it at the plasma membrane. Following recruitment to clathrin-coated pits, the receptor and β -arrestin remain bound together on the surface of endocytic vesicles.

1.3.2 Regulation of β -arrestins and 7TMRs by Ubiquitination

7TMRs are ubiquitinated in response to agonist and this post-translational modification is a requirement for receptor degradation. Interestingly, ubiquitination and degradation of agonist-stimulated 7TMRs such as the β 2AR and V2R is mediated specifically by the β -arrestin2 isoform [68, 69]. For example, studies in β -arrestin1/2 double knockout mouse embryo fibroblasts (MEFs) demonstrated that ubiquitination of the β 2AR does not occur unless the expression of β -arrestin2, but not β -arrestin1, is restored. Given these data, it is likely that β -arrestin is the adapter which brings the E3 ubiquitin ligase in close proximity of the 7TMR.

The distinct patterns of receptor: β -arrestin endocytic behavior also correlate with differential patterns of β -arrestin ubiquitination [68, 70-72]. β -arrestins undergo ubiquitination in response to activation of several 7TMRs which is mediated by the E3 ubiquitin ligase, Mdm2, and, in the case of β -arrestin2, the deubiquitinating enzyme ubiquitin-specific protease 33 (USP33) [68, 73]. This post-translational modification is required for rapid receptor internalization and governs the strength of β -arrestin's interaction with activated 7TMRs. Class A receptors lead to transient ubiquitination while Class B receptors promote sustained β -arrestin ubiquitination [71]. Agonist-stimulated β -arrestin ubiquitination not only regulates 7TMR trafficking of the receptor:arrestin complex, but also appears important for stabilizing signaling functions [70]. Thus, ubiquitination may be the mechanism by which the endocytic and signaling properties of β -arrestin converge.

1.3.3 G protein-Independent Activation of MAP Kinases by β -arrestins

Mitogen-activated protein (MAP) kinases are serine/threonine specific kinases that regulate cellular activities such as cellular proliferation and differentiation, gene expression and cell survival/apoptosis. 7TMRs are capable of regulating the activities of MAPK family members including extracellular signal regulated kinases (ERK1 and ERK2), c-Jun NH₂-terminal kinases (JNKs) and the p38 MAPKs. MAPKs are activated in an evolutionarily conserved cascade involving three enzymes; MAP kinase, MAP kinase kinase (MKK, MEK or MAP2K), and MAP kinase kinase kinase (MAPKKK, MEKK or MAP3K). The MAP3K is activated by extracellular stimuli and then subsequently phosphorylates the MAP2K and this MAP2K in turn activates the MAPK thus forming a signaling cascade.

The discovery that β -arrestins act to scaffold MAPK cascades spawned from studies of 7TMR endocytosis in which β -arrestin-dependent Src recruitment to 7TMRs resulted in ERK activation [64, 74]. Activation of the angiotensin II type 1A receptor (AT₁AR) directs the formation of a β -arrestin2, Raf-1, MEK1 and ERK1/2 signaling complex while stimulation of the protease-activated receptor 2 (PAR2) results in a β -arrestin1, Raf-1 and phosphorylated ERK complex. β -arrestin is similarly capable of scaffolding the JNK3 MAPK cascade and figure 1-4 illustrates β -arrestin scaffolds for both ERK1/2 and JNK3 [75]. Studies have revealed that the β -arrestin functions to assemble the MAPK activation complex and direct its subcellular distribution; however, the downstream targets activated by β -arrestin-dependent ERK remain unknown [76].

β -arrestin-dependent ERK activation is both spatially and temporally distinct from G protein-mediated ERK pathways as evidenced with small interfering RNA (siRNA) experiments [77]. After stimulation of AT_{1A}R, G protein-mediated ERK is maximal within only a couple of minutes after stimulation and contributes little to the cellular pool of phospho-ERK. In stark contrast, β -arrestin2-mediated ERK is minimal until ten minutes, but is responsible for almost 100% of ERK activation beyond 30 minutes. Mutational analysis also supports independent G protein and β -arrestin signaling to ERK for both the β 2AR and AT_{1A}R [78, 79].

Figure 1-4: β -arrestin scaffolds the ERK1/2 and JNK3 MAPK cascades. β -arrestins scaffold the ERK1/2 (a) and JNK3 (b) MAPK cascades through direct interactions with both the MAP3K and MAPK (Raf-1 and ERK1/2; ASK1 and JNK3; respectively). The β -arrestins function not only to assemble the MAPK activation complex, but also direct its subcellular distribution. Adapted from S. M. DeWire et al., *β -arrestins and Cell Signaling*. *Annu. Rev. Physiol.*, 2007. **69**(483): p. 483-510.

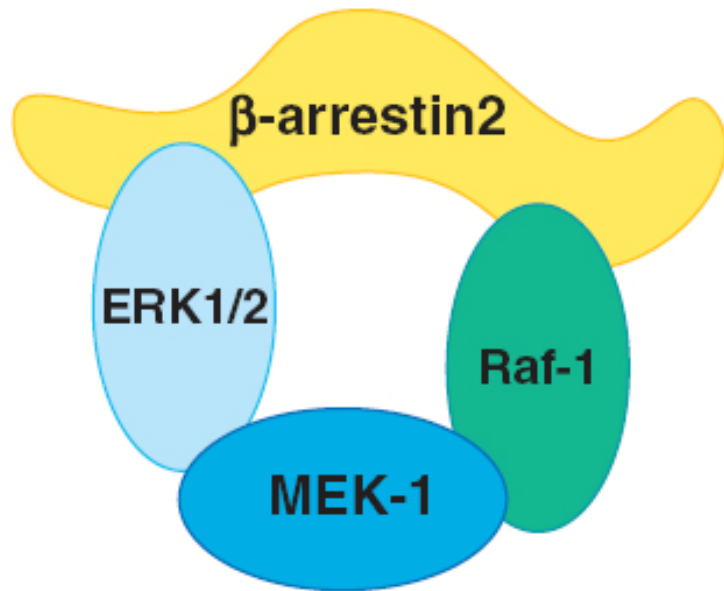
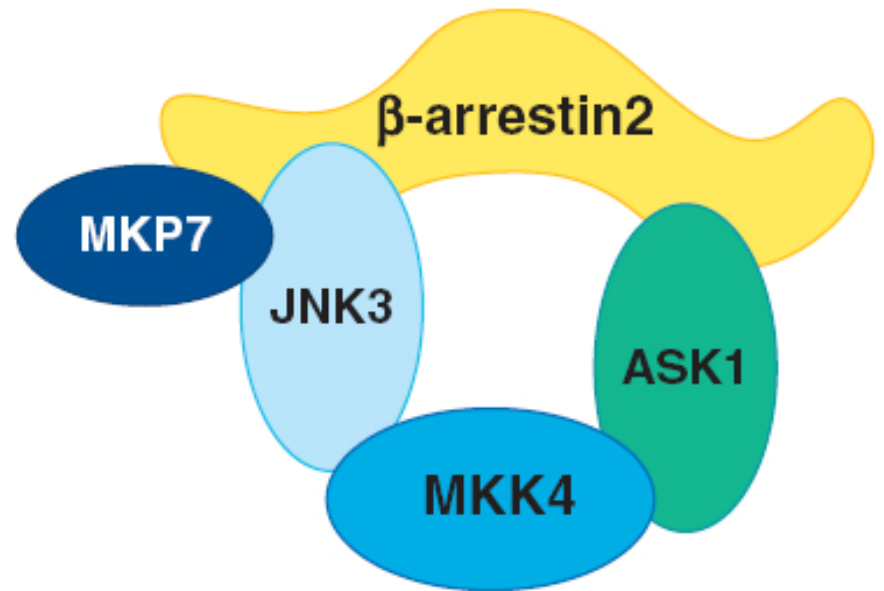
a**b**

Figure 1-4: β-arrestin Scaffolds the ERK1/2 and JNK3 MAPK Cascades.

1.3.4 β -arrestin Bias

Until recently, ligand efficacy for the stimulation of G protein activities was thought to be proportional to β -arrestin recruitment which would restrict 7TMRs to either stimulation or inhibition of all responses. Recent studies with mutant receptors that are uncoupled from G proteins, but still retain the ability to recruit β -arrestin provide the perfect models to study exclusively β -arrestin-mediated signaling [78-80]. For the AT1AR alanine substitution at two conserved residues in the second intracellular loop (AT1AR-DRY/AAY) uncouples the receptor from $G\alpha_q$. Evolutionary trace analysis of the β 2AR led to the construction of a mutant (β 2AR^{TY}) that is devoid of $G\alpha_s$ signaling while maintaining β -arrestin recruitment. Both of these mutant receptors are capable of ERK activation in a β -arrestin-mediated fashion; moreover, in the case of the β 2AR^{TY}, ERK activation is completely blocked in cells treated with β -arrestin2 siRNA which demonstrates exclusive β -arrestin signaling in the absence of G protein activation [78].

A “biased agonist” is a ligand which stabilizes a particular active conformation of a receptor thus stimulating some responses but not others. Whereas classical agonists stimulate both G protein-mediated and β -arrestin-mediated signaling mechanisms, “biased ligands” can selectively activate G protein or β -arrestin functions and thus elicit novel biological effects [81]. A synthetic peptide ligand, termed SI⁴I⁸ Ang II (SII), for the AT1AR cannot activate $G\alpha_q$ signaling, but recruits β -arrestin in the typical Class B pattern and stimulates ERK in an entirely β -arrestin-dependent manner [80]. A β 2AR biased ligand, carvedilol, was recently demonstrated to selectively stimulate β -arrestin-mediated signaling [82]. β -arrestin functions beyond

desensitization represent a new paradigm in 7TMR biology and potentially a wide array of new targets for the development of therapeutics.

Figure 1-5: Mechanism of β -arrestin biased ligands. Classically, agonist (A) activation of a 7TMR stimulates both G protein activation and β -arrestin-mediated functions (left panel). A biased ligand stimulates only one of either G protein or β -arrestin (right panel) such that β -arrestin biased ligands do not activate G proteins but do promote β -arrestin recruitment to the 7TMR.

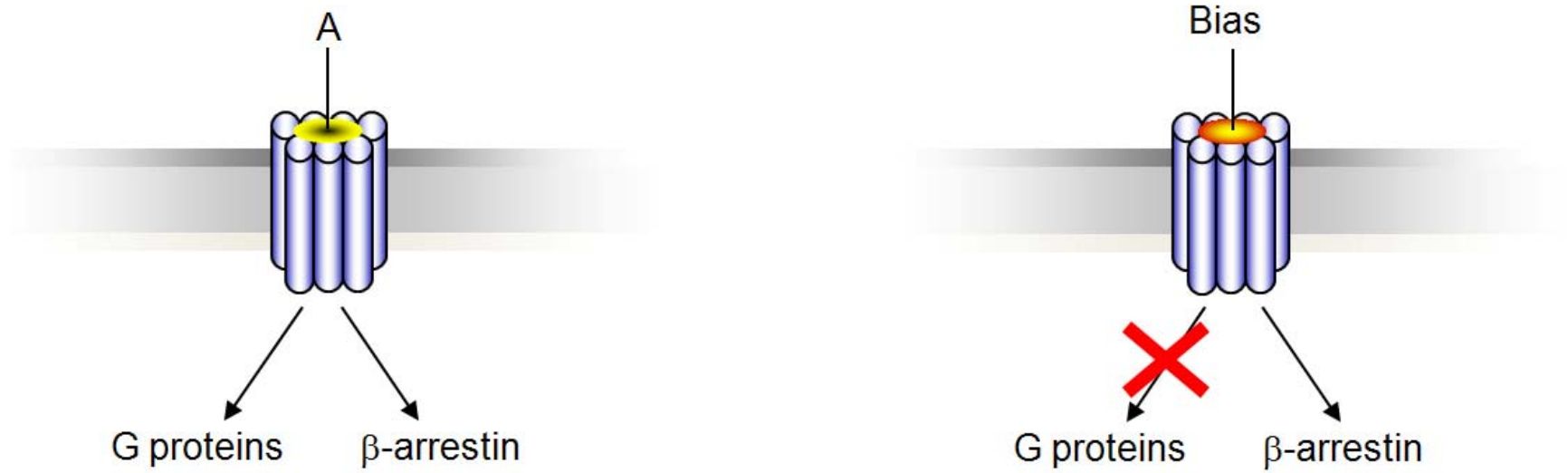


Figure 1-5: Mechanism of β -arrestin biased ligands.

1.4 Objectives for this Dissertation

At the time of this dissertation, it has been well established that phosphorylation of 7TMRs by GRKs plays essential roles in regulation of receptor function by promoting interactions of the receptors with β -arrestins. β -arrestins serve as multifunctional adaptors to desensitize G protein signals, facilitate receptor internalization, and also mediate numerous signaling pathways on their own. A long held notion in 7TMR biology is that receptors exist in one of two states: active or inactive. The recent discovery of β -arrestin biased ligands and the use of mutant receptors that signal exclusively through β -arrestin-dependent mechanisms overturn this notion of a two state receptor model and suggest that both 7TMRs and β -arrestins can adopt multiple active states.

The central hypothesis tested in these studies is that the phosphorylation of distinct sites, or sets of sites, on 7TMRs by the GRKs leads to structurally and functionally distinct conformations of β -arrestins. These distinct conformations imparted to the recruited β -arrestin by GRK “bar codes” thus regulate β -arrestin’s functional activities. Accordingly, the specific aims for this project are as follows:

I. Develop a model system to study β -arrestin conformational changes and demonstrate that β -arrestin's conformation changes in response to 7TMR phosphorylation.

Ia. Demonstrate distinct conformations of β -arrestin in response to different phosphorylation patterns.

Ib. Given recent evidence which suggests that the two β -arrestin isoforms are not functionally redundant, determine if the conformations of the two ubiquitously expressed β -arrestins are different in this model system.

II. Demonstrate that β -arrestin functionality is altered in cultured cells over-expressing the β 2AR in the presence of a full complement of GRKs or when individual GRKs (2 or 6) are depleted.

IIa. Determine if phosphorylation of the β 2AR after silencing either GRK2 or 6 instruct different conformations in β -arrestin.

III. Determine the actual sites of phosphorylation on the β 2AR in response to a full agonist, isoproterenol, from cultured cells using RNAi directed at either GRK2 or 6 in conjunction with mass spectrometry-based quantitative proteomic approaches.

IIIa. Determine the phosphorylation sites on the β 2AR upon stimulation with a β -arrestin biased ligand, carvedilol.

2. Materials and Methods

2.1 Materials and Reagents

Tissue culture reagents were purchased from Invitrogen. Radioligands and ^{32}P orthophosphate were purchased from Perkin Elmer. Anti-phospho-MAPK p42/44 antibody was purchased from Cell Signaling Technologies while the total ERK antibody (anti-MAPK 1 / 2) was purchased from Upstate. GeneSilencer was from Gene Therapy Systems. Chemiluminescent detection was performed with horseradish peroxidase-conjugated secondary antibodies and SuperSignal West Pico reagent from Pierce. β 2AR anti-phospho-S355/S356, GRK2 and GRK6 antibodies were from Santa Cruz. All GloSensor reagents were purchased from Promega. Site-directed mutagenesis was performed using a QuikChange II kit from Stratagene (La Jolla, CA). All other materials were purchased from Sigma unless otherwise noted.

Synthesis of the peptides used in this study, V₂Rnp and V₂Rpp, have been described elsewhere and the sequence of both peptides is as follows with phosphorylation sites bold and italicized: ARGRTPPSLGPQDESC***TT***ASSSLAKDTSS [83]. Two other non-specific synthetic peptides, a 28mer and 30mer, derived from GRK2 were used as controls and have been previously described [83]. The peptide V₂R4P was a gracious gift from Dr. Eric R. Prossnitz and the sequence is as follows with phosphorylation sites in bold and italicized:

ARGRTPPSLGPQDESC***TT***ASSSLAKDTSS.

Small interfering RNAs (siRNAs) were chemically synthesized from Dharmacon as previously described [84, 85]. Briefly, double-stranded siRNAs, with 19-nucleotide duplex RNA and 2-nt 3' dTdT overhangs were used in deprotected and desalted form. The siRNA sequences targeting GRKs are GRK2, 5'-AAGAAGUACGAGAAGCUGGAG-3' (NM_001619, position 268–288); GRK6-1, 5'-AACAGUAGGUUUGUAGUGAGC-3' (AF040751, position 724–744); GRK6-2, 5'-CAG UAG GUU UGU AGU GAGC-3' (position 726-745). Indicated position numbers are relative to the start codon. A nonsilencing RNA duplex (5'-AAUUCUCCGAACGUGUCACGU-3'), as the manufacturer indicated, was used as a control (CTL).

2.2 DNA Plasmids and Cell Lines

Wild-type rat β -arrestin1 and β -arrestin 2 were cloned into a pGEX4T3 expression vector (expresses GST-tagged β -arrestin1 or 2, *i.e.* GST- β -arrestin 1 or 2). All truncations and mutations discussed here were constructed with a QuikChange® II Mutagenesis kit (Stratagene). All constructs were confirmed by DNA sequencing and transformed into *Escherichia coli* strain BL21 (DE3) pLysS. The bioluminescence resonance energy transfer (BRET)-based biosensor of β -arrestin2 was constructed as previously described [86]. In this biosensor, the N-terminus of β -arrestin2 is fused to bioluminescent Renilla luciferase (RLuc) while the C-terminus is fused to yellow fluorescent protein (YFP).

To maintain consistency of expression levels between different experiments, HEK293 cells stably expressing the wild-type human β 2AR with an N-terminal FLAG tag were used unless otherwise noted. Briefly, early passage HEK293 cells were transfected with 1 mg of

FLAG- β 2AR plasmid and positive clones were selected with G418. Receptor expression levels were determined with radioligand binding as described previously [78].

We generated a stable cell line with a cAMP reporter to maintain consistency during desensitization assays. Early passage HEK-293 cells were transfected with 2.5 μ g of GloSensor enzyme plasmid (Promega) and positive clones were selected against hygromycin B (100 μ g/mL). GloSensor expression was confirmed by stimulation of endogenous β 2ARs with isoproterenol in twelve different clonal lines. The clonal line with the highest sensitivity to isoproterenol was then further characterized with forskolin treatment.

2.3 Techniques

Purification of Recombinant Rat β -arrestin 1. To overexpress GST- β -arrestin1, *E. coli* cultures were grown at 37°C to an OD₆₀₀ of 0.8 and the cultures were then equilibrated to 17°C. GST- β -arrestin1 expression was induced with 0.1 mM IPTG for 16 hours and cells were then harvested by centrifugation at 4,500 X g. The bacterial pellet was re-suspended in binding buffer (20 mM Tris-HCl pH 8.0, 150 mM NaCl, 1 mM EDTA, 2 mM DTT, 1 mM PMSF and 1 mM benzamidine) to give a 10% slurry (w/w). Cells were lysed with a cell cracker (Micorfluidics) and then centrifuged at 18,000 X g for 30 minutes. The clarified supernatant was loaded onto a glutathione sepharose (GS) column (Pharmacia) by gravity and washed with 20 column volumes (CV) of column buffer 1 (CB1) (20 mM Tris-HCl pH 8.0, 150 mM NaCl, 1 mM EDTA and 2 mM DTT). The GS resin with GST- β -arrestin1 bound was re-suspended in 2 CVs of CB1 and the GST fusion protein was cleaved with thrombin protease (Haematologic Technologies Inc.) at a mg/mg ratio of 1:1000 of thrombin:GST- β -arrestin1 . The thrombin digestion was

carried out at 4°C for 16 hours with gentle agitation of the GS resin and the supernatant was collected followed by two additional washes of the GS resin with CB1. The washes and supernatant were pooled and the NaCl concentration was diluted dropwise to 50 mM NaCl by the addition of 20 mM Tris-HCl pH 8.0, 1 mM EDTA and 2 mM DTT. The cleaved β -arrestin1, which contains eight additional amino acids at the N-terminus after thrombin cleavage (Figure 1), was then loaded onto a 5 mL HiTrap Mono-Q column (Pharmacia) and then eluted with a 50-500 mM linear NaCl gradient. Fractions were analyzed by SDS-PAGE and those containing β -arrestin1 were pooled and concentrated to 25 mg/ml and then loaded onto a Superdex 75 (Pharmacia) gel filtration column. β -arrestin1 was eluted in 20 mM Tris-HCl pH 8.0, 150 mM NaCl, 1 mM EDTA and 2 mM DTT. Fractions were analyzed by SDS-PAGE and fractions containing β -arrestin1 were pooled and concentrated to 5-25 mg/ml, flash frozen in liquid N₂ and stored at -80°C. Protein purity was >95% as assessed by SDS-PAGE and the yield was 5 mg/liter of cell culture. Recombinant GST- β -arrestin2 was purified as previously described [83].

Limited Trypsin Proteolysis. In all experiments, except where noted, a 5:1 molar ratio of peptide: β -arrestin was used to assess the effects of peptides on the limited tryptic digestion patterns of β -arrestins1 and 2. Prior to proteolysis, β -arrestins were incubated with ligand (V₂Rpp, V₂Rnp, V₂R4p, 28mer, 30mer or heparin) for 30 minutes at 4°C. An average molecular weight of 12,000 Da was used to determine the concentration of heparin. TPCCK treated trypsin to β -arrestin1 ratio of 1:250 was used in all experiments shown; however, ratios of 1:100, 1:500, 1:1,000 and 1:2,000 were also used to assess the effects of the trypsin to β -arrestin1 ratio on the limited proteolysis pattern (data not shown). No proteolysis was seen in experiments containing trypsin: β -arrestin1 ratios of 1:1,000 or 1:2,000. In the case of β -arrestin2, a trypsin to

β -arrestin2 ratio of 1:2,000 was used. Higher trypsin concentrations (1:250, 1:500 and 1:1000) were also tested, but these concentrations of trypsin completely digested β -arrestin2. After incubation with ligand, trypsin was added to the β -arrestin:ligand mixture and the samples were incubated at 25°C for the indicated time points. At each time point, 5 μ l (5 μ g) of β -arrestin1 or 2 were removed and transferred to a new microfuge tube containing 5 μ l of 2X SDS-PAGE buffer and samples were analyzed on 4-20% SDS-PAGE (Invitrogen).

MALDI-TOF MS Analysis. Spectra were collected in positive-ion mode on a Voyager DE Biospectrometry Workstation (Applied Biosystems Incorporated) in linear mode using a N₂ laser (337 nm). The acceleration voltage, grid voltage, guide wire voltage, delay time, low mass gate and laser intensity were set to 25 kV, 92.5%, 0.11%, 1200 ns, 10,000 m/Z and 2500, respectively. Sixty laser shots were collected for each sample and the spectra shown represent the sum of these 60 laser shots. Samples for MALDI-TOF MS analysis were thawed on ice and immediately diluted 25-50 fold in matrix solution (45% acetonitrile, 0.1% TFA and 5 mg/ml sinapinic acid) giving a final β -arrestin1 concentration of 2-4 μ M before depositing 1 μ l of the sample mixture onto the MALDI-TOF target plate (Applied Biosystems). Both internal and external standards were used to calibrate the data. For internal calibration, 1 μ l of carbonic anhydrase was deposited on the MALDI-TOF target after the β -arrestin1 sample had dried. Apomyoglobin and aldolase were used as external calibrants and were deposited on empty target spots. Samples were air-dried at room temperature prior to MALDI-TOF analysis. For each limited tryptic digestion, the mean mass and standard deviations were calculated from at least 5 independent experiments (Table 3-1). For low-abundance peaks, samples were prepared by quenching the tryptic digest with 1 mM PMSF and samples were then passed through a Zip

Tip (Millipore) according to the manufacturer's instructions. Samples were eluted from the Zip Tip with matrix solution and 1 μ l was directly deposited on the MALDI-TOF plate. Protein Prospector (<http://prospector.ucsf.edu/>) was used to determine all theoretical trypsin digestion fragments for rat β -arrestin1. The theoretical trypsin digest was compared to experimentally determined masses to assign candidate fragments for each β -arrestin1 fragment observed in the MALDI-TOF spectra (Table 3-1). The limited proteolytic fragments with only 1 possible theoretical candidate fragment from Protein Prospector were assigned directly. Fragments with more than 1 theoretical candidate were assigned by Western blot analysis with antibodies that recognize either the N- or C-terminus of β -arrestin1 and by determining more accurate masses by liquid chromatography electrospray ionization MS (LC/ESI-MS).

LC/ESI-MS Analysis. β -arrestin1 samples were proteolyzed as described above either in the absence of ligand or in the presence of V₂Rnp or V₂Rpp and flash frozen in liquid N₂ at various time points. Samples were analyzed on a Shimadzu LC system (comprising a solvent degasser, two LC-10A pumps and a SCL-10A system controller) coupled to a QSTAR XL quadrupole time-of-flight tandem mass spectrometer (ABI/MDS-Sciex, Toronto, Canada) equipped with an electrospray source. LC, with a Vydac C4 reverse phase column (2.1 \times 50 mm), was operated at a flow rate of 200 μ L/min with a linear gradient as follows: 100% A was held isocratically for 2 min and then linearly increased to 60% B over 18 min and then increased to 100% B over 5 min. Mobile phase A consists of water:acetonitrile (98:2 vol/vol) with 0.1% acetic acid. Mobile phase B consists of acetonitrile:water (90:10 vol/vol) with 0.1% acetic acid. The acquisition and deconvolution of ESI mass spectra were performed using the Analyst QS software.

Clathrin Binding. To determine the effects of ligand on β -arrestin1 binding to clathrin, 2.5 μ M β -arrestin1 was incubated at 4°C for 30 minutes in the absence or presence of a 5:1 molar ratio of ligand: β -arrestin1 in binding buffer (20 mM Tris-HCl pH 8.0, 150 mM NaCl). The β -arrestin1: ligand mixture was diluted to 50 nM β -arrestin1 (500 μ l) with binding buffer and clathrin was subsequently added at a 1:1 molar ratio to the reaction mixture. The reactions were tumbled at 4°C for 4 hours and then 7 μ l of a clathrin monoclonal antibody (BD Transduction) was added to the mixture and tumbled for an additional 1 hour at 4°C. Fourteen μ l of Protein A Agarose (Roche) beads were then added to the mixture and tumbled for 1 hour at 4°C. The beads were centrifuged at 20,000 X g in a benchtop microcentrifuge and washed with 1 ml of binding buffer five times and re-suspended in 20 μ l of 2X SDS-PAGE loading buffer. β -arrestin1 binding to clathrin was measured by Western blot analysis with an anti- β -arrestin1 antibody (A1CT) (ref). Samples were also subjected to SDS-PAGE and Western blot analysis with an anti-clathrin antibody (BD Transduction) to normalize the amount of clathrin for each reaction.

Cell Culture and Transfection. HEK293 cells were maintained as described above. 40-50 % confluent cells in 150-mm plates, split at least 24 hr before transfection, were transfected with siRNA using the GeneSilencer transfection reagent (Gene Therapy Systems) according to the modified manufacturer's instructions [84, 85]. Briefly, 125 μ l of the GeneSilencer transfection reagent was added to 750 μ l MEM, while RNA mixtures containing 90 μ l of 20 μ M (~20 μ g) RNA, 600 μ l of siRNA diluent, and 450 μ l MEM were prepared. Both solutions were allowed to stand 5-10 min at room temperature and mixed by inversion. Following 10-20 min incubation at room temperature, the entire transfection mixture was added to cells in a 150-mm plate

containing 10 ml of fresh, serum-free MEM. After cells were incubated for 4 hr at 37°C, an additional 12 ml of MEM with 20 % FBS and 2 % penicillin/streptomycin were added to the plate. Following additional incubation for 48 hr, cells were divided as necessary. For assays requiring transient receptor expression, the appropriate amounts of the plasmid encoding the selected receptor were transfected either two days after RNA treatment or simultaneously with RNA at the same time as above. All assays were performed at least three days after RNA transfection or two days after plasmid DNA transfection.

SILAC and Small Interfering RNA (siRNA) Silencing of Gene Expression.

These β 2AR-stable cells were maintained in stable isotope labeling of amino acids in cell culture (SILAC) “light” and “heavy” media side-by-side. The SILAC media were prepared from custom ordered DMEM powder without arginine, lysine and leucine (Gibco, Formula # 03-5080EB) (Gibco/Invitrogen, Carlsbad, CA). 50 mg/L lysine- $^{13}\text{C}_6$, $^{15}\text{N}_2$] and 50 mg/L Leucine- $^{13}\text{C}_6$, ^{15}N] (Cambridge Isotope Laboratories, Andover, MA) were added to the “heavy” medium, whereas equal concentrations of conventional arginine and lysine were added to the “light” medium; and both “heavy” and “light” media were supplemented with 84 mg/L of L-Arginine, 10% dialyzed FBS (Hyclone) (Thermo Scientific, Waltham, MA), 1% penicillin/streptomycin, and 150 $\mu\text{g}/\text{ml}$ G418. In some experiments, 50 mg/L lysine- $^{13}\text{C}_6$, $^{15}\text{N}_2$] and 25 mg/L arginine- $^{13}\text{C}_6$, $^{15}\text{N}_4$] (Cambridge Isotope Laboratories, Andover, MA) were added to the “heavy” medium, whereas equal concentrations of conventional arginine and lysine were added to the “light” medium; and both “heavy” and “light” media were supplemented with 104 mg/L of L-Leucine, 10 mg/L of L-proline, 10% dialyzed FBS (Hyclone) (Thermo Scientific, Waltham, MA), 1% penicillin/streptomycin, and 150 $\mu\text{g}/\text{ml}$ Zeocin. When reached ~ 80% confluence, the cells were

serum-starved for 24 hours. To map the phosphorylation sites on the β 2AR induced by isoproterenol or carvedilol, the “heavy” labeled cells were treated with 10 μ M of isoproterenol or carvedilol for 5 minutes before harvesting, and the “light” labeled cells served as control without any treatment. In some experiments, the “light” labeled cells were treated with agonist and the “heavy” labeled cells served as control.

To map the phosphorylation sites by GRK2 or 6, the “heavy” labeled cells were treated with control siRNA and the “light” labeled cells were treated with GRK2 or 6 siRNA, or vice versa. The sequences of the control, GRK2 and GRK6 siRNAs were published previously [84, 85]. After siRNA treatment, both “light” and “heavy” cells were stimulated 10 μ M of isoproterenol for 5 minutes before harvesting. Equal numbers of “light” and “heavy” cells (generally thirty 150 mm culture dishes for each) were mixed, flash-frozen in liquid nitrogen, and stored at -100 °C. The SILAC experiments were repeated at least three times. Silencing was quantified by immunoblotting. Only experiments with verified silencing were used.

β 2AR purification and digestion. The β 2ARs were purified with an alprenolol-agarose affinity purification procedure as previously described [87]. Briefly, crude membrane fractions were prepared from the HEK-293 line stably expressing 2pmol/mg of FLAG tagged β 2AR and receptors were extracted with 1X buffer (20 mM Tris-HCl, PH 8.0, 100 mM NaCl, 2 mM EDTA) containing 1% DDM (n-Dodecyl β -D-maltoside). Alprenolol-agarose affinity beads were then used to isolate the β 2ARs from the above extracts. Purified receptors were eluted with 150 μ l of 5mM alprenolol in 1X Buffer with 0.01% DDM. Protease and phosphatase inhibitors were added to all the buffers.

Purified β 2ARs were reduced with 5 mM DTT at 65°C for 20 minutes and alkylated with 10 mM iodoacetamide in the dark at room temperature for 20 minutes. In-solution digestion was performed using 5-10 ng/ μ l trypsin (modified, sequencing grade, Promega, Madison, WI) in 50 mM NH_4HCO_3 (pH 8.0) for 18 h at 37°C. To the digested samples, equal volume of 100% acetonitrile (CH_3CN) was added, and dried under vacuum on a speed-vac evaporator. The peptide samples were desalted by using handmade STAGE-tips (refs) and dried by a speed-vac evaporator before subjected to phosphopeptides enrichment or directly to mass spectra analyses.

Immobilized Metal Ion Affinity Chromatography (IMAC). For phosphopeptides enrichment, the dried peptides were resuspended in 150 μ L of IMAC wash/equilibration buffer (25 mM formic acid, 40% acetonitrile) and added to 25 μ L of a 1:1 slurry of pre-charged IMAC resin (Fe(III)-loaded IMAC slurry) (Phos-Select iron affinity gel, Sigma-Aldrich, St. Louis, MO). The IMAC resin was pre-washed 3 times in 1 mL wash/equilibration buffer. Samples were agitated for 90 minutes at room temperature and washed 3 times with 150 μ L of wash/equilibration buffer. Bound peptides were eluted twice with 45 μ L of 50 mM $\text{KH}_2\text{PO}_4/\text{NH}_3$ (pH 10.0) and acidified with 45 μ L of 5% formic acid, 5% acetonitrile. All samples were resuspended in 40 μ L of 5% formic acid and desalted on C18 resin, using handmade STAGE-tips[88]. Peptides were eluted with 5% formic acid, 50% acetonitrile, dried once again by a speed-vac evaporator, reconstituted in 5% formic acid, 5% acetonitrile and subjected to LC/MS/MS analysis.

LC/MS/MS and Data Analyses. Liquid Chromatography/Tandem Mass Spectrometry (LC/MS/MS) analyses were performed on a Thermo Scientific LTQ Orbitrap XL or LTQ-FT mass spectrometer (Thermo Fisher, San Jose, CA) with a Finnigan Nanospray II electrospray ionization source as described previously [57]. Instrument control and primary data processing were done using the Xcalibur software package. The LTQ Orbitrap XL or LTQ-FT was operated in the data-dependent mode using the TOP10 strategy [89]. MS/MS spectra were searched by using the SEQUEST algorithm against a composite database containing the human β 2AR and its interacting proteins. Search parameters allowed for three missed tryptic cleavages, a mass tolerance of ± 80 ppm, a static modification of 57.02146 Da (carboxyamidomethylation) on cysteine, and up to six total dynamic modifications (79.96633 Da (phosphorylation) on serine, threonine, and tyrosine, 15.99491 Da (oxidation) on methionine, 10.00827 Da on arginine, and 8.01420 Da on lysine). Search results were filtered to include <1% matches to reverse sequences by restricting the mass tolerance window, and setting thresholds for Xcorr and dCn' (defined as the normalized difference between Xcorr values of the top-ranked candidate peptide and the next candidate with a different amino acid sequence). All the MS and MS/MS spectra were manually confirmed.

The probability of correct phosphorylation site localization for each phosphorylation site was measured using an Ascore algorithm as describe previously [90]. Sites with Ascore ≥ 13 ($P \leq 0.05$) were considered to be confidently localized, and those with Ascore ≥ 19 ($P \leq 0.01$) were considered to be localized with near certainty. Peptide quantification was performed automatically by using the Vista program as describe previously [91]. In brief, the theoretical mass of both heavy and light variants of each peptide was calculated and used to identify ion

peaks in the high mass accuracy precursor scans for each. The intensity of the peaks was used to construct ion chromatograms. Candidate peaks were required to fall within a tolerance window of ± 10 ppm from the calculated mass and were filtered to require the predicted isotopic distribution. For each isotopic variant, the background-subtracted area under the curve was determined as a function of elution time and used to calculate the heavy to light abundance ratio (Vista ratio). All the quantification data was manually checked.

Immunoprecipitation and Immunoblotting. HEK293 cells stably expressing FLAG-tagged β_2 AR were used for immunoprecipitations unless otherwise noted. Cells were lysed in and adjusted to equal protein concentration by protein assay prior to immunoprecipitation with M2 anti-FLAG beads (Sigma). Equal amounts of protein were separated on Tris-glycine polyacrylamide gels (Invitrogen) and transferred to polyvinylidene fluoride membranes for immunoblotting. GRKs were detected with isoform specific antibodies from Santa Cruz Biotechnology, Inc. according to the manufacturer's protocol. Phosphorylated β_2 AR, phosphorylated ERK1 / 2 and total ERK1 / 2 were detected by immunoblotting with an anti-phospho β_2 AR antibody (Santa Cruz), anti-phospho-p44/42 MAPK antibody (Cell Signaling) and anti-MAPK1/ 2 (Upstate Biotechnology), respectively. Chemiluminescent detection was performed with horseradish peroxidase-coupled secondary antibody (Amersham Biosciences) and SuperSignal West Pico reagent (Pierce). Chemiluminescence was quantified by a charge-coupled device camera (Syngene ChemiGenius2).

β_2 AR Desensitization in GloSensor Cells. HEK293 cells stably expressing Promega's GloSensor enzyme (a luciferase enzyme that produces luminescence upon binding to cAMP), were seeded on 96-well plates 48 hours after GRK siRNA treatment. The next day (72 hrs. post-

transfection), the cells were pre-equilibrated with 2% of the GloSensor cAMP reagent in MEM (supplemented with 10% FBS) for 2 hrs. at 27°C. Endogenous β 2ARs were then stimulated with either a vehicle (DMSO) or 100 nM isoproterenol for five minutes and subsequently washed two times with 150 μ l of MEM (supplemented with 10% FBS and 1% penicillin/streptomycin) for five minutes. After adding 100 μ l of fresh MEM to the cells, β 2ARs were re-challenged with isoproterenol in a dose-dependent fashion. GloSensor luciferase activities were then measured in quadruplicate using the Novostar microplate reader (BMG Labtech) in luminescence mode and the dose-response data were fit using the operational model of Black and Leff [92].

Internalization Assay. Receptor internalization was measured by CGP 12177 radioligand binding on monolayers of cells plated on poly-D-lysine-coated 12-well dishes (Biocoat) in MEM buffered with 10 mM HEPES (pH 7.5) and supplemented with 0.1% BSA (wt./vol). Binding was performed in triplicates with 10 nM CGP 12177 in the presence or absence of 20 μ M ICI (to define non-specific binding). After incubation at 4°C for 90 minutes, the cells were placed on ice and washed several times with phosphate-buffered saline containing calcium and magnesium. Cells were solubilized in 0.1 N NaOH and 0.1% SDS and counted for 3 H. Agonist-induced internalization was defined as loss of cell surface receptors as previously described. GraphPad PRISM software was used for data analyses.

ERK Activation Assay. HEK293 cells stably expressing the β 2AR were grown at low confluence and split to 6- or 12-well plates. Cells were starved in serum free media at least four hours prior to stimulation with either 10 μ M isoproterenol or 10 μ M carvedilol. After stimulation, cells were solubilized directly into 2x SDS-sample buffer followed by sonication with a microtip for 15 seconds. For each experimental condition, an equal portion of cells was

used for protein determination (Bradford). Equal micrograms of cell lysate were separated on 4-20% Tris-glycine polyacrylamide gels and transferred to filters for immunoblotting. GraphPad PRISM software was used for data analyses.

BRET Assay. BRET assays were performed as described [93]. Briefly, 48 h after transfection, cells co-expressing the β 2AR, BRET biosensor and siRNAs were plated on fibronectin coated, 96-well microplates (white wall ,clear bottom). Prior to the assay, cells were washed twice with 100 μ l of PBS at 37°C. The transparent bottom of the plate was then covered with a white back-tape adhesive and cells were then incubated for ten minutes at 37°C with coelenterazine h (5 μ M final concentration). Cells were then stimulated with isoproterenol for 15 minutes and light emission was detected as previously described. The BRET ratio was determined as the ratio of light emitted by YFP and the light emitted by RLuc. The values were corrected by subtracting the background signals prior to isoproterenol stimulation.

Statistical Analysis. All statistics presented were from data analyzed using GraphPad Prism software (GraphPad Software Inc., San Diego, CA). Analysis of variance (ANOVA) was performed where noted and significance was determined with Bonferonni's post-test. P values less than 0.05 were taken as statistically significant.

3. The Active Conformation of β -arrestin1 and its Difference from β -arrestin2

3.1 Introduction

The central hypothesis tested in these studies is that the phosphorylation of distinct sites, or sets of sites, on 7TMRs by the GRKs leads to structurally and functionally distinct conformations of β -arrestin and that these distinct conformations regulate β -arrestin's functional activities. The roles of β -arrestins in 7TMR desensitization, internalization and signaling are agonist-dependent, which demonstrates that β -arrestins must first interact with agonist-occupied, phosphorylated 7TMRs suggesting that the conformation of "receptor-bound" β -arrestin is required to elicit some of its cellular functions. Moreover, β -arrestins 1 and 2 may have different roles in modulating cellular processes, though extant evidence suggests that the two β -arrestin isoforms are structurally very similar.

The arrestin gene family in mammals consists of four members: arrestins 1 and 4 (visual arrestins), and arrestins 2 and 3, also known as β -arrestin1 and 2, respectively. Solved crystal structures of the basal state of visual arrestin1, visual arrestin4 and β -arrestin1 in conjunction with extensive biochemical and mutagenesis studies support the idea that a conformational change occurs in arrestins upon binding activated, phosphorylated 7TMRs [53, 94-115]. The basal conformations of arrestins are elongated two-domain (N- and C-domain) molecules and these domains are connected through a twelve residue linker, or hinge, region (Figure 3-1A) [53]. It has been suggested that upon "activation" of β -arrestins, the N- and C-domains move relative to one another via flexibility of the hinge region. Two major intramolecular interactions have been suggested to stabilize the basal conformation of arrestins. The first is a series of

hydrophobic interactions between α -helix I, β -strand I and the C-terminus of the molecule, which folds back onto the N- domain (Figure 3-1B). The second intramolecular interaction that “holds” arrestins in their inactive state is the polar core; a distinctive interaction of five charged residues which are shielded from water and embedded at the fulcrum of the molecule between the N- and C-domains (Figure 3-1C). This polar core contains elements of both the N- and C-termini of arrestins and also a lariat loop region (R²⁸²-G³⁰⁹). The lariat loop plays a central role in stabilizing the polar core since it contains the primary counterion, D²⁹⁰, for R¹⁶⁹ in the polar core. This loop apparently lacks any secondary structure, yet its tertiary structure is virtually identical in both visual arrestin and β -arrestin1 suggesting that its conformation is essential in stabilizing the basal state of arrestins.

Figure 3-1. The basal conformation of bovine β -arrestin1. (A) The crystal structure of bovine β -arrestin1 is shown as a ribbon diagram with both the N- and C-termini labeled. The diagram is colored by domain with the N-domain in magenta, C-domain in blue and the hinge region in orange. Circled regions of the structure in part A are enlarged in parts B and C. (B) Hydrophobic interactions between α -helix I, β -strand I and the C-tail, which stabilize β -arrestin's basal conformation are shown. α -helix I and β -strand I are shown in magenta and the C-tail is shown in blue. Hydrophobic contributions from α -helix I include three leucines, while phenylalanine residues from the C-tail are also shown. Conserved lysines in β -strand I (K¹⁰ and K¹¹) are also shown as these residues guide receptor-attached phosphates to R¹⁶⁹ in the polar core. (C) The local environment of the polar core (five interacting charged residues) is shown with sticks for residues D²⁶, R¹⁶⁹, D²⁹⁰, D²⁹⁷ and R³⁹³. The polar core is the main phosphate sensor in arrestins and, upon activation, this polar core is disrupted causing release of the C-tail (shown in blue).

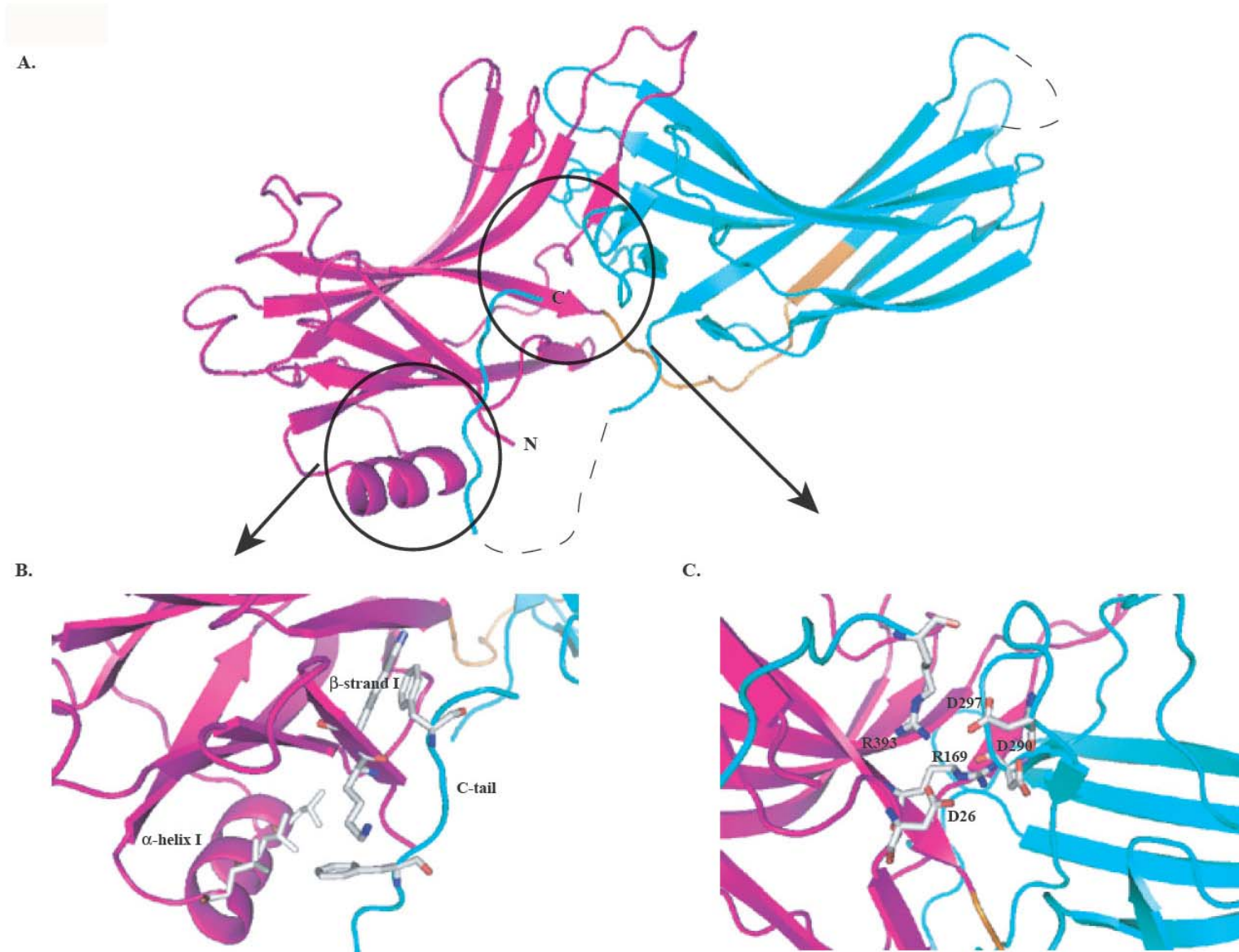


Figure 3-1: The Basal Conformation of Bovine β -arrestin1.

Studies have suggested that upon binding to 7TMRs, the polar core of arrestins is disrupted and its C-terminus is released [53, 83, 95, 104, 105, 109, 110, 114]. The C-termini of β -arrestins contain both clathrin and AP2 binding sites and exposure of this C-terminus is essential for clathrin-mediated receptor internalization [61]. Studies have demonstrated that visual arrestin binding to a phosphorylated peptide corresponding to the last 17 amino acids (C-terminus) of rhodopsin can mimic visual arrestin binding to phosphorylated rhodopsin as assessed by limited trypsin proteolysis [109, 110, 112]. Despite evidence for conformational changes in arrestins, no structure for the active, or receptor-bound, conformation has been determined for any arrestin family member. Moreover, conformational studies of arrestins are primarily limited to the visual arrestin system.

β -arrestins1 and 2 are ubiquitously expressed and their universal regulation of 7TMRs attests to their importance in modulating cellular function. Despite the ubiquitous expression of both β -arrestins1 and 2, recent evidence has suggested that the two isoforms are in fact not functionally redundant. For example, β -arrestin1 is responsible for scaffolding RhoA activation in conjunction with $G_{\alpha q/11}$ and also IGF-1 activation of phosphatidylinositol 3-kinase (PI3K) [116, 117]. β -arrestin2 scaffolds the mitogen-activated protein kinase (MAPK) cascade to activate ERK1/2, c-Jun N-terminal kinase (JNK3) and in some cases, p38 [75, 76, 118-122]. Our lab has previously reported conformational changes in β -arrestin2 with a phosphorylated peptide corresponding to the C-terminus of the human V_2 vasopressin receptor (V_2R_{pp}) as assessed by limited tryptic proteolysis and MALDI-TOF analysis [83]. Using this same approach, we now report that the conformation of β -arrestin1 is also altered upon binding V_2R_{pp} , but in ways which suggest that its activated conformation is different from that of β -arrestin2. Furthermore,

we show that a V₂R phospho-peptide containing different sites of phosphorylation (V₂R4p) is able to elicit a conformational change in β -arrestin1 that is distinct from that induced by V₂Rpp.

3.2 Results

Conformational changes in β -arrestin1 upon V₂Rpp binding

Recombinant β -arrestin1 was purified as described in Experimental Procedures and the primary sequence is shown in Figure 3-2. To study conformational changes in β -arrestin1 upon its association with a 7TMR, we employed an *in vitro* model system utilizing both a phosphopeptide (V₂Rpp) and non-phosphopeptide (V₂Rnp) corresponding to the C-terminus of the human V₂ vasopressin receptor (V₂R peptide sequences are given in Experimental Procedures). β -arrestin1 was incubated in the absence or presence of ligand (a 5:1 molar ratio of ligand: β -arrestin1 was used in all experiments unless otherwise stated) and then subjected to limited tryptic proteolysis. The proteolysis patterns of β -arrestin1 alone or in the presence of V₂Rnp are identical and we will refer to this digestion pattern as “control pattern” (Figure 3-3A, panels I and II). The control pattern in figure 3B illustrates that full-length β -arrestin1 (G⁸-R⁴¹⁸) has an apparent molecular weight of 47 kDa and the addition of trypsin results in slow, continuous digestion generating fragments with apparent molecular weights of 47, 40, 32, 25 and 21 kDa. The addition of the V₂Rpp resulted in a distinct digestion pattern with an accelerated proteolysis of the 40 and 32 kDa species as well as the full-length protein (Figure 3A, panel III). This new digestion pattern also featured the appearance of new species with molecular weights of 44 and 45 kDa and the accumulation of the 21 kDa species over time. The V₂Rpp pattern is depicted schematically in Figure 3-3B. Proteolysis of β -arrestin1 was also

conducted in the presence of two non-specific peptides, a 28-mer and 30-mer, and β -arrestin1 digestion in the presence of these peptides resulted in the control pattern (data not shown).

Figure 3-2. Sequence Alignment of recombinant rat β -arrestins 1 and 2. (A) A sequence alignment of recombinant rat β -arrestins1 and 2 was performed using Geneious software (www.biomatters.com). Both of these recombinant proteins contain additional amino acids at the N-terminus due to thrombin cleavage of the GST tag during purification (number -8 to -1). The top sequence corresponds to β -arrestin1 and the bottom sequence corresponds to β -arrestin2. Residues are colored according to polarity and the numbering is shown only for β -arrestin1. The start M in the sequence of β -arrestin1 is replaced by an L and is followed by the wild type sequence with G at position 2. Important R residues to this study are indicated with arrows ($R^{188/189}$ and $R^{363/364}$ for β -arrestin1 and 2, respectively). β -arrestin's hinge region, residues 173-184 of β -arrestin1, is indicated by a rectangle and arginines 188 and 189, of β -arrestins 1 and 2 respectively, located just outside this region are indicated with an arrow.

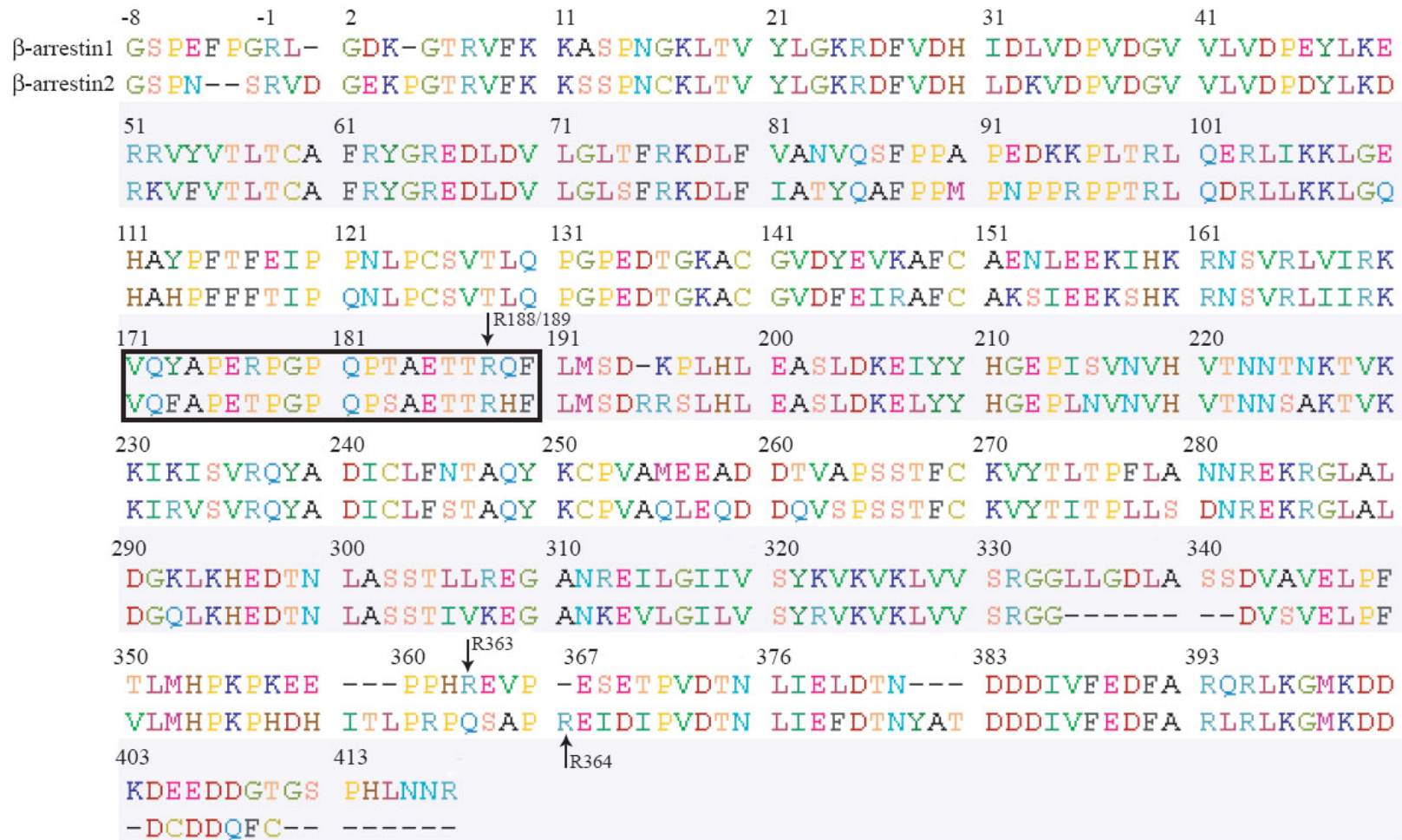


Figure 3-2: Sequence Alignment of Recombinant Rat β -arrestin1 and 2.

Figure 3-3. Limited tryptic proteolysis patterns of β -arrestin1 alone and in the presence of

either V₂Rnp or V₂Rpp. (A) A time-course (0, 5, 30, 60 and 120 minutes) of limited tryptic proteolysis fragments, analyzed by SDS-PAGE, is shown for β -arrestin1 alone (panel I), β -arrestin1 in the presence of V₂Rnp (panel II) and β -arrestin1 in the presence of V₂Rpp (panel III).

The tryptic fragments in panels I and II are identical and the apparent molecular weights by SDS-PAGE are indicated to the right of panel III. The tryptic fragments of β -arrestin1 in the

presence of V₂Rpp are different from those in the absence of peptide or in the presence of

V₂Rnp. Panel III shows the tryptic fragments of β -arrestin1 in the presence of V₂Rpp and the

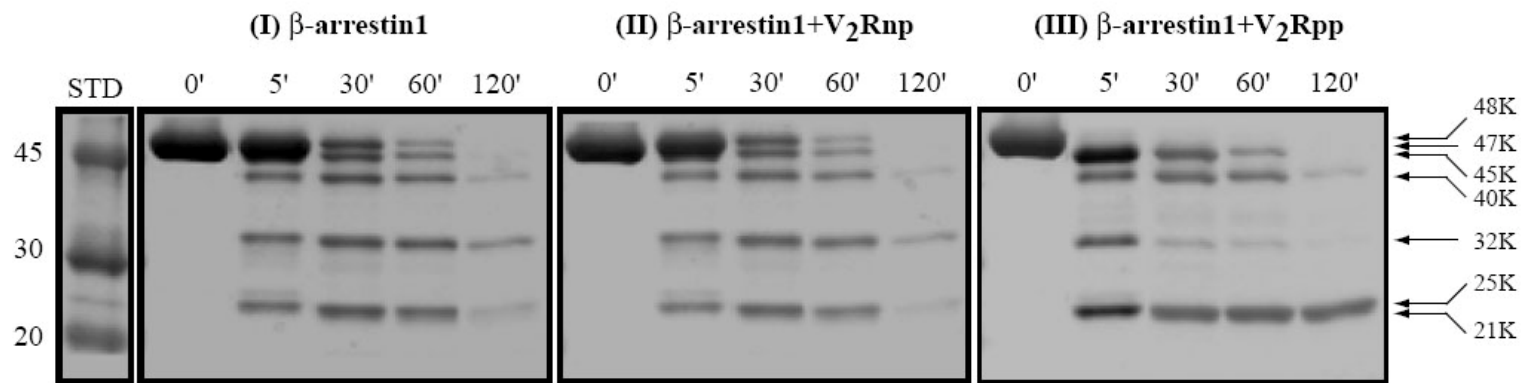
apparent molecular weights of these fragments are indicated to the right of panel III. (B) A

schematic representation of tryptic fragments for β -arrestin1. The control panel on the left is the

pattern seen for limited tryptic digestion of β -arrestin1 alone or in the presence of V₂Rnp. The

V₂Rpp panel is shown on the right.

A.



B.

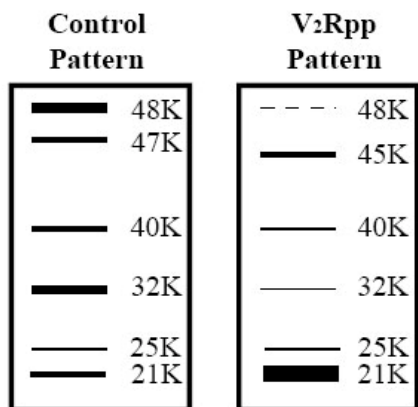


Figure 3-3: Limited Tryptic Proteolysis Patterns of β -arrestin1.

Conformational Changes in β -arrestin1 require phosphate moieties

We have shown that the limited proteolytic digestion pattern of β -arrestin1 is unaltered by the addition of V₂Rnp; the possibility exists that V₂Rnp can indeed bind to β -arrestin1 with a lower affinity than V₂Rpp and binding of V₂Rnp can also induce conformational changes in β -arrestin1 at a higher V₂Rnp to β -arrestin1 ratio. We therefore titrated β -arrestin1 with increasing amounts of peptides and performed limited proteolysis to assess the effects of changes in peptide to β -arrestin1 ratios. V₂Rnp does not alter the digestion pattern of β -arrestin1 even at a peptide to β -arrestin1 molar ratio of 20:1 while V₂Rpp alters the conformation of β -arrestin1 even at a 1:1 molar ratio (Figure 3-4A and 3-4B). We also conducted a competition experiment to determine if high concentrations of V₂Rnp can compete with V₂Rpp for binding to β -arrestin1. In the presence of 1:1 molar ratio of V₂Rpp, addition of a 100-fold molar excess of V₂Rnp did not convert the V₂Rpp pattern to the control pattern, clearly demonstrating that the V₂Rnp is incapable of competing with V₂Rpp binding (Figure 3-4C, lane 6).

Figure 3-4. The effects of different peptide:β-arrestin1 molar ratios on limited tryptic proteolysis patterns and competition binding of V₂Rnp and V₂Rpp to β-arrestin1. (A) β-arrestin1 was incubated without (labeled 0) or with increasing molar ratios of V₂Rnp (1:1 up to 20:1) to determine the effects of peptide concentration on the limited tryptic patterns for β-arrestin1 at a 30 minute time point. (B) β-arrestin1 was incubated without (labeled 0) or with increasing molar ratios of V₂Rpp (1:1 up to 20:1) to determine the effects of V₂Rpp concentration on the limited tryptic digest of β-arrestin1 at a 30 minute time point. (C) Lane 1 shows undigested β-arrestin1 (0 minutes) while lane 2 shows the tryptic digestion pattern of β-arrestin1 alone. In lanes 3 and 4, β-arrestin1 was incubated with a 1:1 molar ratio of either V₂Rnp and V₂Rpp, respectively, prior to limited proteolysis. In lanes 5 and 6, β-arrestin1 was simultaneously incubated with a 1:1 molar ratio of V₂Rpp and increasing concentrations of V₂Rnp. All tryptic fragments shown in lanes 2-6 are of a 30 minute time point. In all panels, the apparent molecular weights of the limited tryptic fragments are shown to the right.

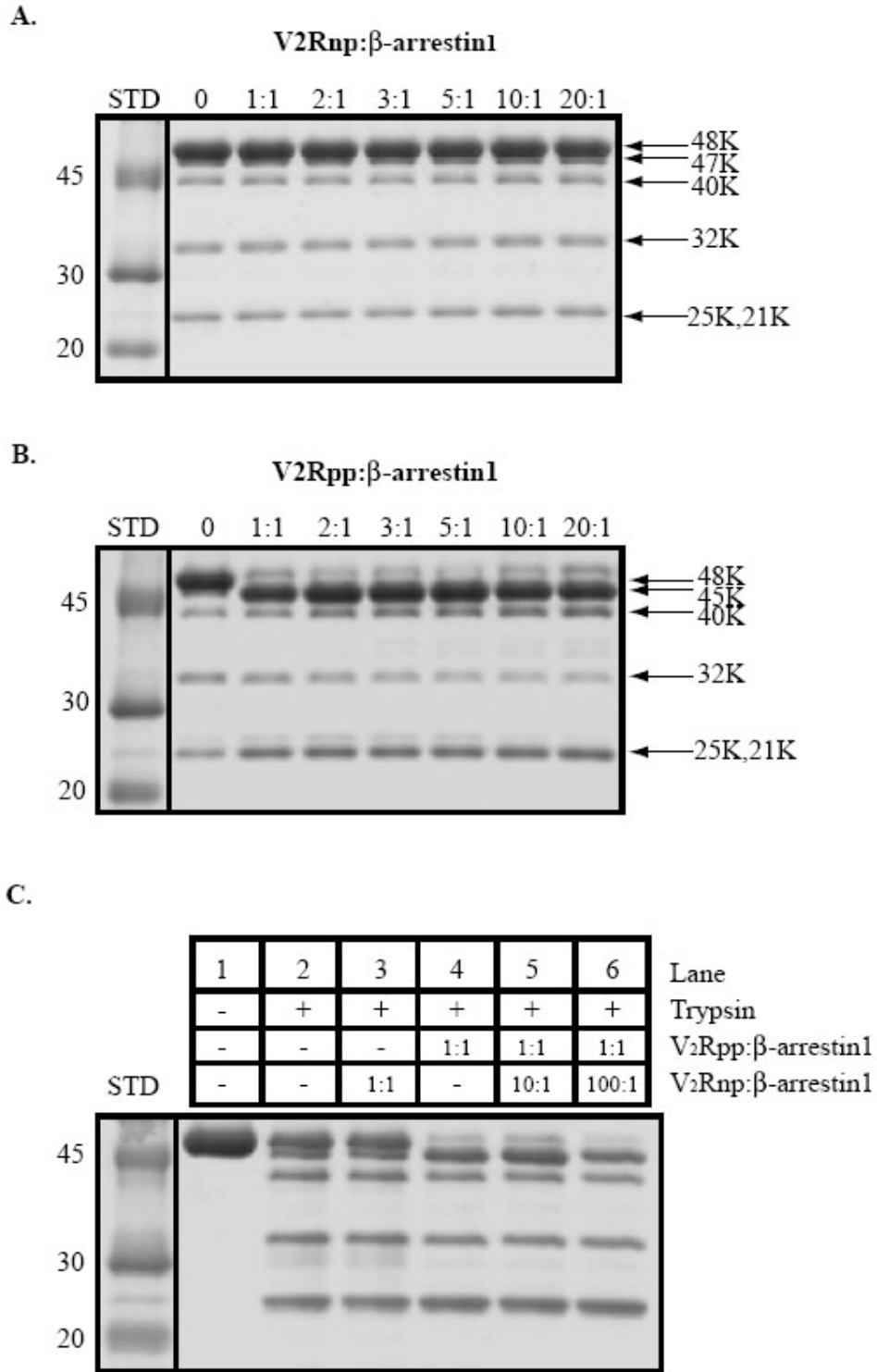


Figure 3-4: Conformation Changes in β -arrestin1 Require Phosphates.

MALDI-TOF MS analysis of limited tryptic proteolysis fragments of β -arrestin1

Limited proteolysis of β -arrestin1 clearly demonstrates a conformational change in the presence of V2Rpp. However, details of these conformational changes could not be obtained due to the low resolution of SDS-PAGE analysis of tryptic fragments. To precisely map regions of β -arrestin1 involved in these conformational changes, we employed MALDI-TOF MS to determine sites of proteolysis by measuring the accurate masses of tryptic fragments. Taking advantage of the high mass accuracy of MALDI-TOF MS, most of the species observed by SDS-PAGE were precisely assigned by comparing the experimental mass value of a protein fragment to its theoretical value (Table 3-1). For those fragments which could not be definitively assigned by MALDI-TOF MS, we used the more accurate liquid chromatography electrospray ionization (LC/ESI) MS with a higher mass accuracy (within less than 1.0 Da for a μ kDa peptide) to help with assignments. Additionally, to assign some fragments, we also conducted Western blot analysis with antibodies that recognize different domains of β -arrestin1 (N- or C-domain).

Table 3-1. The final assignment of all β -arrestin1 tryptic fragments are shown in the first column. Candidate fragments generated from a theoretical trypsin digest of β -arrestin1 (<http://prospector.ucsf.edu/>) are shown in the next column followed by their predicted masses. Mean experimental masses and standard deviations from at least 5 independent experiments were generated from MALDI-TOF data of β -arrestin1 proteolysis. Apparent molecular weights of all fragments by SDS-PAGE and those fragments which were confirmed by ESI-MS are shown in the last two columns.

Table 3-1: Final assignment of limited tryptic proteolytic fragments of β -arrestin1

Final Assignment of Tryptic Fragments	Candidate Fragments (theoretical)		MALDI-TOF m/z (experimental)			Apparent MW by SDS-PAGE (kDa)	Confirmed by ESI-MS
	Predicted tryptic fragments (amino acid)	Predicted m/z within standard deviations	β -arrestin1	β -arrestin1 + V2Rnp	β -arrestin1 + V2Rpp		
G ⁸ -R ⁴¹⁸	G ⁸ -R ⁴¹⁸	47830	47841+/-35	47840+/-41	47853+/-32	48	
L ¹ -R ⁴¹⁸	L ¹ -R ⁴¹⁸	47003	47022+/-19	46995+/-28	NA	47	
G ⁸ -R ³⁹³	G ⁸ -R ³⁹³ L ¹ -K ⁴⁰⁰	44993 45007	NA	NA	45014+/-28	45	+
L ¹ -R ³⁹³	L ¹ -R ³⁹³	44165	NA	NA	44181+/-30	44	
L ¹ -R ³⁶³	L ¹ -R ³⁶³	40744	40739+/-24	40731+/-25	40725+/-24	40	
1 L ¹ -R ²⁸⁵	L¹-R²⁸⁵ K ¹⁰⁷ -R ³⁹⁵	32335 32346	32335+/-22	32321+/-28	32342+/-9	32	
1 G ⁵ -R ²⁸⁵ ?	K ¹¹ -K ²⁹² E ⁵⁰ -R ³³¹ L ¹ -R ²⁸² G⁵-R²⁸⁵ L ¹⁰⁸ -R ³⁹³	31888 31913 31922 31922 31934	31905+/-48	31900+/-37	31920+/-41	32	
1 D ²⁶ -K ²⁵⁰	D²⁶-K²⁵⁰ V ¹⁷¹ -K ⁴⁰⁰ Q ¹⁸⁹ -R ⁴¹⁸	25732 25737 25752	25742+/-17	25736+/-41	NA	25	
1 L ¹ -R ¹⁸⁸	E ²⁰⁶ -R ³⁹⁵ L¹-R¹⁸⁸	21244 21270	21260+/-19	21262+/-23	21260+/-17	21	+

1 Recognized by F4C1.

MALDI-TOF MS analysis over the range of m/z 20,000-50,000 was conducted on tryptic fragments from β -arrestin1 alone or in the presence of either V₂Rnp or V₂Rpp. At an early time point (5 min), the spectra for β -arrestin1 alone or in the presence of V₂Rnp are identical and we have therefore shown spectra of β -arrestin1 with V₂Rnp only. The major peaks are 48 and 47 kDa and minor peaks at 25 and 21 kDa (Figure 3-5A, left panel). In the presence of V₂Rpp, the major peaks are left-shifted with masses of 45 and 44 kDa and a minor peak is also observed at 21 kDa (Figure 3-5A, bottom of left panel). The most notable difference in spectra collected at an early time point is the accelerated proteolysis of β -arrestin1 in the presence of V₂Rpp resulting in a left-shift of the major peaks.

MALDI-TOF MS of an early time point (5 min.) of β -arrestin1 tryptic fragments in the presence of V₂Rnp indicates that the major species is full-length β -arrestin1 (G⁻⁸-R⁴¹⁸), which has an experimental mass (m/z) of 47840±41 Da (Figure 3-5A). Full-length β -arrestin1 is then slowly proteolyzed to residues L¹-R⁴¹⁸ due to an N-terminal clip at position R⁻¹ (Figure 5A). In the presence of V₂Rpp, β -arrestin1 proteolysis is initially accelerated and then slow and continuous over time giving rise to a 45 kDa fragment (45014±28 Da) corresponding to amino acids G⁻⁸-R³⁹³ as is evident in both the MALDI-TOF spectra and by SDS-PAGE (Figures 5A and 5B). The assignment for this fragment was confirmed by LC/ESI-MS, which gave a mass of 44992 Da (Table 3-1). We further confirmed the assignment of this 45 kDa peak (G⁻⁸-R³⁹³) by the presence of the 24 amino acid C-terminal peptide, R³⁹³-R⁴¹⁷, which had a mass of 2854.3 Da by LC/ESI-MS (data not shown). In addition, we also identified a peptide corresponding to amino acids R³⁹⁵-R⁴¹⁷ with an apparent mass of 2570.2 Da, which demonstrates that β -arrestin1 is actually

proteolyzed at both R³⁹³ and R³⁹⁵ in the presence of V₂Rpp though we could not resolve these two species by MADLI-TOF MS or SDS-PAGE (data not shown). N-terminal proteolysis also occurs on this 45 kDa fragment at the R⁻¹ position resulting in a peak at 44 kDa (44181±30 Da) in the MALDI-TOF spectra, which corresponds to residues L¹-R³⁹³ (Figure 3-5A). Figure 3-5C is a ribbon diagram of β-arrestin1's crystal structure with R³⁹³ shown, which displays increased accessibility in the presence of V₂Rpp. R³⁹⁵ is not present in the solved crystal structure of β-arrestin1 since this structure is of a truncated β-arrestin1 (M¹-R³⁹³) and is therefore not shown in Figure 3-5C.

Spectra collected at a late time point (60 min) of β-arrestin1 alone or in the presence of V₂Rnp are also identical and we have again only shown a representative spectrum of β-arrestin1 in the presence of V₂Rnp (Figure 3-5A, right panel). The major peaks for these spectra are 47, 40, 32, 25 and 21 kDa and the 47 kDa peak remained protected over time from the early (5 min) time point. In the spectra for β-arrestin1 with V₂Rpp, the major peaks occur at 44 kDa and 21 kDa, with minor peaks at 40, 32 and 31 kDa. The 44 kDa fragment that occurs from β-arrestin1 with V₂Rpp remained protected over time and also occurs in the early (5 min) time point spectrum. A striking difference at the late time point (60 min) is that two peaks are observed at 32 and 31 kDa for β-arrestin1 with V₂Rpp whereas only one (32 kDa) peak is observed in the control situation.

The 32 kDa fragment of β-arrestin1 is present in all the samples that were analyzed (Figure 3-5A) and the experimental masses for this species with both V₂Rnp (top spectrum) and V₂Rpp are 32321±28 and 32342±9 Da, respectively. There are two candidate fragments from the theoretical trypsin digest of β-arrestin1 for the 32 kDa species which correspond to either

residues L¹-R²⁸⁵ or K¹⁰⁷-R³⁹⁵ (Table 3-1). This tryptic fragment is consistent with L¹-R²⁸⁵ because it is recognized by an N-terminal antibody (F4C1) whose epitope is residues D³⁸-D⁴⁴ (data not shown). Interestingly, fragment L¹-R²⁸⁵ is more readily proteolyzed in the presence of V₂Rpp, as assessed by SDS-PAGE (Figure 5D), and two species are observed by MALDI-TOF MS with masses of 31920±41 and 32342±9 Da, respectively (Figure 5A, bottom spectrum). There are five candidate fragments for the 31 kDa species that occurs in the presence of V₂Rpp (Table I), which cannot be assigned; however, the most likely assignment of this fragment is residues G⁵-R²⁸⁵ because it represents further proteolysis of the already assigned 32 kDa species (L¹-R²⁸⁵). Figure 5C shows the location of R²⁸⁵ on the crystal structure of bovine β-arrestin1 (PDB code 1G4R).

Perhaps the most striking feature of our β-arrestin1 study is the rapid appearance of a 21 kDa species in the presence of V₂Rpp, which persists even up to two hours after digestion (Figure 3-3A, panel III) and the complete absence of a 25 kDa peak in the MALDI-TOF MS. MALDI-TOF analysis over the range *m/z* 20,000-30,000 revealed that there are in fact two species, with masses of 25 and 21 kDa, for β-arrestin1 alone or in the presence of V₂Rnp or V₂Rpp (Figure 3-5A, right panel). The 25 kDa species in all experiments is not visible by SDS-PAGE; however, this low abundance species is visible by MALDI-TOF analysis in the late time point (Figure 3-5A, right-hand spectra). Experimental masses for the 25 kDa species were determined to be 25742 ± 17 and 25736 ± 41 for β-arrestin1 alone or in the presence of V₂Rnp, respectively (Table 3-1). There are three candidate fragments (D²⁶-K²⁵⁰, V¹⁷¹-K⁴⁰⁰ and Q¹⁸⁹-R⁴¹⁸) for the 25 kDa species and it is visible by Western blot analysis and it is recognized by an N-terminal antibody, F4C1 (Table 3-1). Only one of the three candidate fragments is from the N-domain of β-arrestin1 and we have therefore assigned this fragment as residues D²⁶-K²⁵⁰.

Figure 3-5. MALDI-TOF spectra of β -arrestin1 tryptic fragments with either V₂Rnp or V₂Rpp.

(A) The MALDI-TOF spectra from two different time points, one early (5 min) and one late (60 min), are shown for β -arrestin1 in the presence of V₂Rnp or V₂Rpp (spectra of β -arrestin1 alone are identical to those in the presence of V₂Rnp and therefore not shown). Each peak is labeled with the mean molecular weight, standard deviation and corresponding residues as determined from at least five independent experiments. An internal standard, carbonic anhydrase, was used to correct the molecular weights for each collected spectrum and the peak for the standard is labeled "STD". Peaks that are not labeled or indicated with a dashed line represent doubly charged species. (B) An SDS-PAGE analysis of tryptic fragments. High molecular weight (>40 kDa) fragments are labeled on the gel. All species labeled in parts B and D are highlighted in the MALDI-TOF spectra in part A. (C) The structure of β -arrestin1 with important tryptic arginines to this study shown. The accessibility of residues 188, 285 and 393 changed upon addition of V₂Rpp. (D) An SDS-PAGE analysis of low molecular weight (<40 kDa) tryptic fragments important to this study.

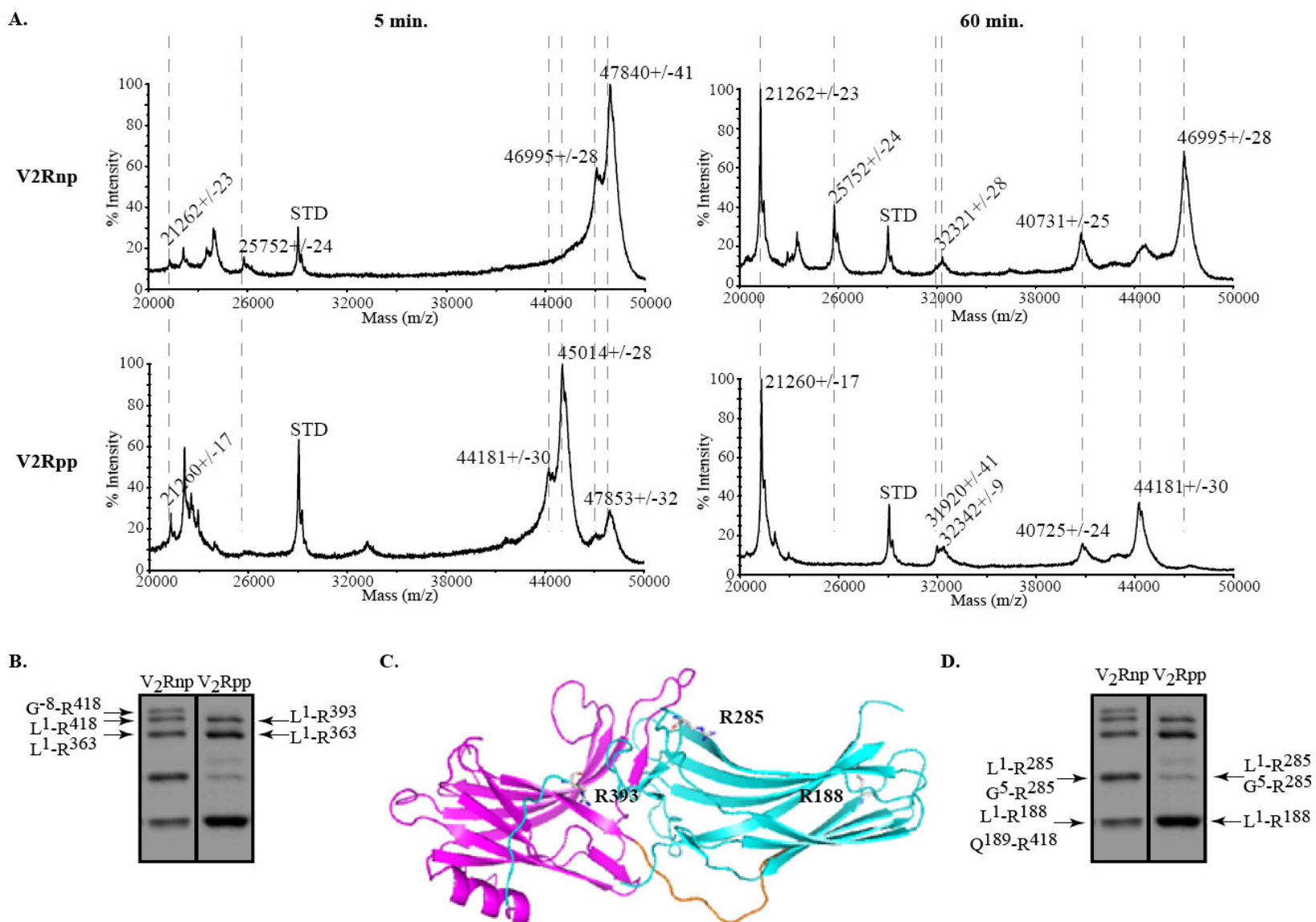


Figure 3-5: MALDI-TOF Spectra of β -arrestin1 Tryptic Fragments.

Functional consequences of conformational changes in β -arrestin1

To assess the functionality of our β -arrestin1:V2Rpp system and the biological ramifications of conformational changes induced in β -arrestin1, we tested β -arrestin's *in vitro* binding to clathrin (Figure 3-6). Clathrin was bound to Protein A beads through a monoclonal antibody that recognizes clathrin heavy chain and β -arrestin1 was then incubated with the clathrin beads (clathrin-protein A beads) either in the absence or presence of V2R peptides. We assessed β -arrestin1 binding to clathrin by Western blot analysis. Figure 3-6A indicates the input for each experiment. β -arrestin1 interacts weakly and non-specifically with empty protein A beads (Figure 3-6B, lane 1) and this low background binding is not altered by the addition of either clathrin-protein A beads or by the pre-incubation of β -arrestin1 with V2Rnp (Figure 3-6B, lanes 2 and 3). However, in the presence of V2Rpp, β -arrestin1 binding to clathrin-protein A beads is significantly enhanced (Figure 3-6B, lane 4). Figure 3-6C shows a Western blot for clathrin to ensure equal loading of clathrin for all experimental conditions tested. Quantitation of β -arrestin1 binding to either empty protein A beads or clathrin-protein A beads from five independent experiments is shown in Figure 3-6D. β -arrestin1 binding to clathrin-protein A beads is normalized to 100% and shows enhanced binding over β -arrestin1 in the presence of V2Rnp ($29.7 \pm 4.1\%$) or absence of ligand ($21.3 \pm 4.5\%$ for β -arrestin1 alone and $29.1 \pm 1.5\%$ for β -arrestin1 with clathrin).

Figure 3-7 depicts a model of β -arrestin1 activation upon binding V2Rpp. Release of β -arrestin's C-terminus promotes clathrin interaction and is evidenced by increased accessibility of R393. The two domains move relative to one another in response to V2Rpp which is indicated by increased accessibility of R285 and protection of the N-domain.

Figure 3-6. Enhancement of clathrin binding to β -arrestin1 in the presence of V₂Rpp. (A) The table indicates the reaction components for each lane. (B) The panel shows an immunoblot for β -arrestin1 to measure the amount of β -arrestin1 that bound to clathrin. (C) Each experiment was normalized by the amount of clathrin loaded per lane. This panel is an immunoblot of clathrin to show equal loading. (D) The graph is quantitation of five independent clathrin binding experiments. The mean and standard error of the mean (SEM) are indicated for each experimental condition. The background from an empty lane was subtracted from all values and the maximal signal (in the presence of V₂Rpp) was normalized as 100%.

A.

Protein A Beads	+	+	+	+	+
Ligand	-	-	V2Rnp	V2Rpp	-
Clathrin	-	+	+	+	+
β -arrestin1	+	+	+	+	-

B.

IB: β -arrestin1



C.

IB: Clathrin



D.

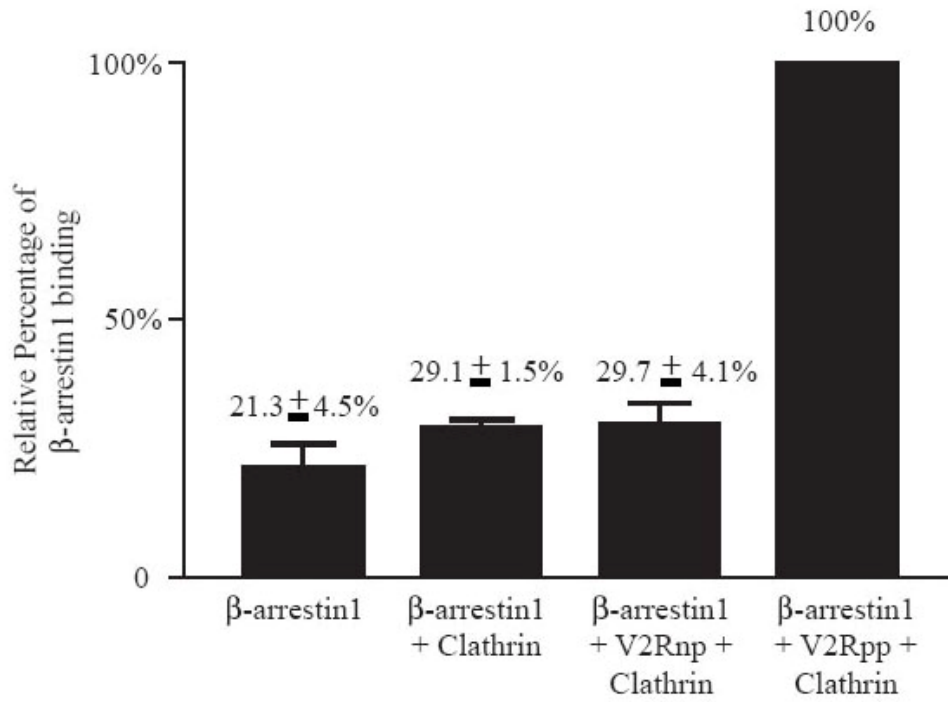


Figure 3-6: Enhancement of Clathrin Binding to β -arrestin1 in the Presence of V2Rpp.

Figure 3-7. Model of β -arrestin1 activation in the presence of V₂Rpp. β -arrestin1's N-domain is shown in blue while the C-domain is shown in green. The inactive conformation is shown on the right with β -arrestin1's polar core intact. Upon V₂Rpp binding, the two domains move relative to one another which causes the release of its C-terminus, as evidenced by enhanced accessibility of R393, and increased accessibility of R285 and R188 (1). Release of the C-terminus promotes clathrin binding (2). Adapted from K. Xiao, et al., *Activation-dependent Conformational Changes in β -arrestin2*. JBC, 2004, **279**(53): p. 55744-53.

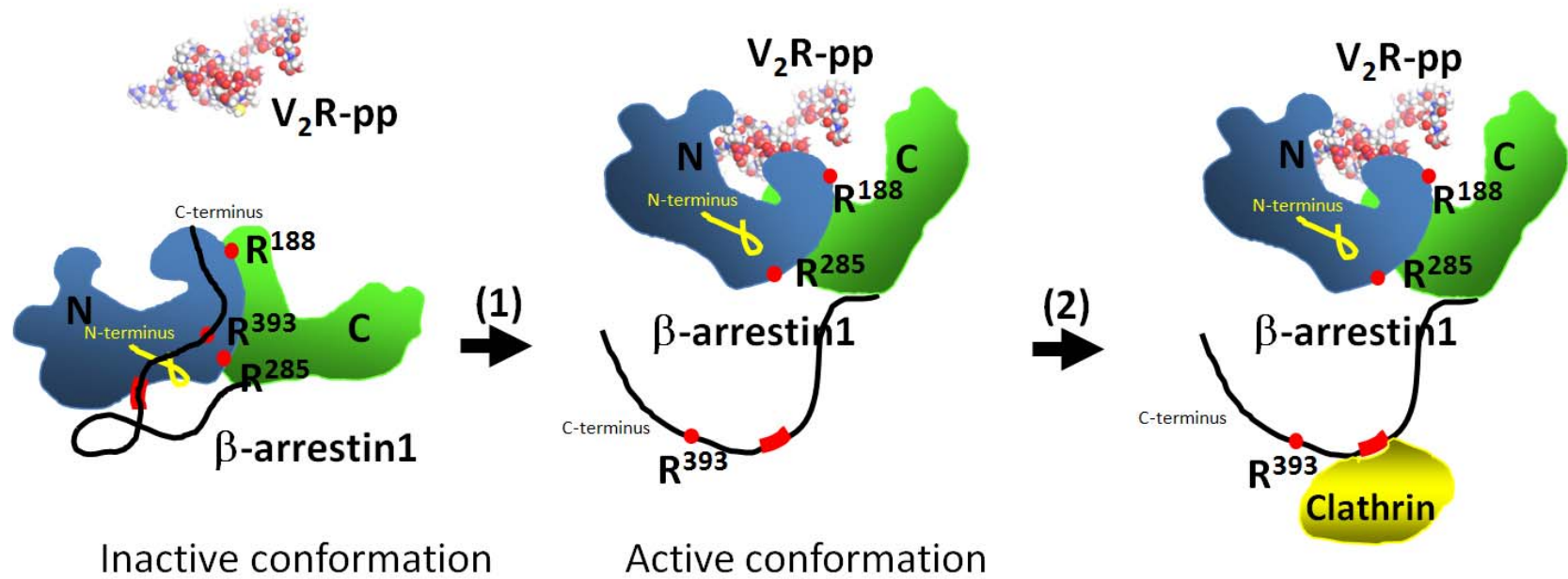


Figure 3-7: Model of β -arrestin1 activation in the presence of V₂Rpp.

Different V₂R Phosphorylation Patterns Induce Distinct Conformations of β -arrestin1

There are four ubiquitously expressed GRKs (2, 3, 5 and 6) that phosphorylate 7TMRs in response to agonist stimulation. Given the variety of cellular functions carried out by only two isoforms of β -arrestin, it is conceivable that the different GRKs phosphorylate distinct sites on the receptor which in turn induce different conformations of β -arrestin. We conducted limited trypsin proteolysis on β -arrestin1 in the presence of a V₂R peptide that contains only four phosphates (V₂R4p) (as described in Materials). β -arrestin1 was incubated in the presence of V₂Rnp, V₂Rpp or V₂R4p at a 5:1 molar ratio and then subjected to limited tryptic proteolysis. The proteolysis pattern observed for β -arrestin1 in the presence of V₂R4p is distinctly different than that observed with V₂Rpp (Figure 3-8 A). The accelerated proteolysis of β -arrestin1 with V₂Rpp which gives rise to a 45 kDa fragment does not occur with V₂R4p (compare panels II and III in Figure 3-8). However, the 21 kDa fragment (or N-domain) of β -arrestin1 is protected over time in the presence of V₂R4p as is similarly observed with V₂Rpp. These data taken together indicate a different and distinct conformation of β -arrestin1 in the presence of V₂R4p when compared to the conformation of β -arrestin1 in the presences of V₂Rpp.

Figure 3-8. Differentially phosphorylated V₂R peptides induce distinct β -arrestin1

conformations. (A) A time-course (0, 5, 30, 60 and 120 minutes) of limited tryptic proteolysis fragments, analyzed by SDS-PAGE, is shown for β -arrestin1 in the presence of V₂Rnp (panel I), β -arrestin1 in the presence of V₂Rpp (panel II) and β -arrestin1 in the presence of V₂R4p (panel III) which contains only four phosphates. The apparent molecular weights of the tryptic fragments by SDS-PAGE are indicated to the right of panel III. The tryptic fragments of β -arrestin1 in the presence of V₂R4p are different from those in the presence of either V₂Rnp or V₂Rpp. (B) A schematic representation of tryptic fragments for β -arrestin1. The control panel on the left is the pattern seen for limited tryptic digestion of β -arrestin1 alone or in the presence of V₂Rnp.

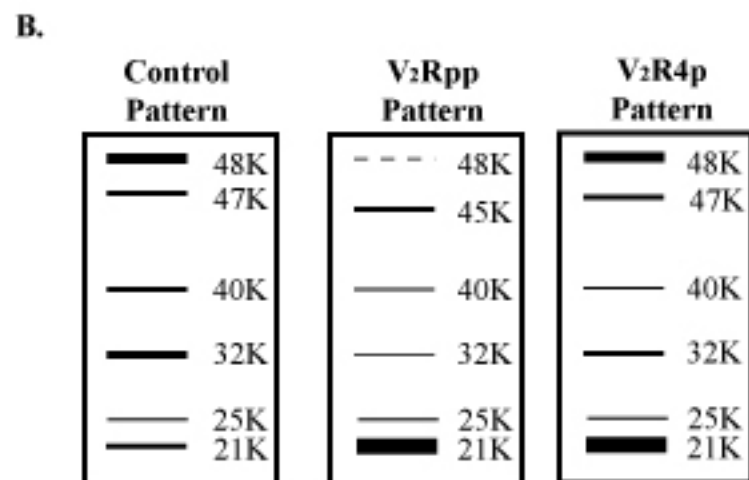
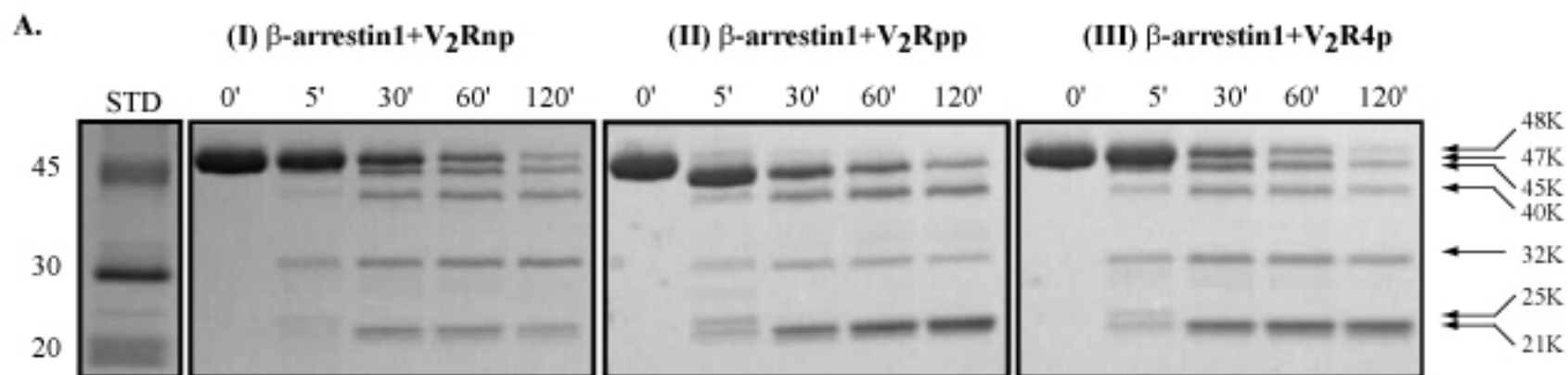


Figure 3-8: Differentially phosphorylated V2R peptides induce distinct β -arrestin1 conformations.

The “active” conformations of β -arrestin1 and 2 are different

A previous study from our laboratory reported conformational changes in β -arrestin2 upon its interaction with V₂Rpp [83]. However, this study did not include information on tryptic fragments below 30 kDa, which would exclude information on β -arrestin2's individual N- and C-domains. Thus, we conducted limited tryptic proteolysis on β -arrestin2 as described in Experimental Procedures in order to directly compare conformational differences between the two β -arrestin isoforms (Figure 3-9). Figure 3-9A shows a limited tryptic digestion of β -arrestin2 alone (Panel I), or β -arrestin2 in the presence of either V₂Rnp (Panel II) or V₂Rpp (Panel III). In the control situation (β -arrestin2 alone or in the presence of V₂Rnp), we see both tryptic fragments with apparent molecular weights of 25 and 21 kDa identical to those seen for β -arrestin1. For β -arrestin2, however, both the 25 and 21 kDa species are generated more slowly from the 42 kDa parent species and persist up to 2 hours post-digestion in the presence of V₂Rpp (Figure 3-4B, Panel II). We have verified via Western blot analysis with F4C1 (epitope is residues D³⁸-D⁴⁴) that both the 25 and 21 kDa species of β -arrestin2 are in fact N-domain fragments. Figure 3-9B shows a schematic representation of β -arrestin2 tryptic digestions either alone or in the presence of V₂Rpp (Panels I and II) and the representation of a β -arrestin1 digestion in the presence of V₂Rpp (Panel III). The major species present in all β -arrestin2 digestions is a 42 kDa species, which was previously reported as G⁻⁷-R³⁶⁴, and this species is significantly protected in the presence of V₂Rpp (Figure 3-9A, compare panels II and III). Residues G⁻⁷-R³⁶⁴ of β -arrestin2 includes both the N-domain and most of the C-domain; thus, in the presence of V₂Rpp, the majority of β -arrestin2 is protected over time with only the last 52 C-

terminal residues missing from this fragment. This is, however, not the case for β -arrestin1 as only the N-domain itself, L¹-R¹⁸⁸, is protected in the presence of V₂Rpp (Figure 3-9B, Panel III). These data suggest that the V₂Rpp-bound, or “active”, conformations of β -arrestins1 and 2 are different.

Figure 3-9. Conformational difference between β -arrestins1 and 2. (A) Limited tryptic proteolysis was performed on β -arrestin2 to assess changes in fragments below 30 kDa. Panels I through III show SDS-PAGE analysis of limited tryptic fragments of β -arrestin2 alone and in the presence of either V₂Rnp or V₂Rpp, respectively. Apparent molecular weights for tryptic fragments are shown to the right of panel III. (B) A schematic diagram of tryptic fragments from β -arrestin2 alone or in the presence of V₂Rnp (termed β -arrestin2 control panel) is shown in panel I. Schematic diagrams of tryptic fragments for β -arrestins2 and 1 in the presence of V₂Rpp are shown in panels II and III, respectively.

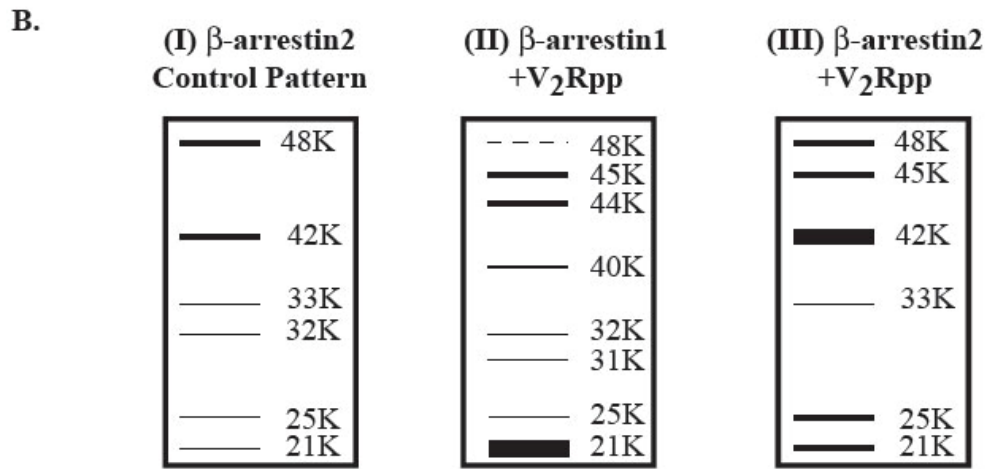
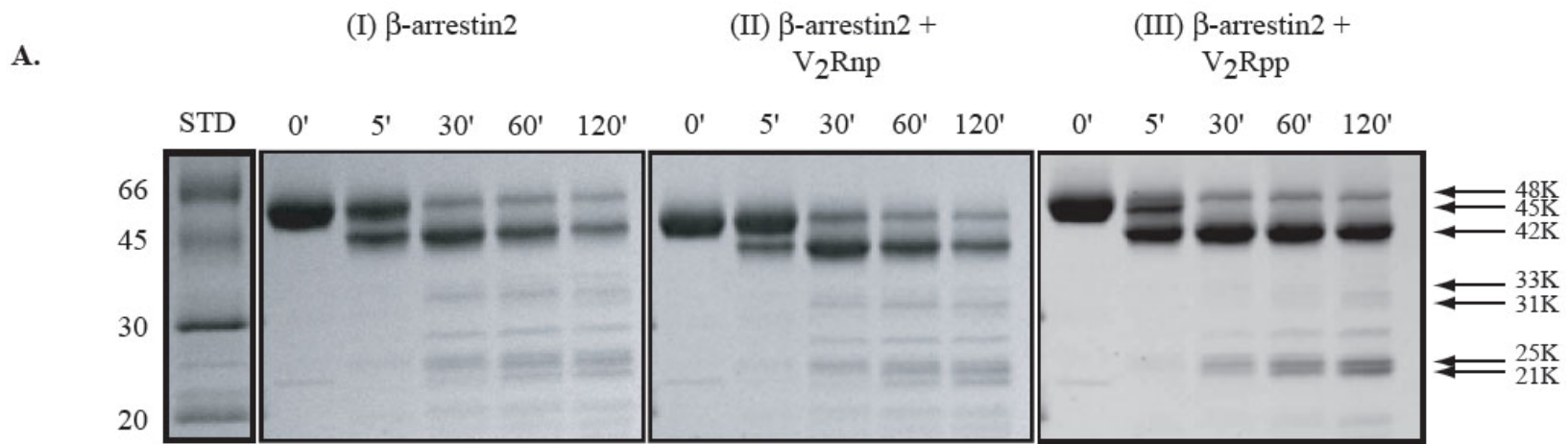


Figure 3-9: Conformational Differences Between β -arrestin1 and 2.

3.3 Discussion

β -arrestins, initially discovered for their role in terminating 7TMR signaling, have been shown more recently to interact with over a dozen nonreceptor partners and thereby serve as scaffolds for MAPK cascades initiating a second wave of signaling independently of G-proteins [54]. The majority of all β -arrestin functions are receptor activation-dependent, and the obvious corollary for this is that β -arrestins undergo a conformational change when bound to agonist-occupied 7TMRs. The solved crystal structure of β -arrestin1 shows that both the N and C termini are in close proximity in the overall fold of the molecule and that intramolecular interactions of these termini stabilize the basal conformation of the protein [53]. The C terminus of β -arrestin1 contains both clathrin- and AP2-binding sites, and the release of this terminus from the fulcrum of the molecule is required to expose these sites [62]. Clathrin and AP2 recruitment to 7TMRs via β -arrestin1 occurs only when 7TMRs are both active and phosphorylated, which demonstrates that β -arrestin1 must be in its active conformation for this now classical function. This study clearly demonstrates that, in the presence of V₂Rpp, both the N and C termini are more flexible and, furthermore, that the C terminus is released as evidenced by accessibility of the previously shielded Arg³⁹³ and enhanced clathrin binding.

The mechanism by which visual arrestins and β -arrestins interact with activated, phosphorylated 7TMRs has been studied through a series of mutagenesis and biochemical studies in addition to solved crystal structures [53, 83, 94-96, 98-100, 104, 107, 108, 110, 112-114, 123-125]. One of the most striking features of all arrestin structures is the presence of a distinctive polar core, a series of five interacting charges completely shielded from water and embedded at the center of the molecule. Disruption of this polar core is necessary for arrestin

activation, and we have demonstrated disruption of the polar core of β -arrestin1 in the presence of V₂Rpp by increased accessibility of Arg²⁸⁵. This residue is actually located in what is termed the “lariat loop” (Arg²⁸²-Gly³⁰⁹) region. The lariat loop, in part, maintains the basal conformation of β -arrestin because it contains Asp²⁹⁰, the primary counterion for Arg¹⁶⁹ in the polar core (Figure 3-1C). The primary sequence of the lariat loop is not conserved among the four mammalian arrestins; however, the secondary structure appears to be conserved in all solved crystal structures of arrestin family members to date [53, 94, 97, 99, 107]. Arg¹⁶⁹ of β -arrestin1 is the primary phosphate sensor because a charge reversal mutation (R169E) results in a phosphorylation-independent mutant. Our data represent the first direct biochemical evidence that “activation” of β -arrestin1 is dependent on both the disruption of the polar core of β -arrestin1 and thereby release of its C terminus to carry out functions such as clathrin binding.

Previous studies with both visual arrestin and β -arrestin1 have shown that the N-domain of the molecule contains the main phosphate sensor for phosphorylated 7TMRs (reviewed in [105]). These studies have localized the main sensor to a single residue, Arg¹⁶⁹. To date, only mutagenesis studies and structural activation models have been used to localize the phosphate sensor of β -arrestin. One of the most notable features of our β -arrestin1 limited tryptic proteolysis study is the rapid appearance and protection of a 21-kDa species in the presence of V₂Rpp. MALDI-TOF MS analysis of this tryptic fragment confirms that it is indeed the N-domain of β -arrestin1 (Leu¹-Arg¹⁸⁸), and this fragment persists even up to 2 h post-digestion, which indicates great stability of this domain when in complex with V₂Rpp. Although our study does not show direct biophysical evidence of V₂Rpp binding to the N-domain of β -arrestin1, our data are in accordance with previously published models based on

crystal structures indicating that the more flexible N-domain of β -arrestin1 is responsible for recognizing the phosphate elements of 7TMRs, whereas the more rigid C-domain most likely serves as a structural scaffold for β -arrestin1 binding partners [53]. The intact C-domain itself is never apparent as a separate entity once cleaved from the N-domain, which leads us to believe that a binding partner such as clathrin would be necessary to stabilize this domain and protect it from complete digestion. Our study represents the first direct evidence that the N-domain itself is in fact responsible for phosphate recognition.

One of the most valuable aspects of our *in vitro* model system is that it can be used to study conformational changes in β -arrestins with various phosphor-receptor peptides and can also be used to study conformational differences between β -arrestin1 and -2. Given the complexity of mechanisms carried out by only two isoforms of β -arrestin, it is conceivable that different GRKs phosphorylate distinct sites on 7TMRs which then instruct β -arrestin's conformation. We compared the limited tryptic fragments of β -arrestin1 in the presence of V₂Rpp, an eight phosphate containing peptide, to those of V₂R4p that contains only four sites of phosphorylation. The digestion patterns of β -arrestin1 are distinctly different with either V₂Rpp or V₂R4p. First, binding of V₂Rpp causes the release of β -arrestin1's C-terminus which gives rise to accelerated proteolysis and the appearance of a 45 kDa fragment corresponding to this C-terminus. The accelerated proteolysis of β -arrestin1's C-terminus is not observed in the presence of V₂R4p. However, both V₂Rpp and V₂R4p are capable of protecting β -arrestin1's N-domain as is evidenced by an increased amount of the 21 kDa species for up to two hours post-digestion. These data suggest that differentially phosphorylated peptides corresponding to the V₂R tail are

able to induce distinct conformations in β -arrestin1 which may be valuable tools for determining the molecular mechanisms of β -arrestin functions at the structural level.

Numerous crystal structures have been solved for β -arrestin1, but the crystal structure of β -arrestin2, however, remains elusive, so any information on structural differences between the two isoforms will have to be garnered from direct biochemical assays. Conformational changes in β -arrestin2 with V₂Rpp have been previously described from our laboratory [83]. Briefly, this study similarly demonstrated the release of the C terminus of β -arrestin2 from the fulcrum of the molecule by accessibility of Arg³⁹⁴ (homologous to Arg³⁹³ of β -arrestin1) and disruption of the polar core of β -arrestin2 by increased accessibility of Arg²⁸⁷ (homologous to Arg²⁸⁵ of β -arrestin1). This previous study, however, contained no information on the tryptic fragments of β -arrestin2 below 30 kDa, which would preclude any information of individual N- and C-domains of β -arrestin2.

Accordingly, we directly compared tryptic fragments below 30 kDa for both β -arrestin1 and -2 (Figure 3-9). The major protected species for β -arrestin1 is the N-domain (Leu¹-Arg¹⁸⁸), and the major protected species for β -arrestin2 is both the N- and C-domains (a 42-kDa species) corresponding to residues Gly⁷-Arg³⁶⁴. Although similar N-domain fragments are observed for β -arrestin2 (25- and 21-kDa species), they are not more rapidly generated nor protected over time in the presence of V₂Rpp. These data taken together suggest that although the overall activation mechanism is the same for β -arrestin1 and -2, the final conformations in the presence of V₂Rpp are in fact different. We first need to exclude two obvious explanations for the observed differences in the active conformations, namely stoichiometric differences in peptide

binding to the β -arrestins and primary sequence differences that would result in altered final conformations.

First, the stoichiometry of the binding of V₂Rpp to β -arrestin1 and -2 may be different. If, for example, β -arrestin2 were to bind two phosphopeptides, then it would make sense that both the N- and C-domains (Gly⁷-Arg³⁶⁴) are protected, whereas β -arrestin1 binding a single peptide would explain protection of only the N-domain (Leu¹-Arg¹⁸⁸). We have shown in this study, by limited proteolysis, that different molar ratios of V₂Rpp: β -arrestin1 do not alter the digestion pattern. A 1:1 molar ratio of V₂Rpp: β -arrestin1 is both necessary and sufficient to induce the observed conformational differences. Similarly, this same experiment in a previous study with β -arrestin2 demonstrated that increasing the molar ratio of V₂Rpp: β -arrestin2 did not alter the digestion pattern [83]. These data taken together suggest that a 1:1 molar ratio of V₂Rpp to either β -arrestin1 or -2 is sufficient to induce the active conformation. Moreover, we also performed native PAGE of β -arrestin1 and -2 in the presence of increasing amounts of V₂Rpp and have determined via a mobility shift that a 1:1 molar ratio of V₂Rpp: β -arrestin suffices for the same shift that we observe at a 5:1 molar ratio. These data indicate that the stoichiometry of binding for V₂Rpp to β -arrestin1 and -2 is in fact 1:1, and thus the conformational differences observed between the two isoforms is not because of a difference in the stoichiometry of peptide binding to the two β -arrestins.

Second, differences in the active conformation of β -arrestin1 and -2 could simply be due to differences in their primary sequences. Figure 3-2 shows the sequence alignment for recombinant rat β -arrestin1 and -2 used in this study. The two isoforms are 78% identical, and the two sequences are well conserved up to the residue numbered 340. We observed a 40-kDa

fragment in all β -arrestin1 digests that corresponds to residues Leu¹-Arg³⁶³. This fragment was protected in the early time points but was not the major protected species for β -arrestin1. In the case of β -arrestin2, cleavage was observed at Arg³⁶⁴ producing a 42-kDa fragment that was significantly protected over time in the presence of V₂Rpp. Although these two arginines in β -arrestin1 (Arg³⁶³) and β -arrestin2 (Arg³⁶⁴) do not align, we still see a somewhat similar pattern of digestion in this portion of their C termini. The striking difference, however, is that β -arrestin2 digests show significant protection of the 42-kDa species, whereas β -arrestin1 digests do not show as dramatic a protection of the corresponding 40-kDa species (Leu¹-Arg³⁶³). We do not believe that differences seen in the digestion patterns of β -arrestin1 and -2 are because of primary sequence differences, and therefore, we conclude that the observed differences are in fact because of conformational differences in the final fold of the two proteins.

Because the major product in β -arrestin1 digestions in the presence of V₂Rpp is Leu¹-Arg¹⁸⁸, we also inspected the sequence alignment of β -arrestin1 and -2 in this region (Figure 3-2). The sequence of β -arrestin1 and -2 containing Arg¹⁸⁸ and Arg¹⁸⁹, respectively, is just upstream of a flexible 12-residue interdomain hinge (*boxed* in Figure 3-2) that connects the N- and C-domains. The primary sequence of the hinge region is very well conserved, and Arg¹⁸⁸ of β -arrestin1 aligns perfectly with Arg¹⁸⁹ of β -arrestin2. We do see tryptic fragments in the digestion of β -arrestin2 with V₂Rpp that correspond to the N-domain, but these fragments are generated more slowly from the 42-kDa parent fragment and are only slightly protected over time. Conversely, in the digestion of β -arrestin1 with V₂Rpp, the N-domain is dramatically protected over time and persists up to 2 hours post-digestion. The protection of the hinge region tryptic residues in the final fold of β -arrestin2 makes this region, specifically Arg¹⁸⁹, less susceptible to

tryptic proteolysis. In summary, the major protected species for β -arrestin1 in the presence of V₂Rpp is the N-domain (Leu¹-Arg¹⁸⁸), whereas for β -arrestin2 it is both the N- and C-domains (Gly⁷-Arg³⁶⁴). These data suggest that the conserved hinge region becomes more accessible in β -arrestin1 (as evidenced by proteolysis at Arg¹⁸⁸) than β -arrestin2 because proteolysis at the corresponding Arg¹⁸⁹ is less rapid in the presence of V₂Rpp. This study shows, for the first time, that the flexibility of this hinge region is in fact different for the two β -arrestin isoforms. Moreover, other studies, including mutagenesis and solved crystal structures, have suggested that the two domains of β -arrestin move relative to one another upon binding 7TMRs, and this hinge region is responsible for the movement of the two domains [53, 94, 97, 99, 105, 107, 112, 113, 125]. Interestingly, successive shortening of the hinge region of the visual arrestin abolishes its ability to bind light-activated, phosphorylated rhodopsin [112]. We have evidenced here that this movement in β -arrestin1 and -2 is in fact different when bound to V₂Rpp.

Because structure dictates function, it follows that the two isoforms have different final conformations because evidence exists demonstrating that β -arrestins1 and -2 are functionally nonredundant, and such individual, nonoverlapping roles in 7TMR regulation are very compatible with distinct receptor-bound conformations. The first evidence to suggest that β -arrestins1 and -2 are in fact not functionally redundant lies in their differential binding to 7TMRs. 7TMRs are broadly broken down into two classes, class A and B [54]. Class A receptors, such as the β_2 AR, have a higher affinity for β -arrestin2 than β -arrestin1; however, the interaction of these 7TMRs with β -arrestin is transient in that internalization of class A receptors leads to dissociation of the β -arrestin-receptor complex. Class B receptors, such as the AT_{1a}R and V₂ vasopressin receptor, display equal affinity for both β -arrestin isoforms and form more stable

β -arrestin-receptor complexes. This preference for one isoform *versus* the other in receptor binding was the first evidence to suggest that β -arrestins do not serve redundant roles, but rather that the two isoforms have nonoverlapping, distinct functions.

In addition to differential receptor regulation, the two β -arrestin isoforms also display functional differences with nonreceptor partners. β -Arrestins are multiadaptor scaffold proteins that regulate 7TMR signaling, and multiple lines of recent evidence have shown that β -arrestins1 and -2 are also nonredundant in this function (reviewed in [56, 126]). Over a dozen nonreceptor partners have been shown to interact with β -arrestins, and the majority of these interactions occur in an agonist-dependent manner indicating that β -arrestins must be in the active or receptor-bound conformation to elicit these functions. The first evidence that β -arrestins play a role in 7TMR signaling stemmed from the discovery that β -arrestin1 specifically, and not β -arrestin2, interacts with c-Src, a nonreceptor tyrosine kinase [47, 74].

Studies following the discovery of the role of β -arrestin1 in c-Src recruitment and ERK activation led to what is now a newly appreciated paradigm, the idea that β -arrestins may in fact play a role in scaffolding MAPK cascades. In terms of ERK signaling, it appears as though different 7TMRs prefer one β -arrestin isoform over the other. In the case of the protease-activated 2 receptor, it has been demonstrated that agonist stimulation leads to complex formation containing receptor, β -arrestin1, Raf-1, and active ERK [74]. However, for angiotensin 1A receptor (AT_{1a}R) stimulation of ERK activation via β -arrestins, β -arrestin2 carries the signal, whereas β -arrestin1 actually functions antagonistically [77, 121]. It has also been recently reported that in some receptor systems such as the parathyroid hormone receptor (PTH1R), agonist stimulation of ERK through β -arrestin requires both isoforms [119]. Thus, in the case of

β -arrestin scaffolding of ERK via 7TMR stimulation, it appears as though different receptor systems, in general, display differential preference for either β -arrestin1 or -2, and in some cases both isoforms may be necessary. Although the ERK MAPK cascade has emerged as the prototypical β -arrestin scaffold function studied, it has also been demonstrated that β -arrestins directly scaffold the activation of JNK3 and possibly indirectly p38 activation, although these systems have not been studied to the same extent as the role of β -arrestins in ERK signaling [75, 122, 127, 128]. Nonetheless, the scaffolding of the JNK3 MAPK cascade has only been shown for β -arrestin2, yet again indicating isoform specificity and functional nonredundance for the β -arrestins. Additionally, β -arrestin1, but not β -arrestin2, has been shown to signal coordinately with $G\alpha_{q/11}$ to activate RhoA, a small G-protein, through $AT_{1a}R$ activation [116].

The different active conformations documented here for β -arrestins1 and -2 are thus consistent with numerous functional differences demonstrated by a multitude of studies. Furthermore, the differences in the conformational changes observed in both β -arrestins1 and -2 may in fact be due to differences in the flexibility of their interdomain hinge regions. This hypothesis could be easily tested by simply swapping the hinge regions of the two isoforms and determining if their functions in various systems are reversed.

Moreover, we demonstrate here, for the first time, that β -arrestin1 is able to adopt multiple conformations in the presence of differentially phosphorylated peptides. The model system used in this study provides an excellent means for determining conformational differences not only between β -arrestin1 and -2, but also in comparing the conformational differences that occur when β -arrestin1 and -2 are bound to phospho-receptor peptides from various 7TMRs or differentially phosphorylated 7TMR peptides. This study thus provides the first evidence to

suggest that β -arrestin's multifunctional properties may in fact be due to its ability to adopt multiple active conformations in response to differential 7TMR phosphorylation.

4. Distinct GRK Phosphorylation Sites on the β 2AR: A “Bar Code” Which Differentially Encodes β -arrestin Functions

4.1 Introduction

Phosphorylation of 7TMRs on their carboxyl termini and intracellular loops by GRKs is generally pre-requisite for β -arrestin binding [39]. In stark contrast to the multiplicity of 7TMRs, there are only seven members in the GRK family; and of those only GRKs 2, 3, 5 and 6 are ubiquitously expressed. Recent studies, using “loss of function” techniques such as siRNA to delete individual GRKs or combinations of GRKs, have suggested that distinct GRKs may contribute differently to the processes of receptor desensitization, endocytosis and signaling [84, 85]. Given that β -arrestins serve as multifunctional adaptors and signal transducers, it follows that the β -arrestins may be able to adopt multiple conformations in response to receptor phosphorylation which would impart different functions to the receptor-bound β -arrestin.

The *in vitro* studies conducted in Chapter 2 support the idea that β -arrestin is indeed capable of adopting multiple conformations and this finding in addition to studies with GRK siRNAs raises the provocative question of how receptor phosphorylation by different GRKs might enable distinct functions of β -arrestins. We hypothesized that the different GRKs might phosphorylate distinct sets of sites on the carboxyl terminus and/or internal loops of the receptor, thereby establishing a “bar code” which would then somehow instruct or determine the conformation assumed by the β -arrestin, which would in turn, determine its functional capabilities. In order to test this hypothesis, we set out to determine all the sites of agonist induced phosphorylation on the β 2AR; the GRKs responsible for phosphorylation of the

different sites; and the functional capabilities of β -arrestin bound in response to the different GRKs.

Whereas classical agonists stimulate both G protein-mediated and β -arrestin-mediated signaling mechanisms, “biased ligands” can selectively activate G protein or β -arrestin functions and thus elicit novel biological effects [81]. For example, carvedilol (Coreg®), a β -blocker was recently demonstrated to selectively stimulate β -arrestin-mediated signaling [82, 129]. Accordingly, we also sought to determine whether a β -arrestin biased ligand such as carvedilol might induce phosphorylation events distinct from those induced by an unbiased agonist such as isoproterenol.

4.2 Results

Silencing of either GRK2 and/or 6 impairs β 2AR desensitization

We initially set out to determine which GRKs empower which β -arrestin functions. We used a live cell biosensor, GloSensor, to monitor the level of G_s -dependent cAMP generation by β 2AR upon altering its phosphorylation pattern with GRK siRNAs [130]. Endogenous β 2ARs in GloSensor HEK293 stable cells were pre-stimulated with either vehicle (DMSO) or 100 nM isoproterenol for five minutes, then washed and re-challenged with isoproterenol in a dose-dependent manner. Figure 4-1A illustrates that this preincubation with isoproterenol induces a 50% loss of the maximal cAMP signal when re-challenged in cells transfected with control siRNA. Cells transfected with either GRK2, GRK6 or GRKs 2 and 6 siRNA show impairment of this desensitization shown in control cells (Fig. 4-1B, C and D, respectively).

We utilized the operational model of Black and Leff to analyze and fit these dose response curves and quantify desensitization [92]. Using this model, a parameter τ can be calculated according to the equation:

$$\tau = [R_0]/K_E$$

Where R_0 = active receptor and K_E =coupling efficiency. τ itself is a measure of the relative efficacy of receptors in stimulating adenylylate cyclase and the decline in τ after isoproterenol preincubation can be taken as a measure of receptor desensitization. The percent functionally active receptor is described as follows:

$$\% \text{ active receptor} = \frac{[R_0]_t}{[R_0]_{nt}} = \tau_t/\tau_{nt}$$

Where $\tau_{i=}$ values for isoproterenol treated β 2AR and $\tau_{nt=}$ values for DMSO treated β 2AR. This analysis revealed that the 50% reduction in the maximal cAMP signal and right shifted dose response curve observed with isoproterenol pre-stimulation for the control siRNA transfected cells corresponds to only 4% residual receptor activity or 96% desensitization (Figure 4-1A and E). In contrast, GRK2 or GRK6 siRNA-transfected cells show dramatically lesser degrees of receptor desensitization (Figure 4-1E). There was no further decrease in desensitization when both GRKs were knocked down together. Figure 4-1F shows quantification of data from at least six independent experiments in which GRK2, GRK6 or both were depleted by siRNA. Silencing of each GRK or the two in combination was typically 80% for each experiment presented and a representative immunoblot (IB) is shown.

It should be noted that in a previous study from our laboratory which also used HEK293 cells we reported that GRK6 was the primary GRK responsible for mediating β 2AR desensitization, as assessed from a quantitative analysis of real time cAMP dynamics [131]. However, the experimental approach utilized in the present work differs in a number of respects. These include the use of a preincubation/re-challenge protocol separated by a washing step versus continuous monitoring of cAMP levels in the earlier study. In addition, there are significant differences in assay methodology: isoproterenol concentrations; the presence or absence of PKA inhibitors in cellular incubations; monitoring in different time frames; and different cAMP biosensors which display different kinetics. Thus the two experimental approaches are likely monitoring somewhat different patterns of cellular desensitization with different contributions by the two GRKs.

Figure 4-1: Desensitization of the β_2 AR after GRK2, 6 or 2&6 siRNA treatment. HEK293 cells stably expressing the GloSensor reporter and transfected with either control (A), GRK2 (B), GRK6 (C) or GRKs 2 and 6 siRNAs (D) were pretreated with 100 nM isoproterenol for 5 minutes, washed 2-3 times over ten minutes and then assayed for cAMP accumulation after re-stimulation with isoproterenol at the indicated concentrations (10^{-9} to 10^{-4}). (E) Tau (τ) analysis of the desensitization data shown in A-D. All data shown are the mean \pm SEM for four independent experiments. ***, $P < 0.001$; **, $P < 0.01$ between control versus either GRK2-, GRK6- or GRK2+6-siRNA transfected cells. (F) A representative immunoblot (IB) for silencing of GRK2, GRK6 or both in conjunction demonstrates the siRNA transfection efficiency. Quantification (S.E. \pm SEM) of at least six independent siRNA transfections used for various experiment types is shown.

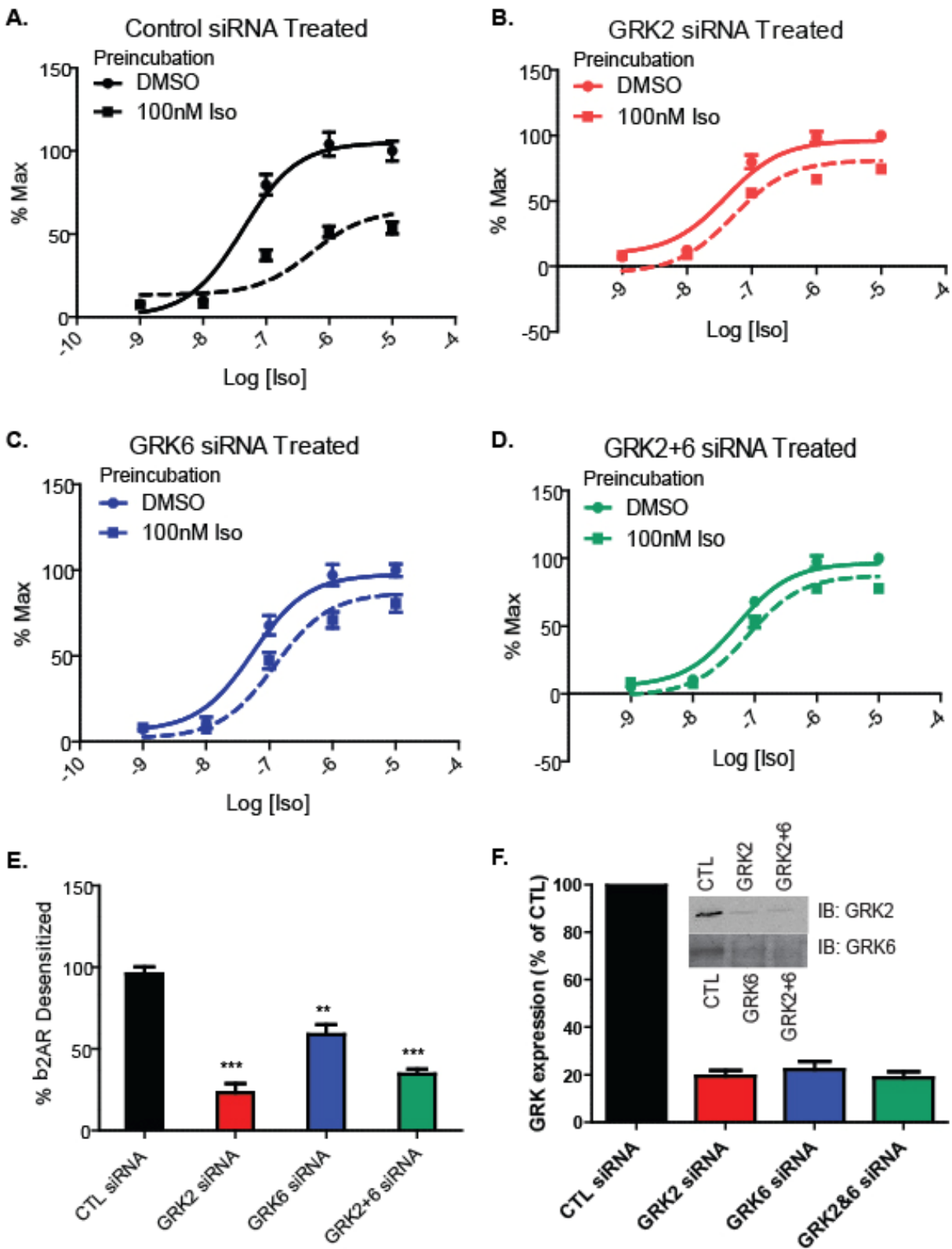


Figure 4-1: Desensitization of the β 2AR After GRK2, 6 or 2+6 siRNA Treatment.

Internalization of the β 2AR is inhibited by knocking down GRK 2 or 6 expression

Previous studies have demonstrated that β -arrestins scaffold elements of the endocytic machinery such as AP-2 and clathrin, which target agonist activated 7TMRs to clathrin coated pits for internalization [73]. Accordingly, we studied the internalization patterns of the receptor after depletion of either GRK2 or GRK6 alone or in combination. In control siRNA-transfected cells, stimulation with 10 μ M isoproterenol led to rapid internalization with a maximum of 50% of the β 2AR being internalized by thirty minutes (Figure 4-2A, black). Depletion of GRK2 slowed the initial rate of internalization and dramatically reduced the maximum internalization to 20% (Figure 4-2A, red). GRK6 siRNA treatment also slowed the initial rate of β 2AR internalization and significantly lowered maximum internalization (to 35%) but less dramatically than observed for GRK2 depletion (Figure 4-2A, blue). Ablation of both GRKs 2 and 6 together almost completely blocked receptor internalization (Figure 4- 2A, green).

Effects of GRK siRNA on β 2AR-stimulated pERK

Previous studies have demonstrated that the β 2AR can signal to ERK via a β -arrestin dependent pathway in response to either isoproterenol or carvedilol stimulation [78, 82]. However, these studies have not assessed how receptor phosphorylation regulates β -arrestin-mediated signaling to ERK. To test whether GRK2 or 6 can specifically promote β -arrestin mediated ERK activation through the β 2AR, we stimulated HEK293 cells stably expressing the β 2AR with either isoproterenol or carvedilol after they had been treated with GRK-specific siRNAs (Figure 4-2B and C, respectively). We followed the time course of activation to determine the effects of silencing the GRKs. Previously we have shown that after isoproterenol

stimulation, G-protein-mediated ERK activation peaks at early time points; e.g. two to five minutes whereas β -arrestin-dependent ERK activation peaks at late times e.g. fifteen minutes [78]. In isoproterenol-stimulated, control siRNA-transfected cells, ERK1/2 activation was robust at the five minute time point (typically 14-fold over basal) while the fifteen minute time point showed a lesser amount of ERK1/2 activation (4-fold over basal) (Figure 4-2B; black bars). Carvedilol stimulation in control siRNA-transfected cells led to lesser degrees of ERK activation (Figure 4-2C; black bars) (note different ordinate scale).

GRK2 depletion by siRNA tended to increase ERK activation stimulated by isoproterenol or carvedilol (Figure 4-2B and C; red bars). In stark contrast, GRK6-siRNA transfected cells stimulated with either isoproterenol or carvedilol showed significantly less ERK1/2 activation at the fifteen minute time point when compared with control-siRNA transfected cells (Figure 4-2B and C; blue bars). These results demonstrate that GRK6-mediated phosphorylation of the receptor is a crucial step for β -arrestin-dependent ERK activation.

Figure 4-2: The Roles of GRK2 and 6 in β 2AR Internalization and ERK activation. (A) Effect of control (CTL, black), GRK2 (red), GRK6 (blue) or GRKs 2 and 6 together (green) on the internalization of the β 2AR. Internalization was determined using ^3H -CGP and ICI as described under Materials and Methods. The percent receptor internalized is expressed as a loss of ^3H -CGP binding and the values represent the mean \pm SEM from at least three independent experiments. Statistical comparison of the curves was determined by using two-way ANOVA between GRK siRNA-transfected cells and control cells (***, $P < 0.001$). (B) and (C) Effects of siRNA-attenuated expression of GRKs 2 and 6 on β 2AR-mediated ERK activation upon stimulation with isoproterenol or carvedilol, respectively. siRNA-transfected cells stably expressing the β 2AR were serum starved and then stimulated with either 10 μM isoproterenol (B) or 10 μM carvedilol (C) at 37°C for the indicated time points. Both phospho-ERK (pERK) and total ERK (tERK) were visualized (lower panel) and quantified (upper panel) as described under “Materials and Methods.” Values are expressed as the percent of phosphorylation of ERK1/2 obtained at the 5 minutes stimulation in control (CTL) siRNA-transfected cells. Data represent the mean \pm SEM from at least three independent experiments. Statistical significance was determined by using a one-way ANOVA with Bonferroni’s post-test to correct for multiple comparisons between each GRK siRNA-transfected and control transfected cells (**, $P < 0.01$; *, $P < 0.05$).

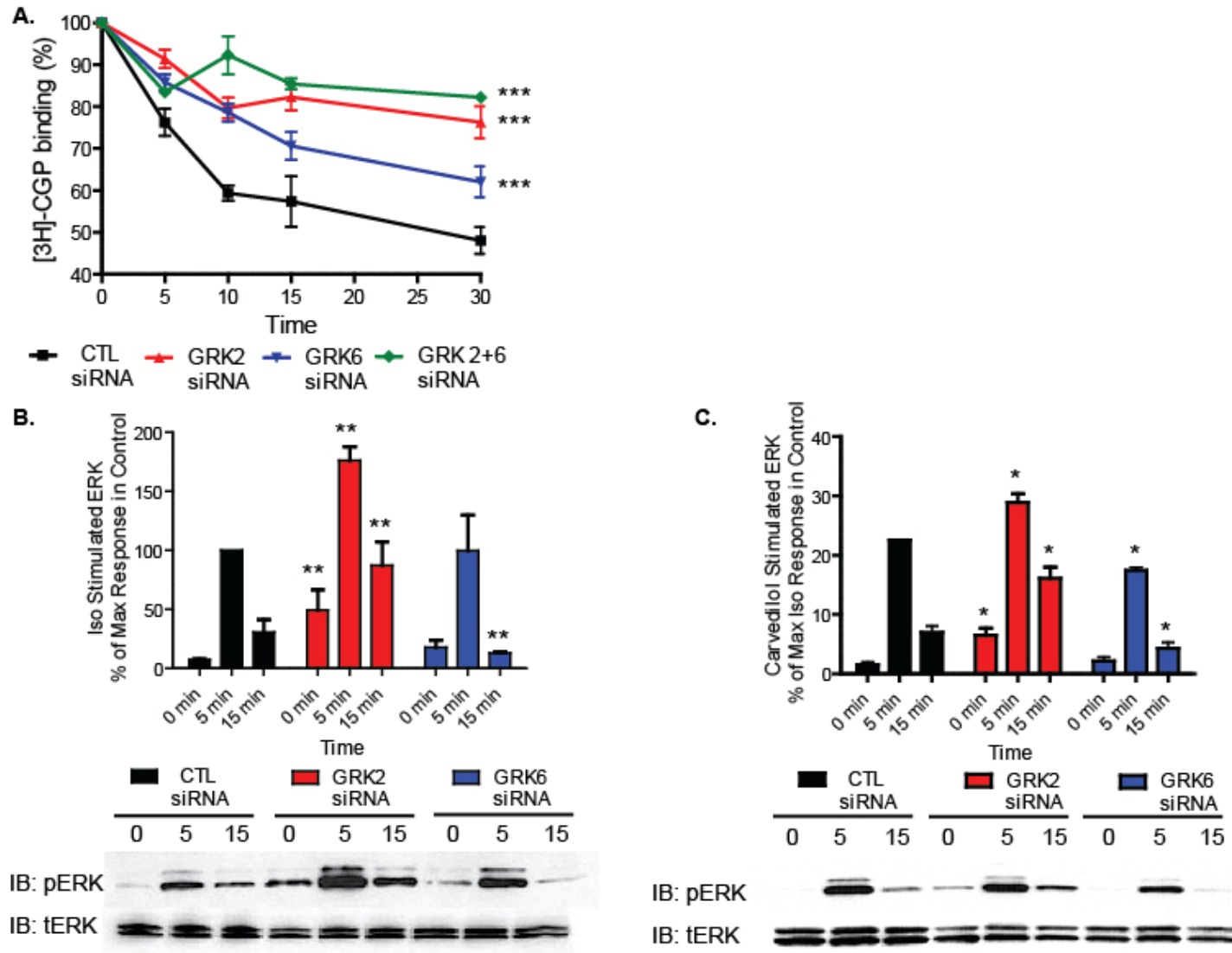


Figure 4-2: The Roles of GRK2 and 6 in β 2AR Internalization and ERK Activation.

GRK2 and 6 Phosphorylation Dictate β -arrestin2 Conformation

To test the hypothesis that phosphorylation of the β 2AR, mediated by either GRK2 or GRK6, can elicit distinct conformations of β -arrestin, we used a bioluminescence resonance energy transfer (BRET)-based biosensor of β -arrestin2 [86, 93]. In this biosensor, the N-terminus of β -arrestin2 is fused to bioluminescent Renilla luciferase (RLuc) while the C-terminus is fused to yellow fluorescent protein (YFP) (Figure 4-3). Previously published data from our laboratory showed that biased ligands and mutant receptors capable of inducing only β -arrestin-mediated signaling display directionally opposite changes in BRET signals when compared to classical agonists and wild type receptors [93]. In the present study, HEK293 cells transiently co-expressing the β 2AR and the β -arrestin2 BRET biosensor (RLuc- β -arr-YFP) were stimulated with 10 μ M isoproterenol after treatment with GRK-specific siRNAs (Figure 4-4A).

Isoproterenol stimulation of control-siRNA transfected cells results in an increase in the intramolecular BRET as we have observed before, which is indicative of a conformational change in β -arrestin2 upon recruitment to the β 2AR (Figure 4-4A CTL siRNA). In stark contrast, however, isoproterenol stimulation of β 2AR after GRK2 siRNA treatment leads to a decrease in intramolecular BRET (Figure 4-4A GRK2 siRNA, red), indicating a different conformation of β -arrestin in the GRK2-siRNA transfected cells compared to that in the CTL-siRNA transfected cells. Interestingly, GRK6-siRNA transfected cells showed no significant change in the BRET signal (Figure 4-4A GRK6 siRNA, blue), suggesting that the β -arrestin conformation in the GRK6-siRNA transfected cells is different from that in either CTL- or GRK2-siRNA transfected cells. The differences in intramolecular BRET signals seen here with CTL-, GRK2- or GRK6-siRNA treatment, indicate that β -arrestin is adopting unique

conformations in all three cases and, taken together, suggest, that phosphorylation on the β 2AR by the two different GRKs results in distinct β -arrestin conformations.

It should be noted that one mechanism by which GRK siRNA treatment could alter the BRET signals is by reducing the amount of β -arrestin recruited to the receptor. Previously published data from our laboratory has indicated that silencing of individual GRKs in HEK293 cells reduces only the rate but not the extent of β -arrestin recruitment as assessed by fluorescence resonance energy transfer (FRET) [131]. However, to confirm this, we tested β -arrestin recruitment via cross-linking to the receptor under the exact experimental conditions used in all of the biological assays presented in this study (eg. 10 μ M isoproterenol stimulation at fifteen minutes). As shown in Figure 4-3B, β -arrestin recruitment is equivalent in CTL-, GRK2- and GRK6-siRNA transfected cells.

Figure 4- 3: BRET-Based Biosensor of β -arrestin2. The N-terminus of β -arrestin2 is fused to the bioluminescent Renilla luciferase (shown in turquoise) while the C-terminus is fused to yellow fluorescent protein (YFP) (shown in yellow). Luminescence of the RLuc substrate causes excitation and emission of the YFP or resonance energy transfer. By monitoring emission at both the RLuc substrate and YFP wavelengths, a ratio of RLuc to YFP is calculated and a change in this ratio demonstrates a conformational change in β -arrestin2. Adapted from A. K. Shukla et al., *Distinct Conformational Changes in Beta-arrestin Report Biased Agonism at Seven Transmembrane Receptors*. PNAS, 2008. **105**(29): p. 9988-93.

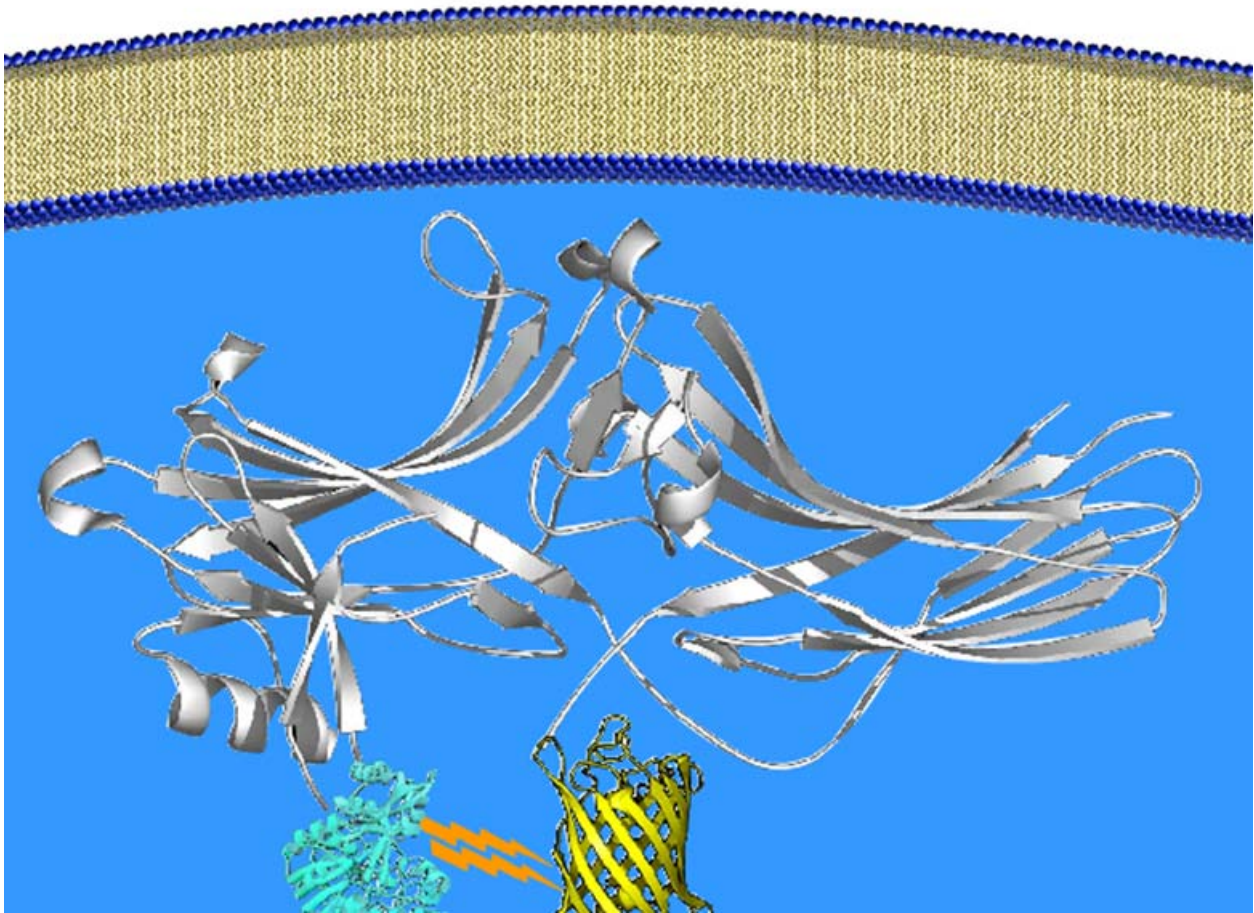
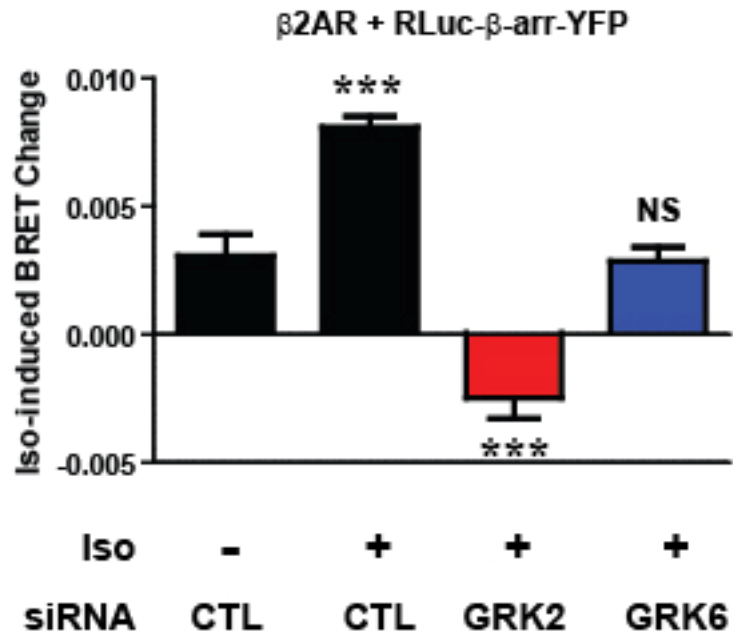


Figure 4-3: β -arrestin2 BRET Biosensor.

Figure 4- 4: β 2AR Phosphorylation Dictates β -arrestin Conformation. (A) HEK293 cells overexpressing β 2AR and β -arrestin2 BRET biosensor (β 2AR + RLuc- β -arr-YFP) were transfected with either control (CTL), GRK2 or GRK6 siRNAs. Changes in intramolecular BRET upon stimulation of β 2AR by isoproterenol (10 μ M for 15 minutes) were measured. Data are the mean \pm SEM of six independent experiments, each performed in quadruplicate. ***, $P < 0.001$; NS, not significant between basal and stimulated conditions as determined by one-way ANOVA with Bonferroni's post-test. (B) The extent of β -arrestin recruitment to β 2AR is unaffected by GRK2 or 6 siRNA treatment. Immunoprecipitation of stably expressed FLAG- β 2AR and Western blot analysis shows agonist-induced β -arrestin association after 15 minutes stimulation with 10 μ M isoproterenol. Treatment with either GRK2- or GRK6-siRNA does not significantly impair this association. Data shown are the mean \pm SEM from three independent experiments. One-way ANOVA and Bonferonni post-test indicated no significant difference between the groups of data when compared to control (CTL).

A.



B.

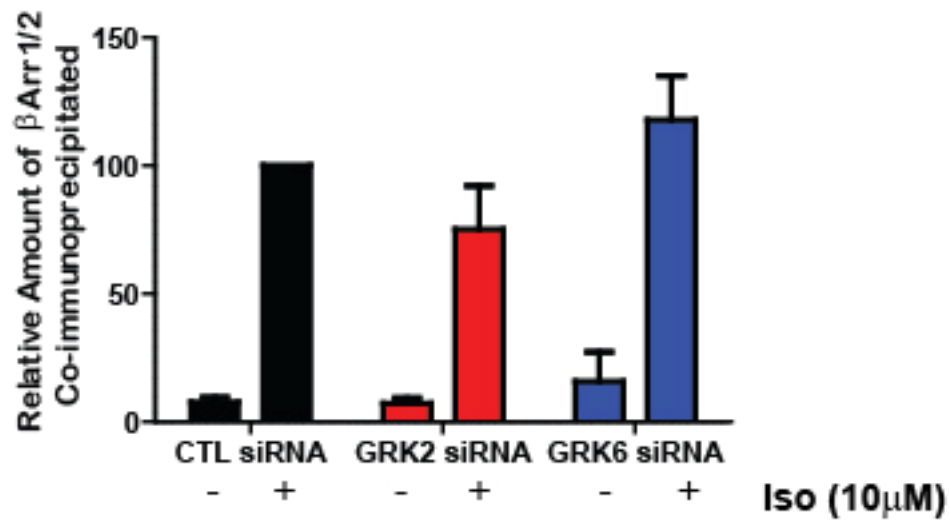


Figure 4-4: β 2AR Phosphorylation Dictates Distinct β -arrestin Conformations.

Identification of Thirteen Phosphorylation Sites on the β 2AR by Mass Spectrometry

To determine if GRKs 2 and 6 target distinct sites, we characterized the phosphorylation sites on the β 2AR by a mass spectrometry (MS)-based proteomic approach (Figure 4-5). A stable isotope labeling with amino acids in cell culture (SILAC) strategy [132] was used to detect the differences in relative levels of phosphorylation (Figure 4-5, I). Receptors were isolated from HEK293 cells stably expressing human β 2AR incubated with or without isoproterenol. Purified β 2ARs (Figure 4-5, SDS-PAGE insert) were digested and phosphopeptides were enriched by immobilized metal ion affinity chromatography (IMAC) [133] (Figure 4-5, II-IV) and then analyzed by online liquid chromatography/tandem mass spectrometry (LC/MS/MS) (Figure 4-5, V). Panels A, B, D and E of figure 4-6 show an example of raw MS/MS data obtained for the phosphorylation of S246. The phosphorylation level at this site decreased by 50% upon isoproterenol stimulation and we confirmed this dephosphorylation event using a specific phosphopeptide antibody (Figure 4-6C and F). In summary, we identified 13 phosphorylation sites (S246, S261, S262, S345, S346, S355, S356, T360, S364, S396, S401, S407 and S411) on the β 2AR. Upon isoproterenol stimulation, the phosphorylation of these sites increased 10- to more than 300-fold and these results are summarized in Figure 4-7.

Figure 4-5: β_2 AR phosphorylation analysis by MS-based quantitative proteomics.

Quantitative β_2 AR phosphorylation analysis involves receptor purification, digestion, phosphopeptide enrichment and LC-ESI/MS/MS analysis (II-V). Briefly, HEK293 cells stably expressing human β_2 AR were cultured using a stable isotope labeling with amino acids in cell culture (SILAC) strategy to prepare receptor samples for subsequent MS-based proteomics (I). For quantitative analysis of phosphorylation levels of each site before and after isoproterenol stimulation, “light” labeled cells were treated with (+) 10 μ M isoproterenol or carvedilol for 5 minutes, and “heavy” labeled cells served as controls without (-) agonist treatment, or vice versa. For quantitative analysis of phosphorylation levels of each site when individual GRKs were depleted from cells, “light” cells were treated with GRK2 or 6 siRNA and “heavy” cells were treated with control siRNA, or vice versa. In the presence of GRK siRNA, both “heavy” and “light” cells were treated with 10 μ M isoproterenol for 5 minutes and subsequently mixed at a 1:1 ratio. The β_2 ARs were purified from the mixed “heavy” and “light” cells using an alprenolol-agarose affinity purification procedure (step II). Purified β_2 ARs were digested by trypsin in-solution (step III). Phosphopeptides were enriched by IMAC (step IV) and were analyzed by online liquid chromatography/tandem mass spectrometry (LC/MS/MS) (step V and VI). Details are described in chapter two. The insert shows a representative Coomassie stained SDS-PAGE gel of the purified β_2 AR. The position of the receptor is indicated by the molecular weights (kDa) of protein standards (Std).

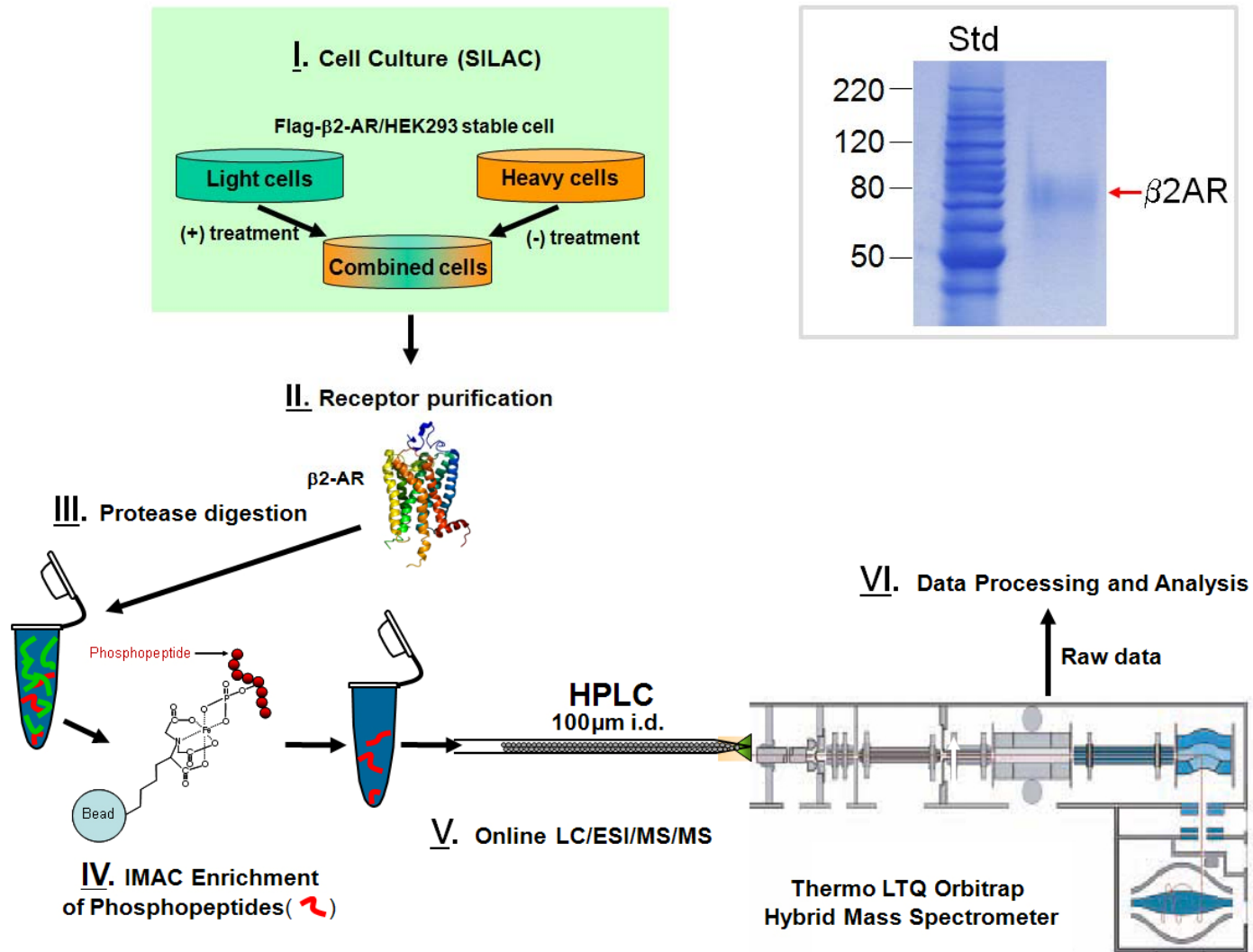


Figure 4-5: β 2AR Phosphorylation Analysis by MS-Based Quantitative Proteomics.

Figure 4-6: Dephosphorylation of β 2AR Ser246 by isoproterenol stimulation.

Phosphorylation of S246 on β 2AR was used as an example to demonstrate how the quantitative analyses were performed. The upper panels (A, B and C) show the quantification procedure for a tryptic non-phosphopeptide FHVQNLSQVEQDGR of β 2-AR and the lower panels (D, E and F) show that for the corresponding phosphopeptide FHVQNL_pSQVEQDGR. A) and D) present the annotated MS/MS fragmentation spectra for the “light” versions of the nonphosphopeptide and phosphopeptide, respectively. The peptide sequences are shown at the top of the MS/MS spectra with phosphorylated residues highlighted in red. The identified fragmentation y (red color) and b (blue color) ions are indicated. B) and E) are the expanded MS spectrum sections showing two isotope envelopes (peaks) corresponding to “light” and “heavy” forms of the unfragmented nonphosphopeptide and phosphopeptide, respectively. The “light” peaks (labeled with red color) represent the peptide from the agonist stimulated sample, whereas “heavy” peaks (labeled with blue color) represent those from the nonstimulated sample. C) and F) show the extracted ion chromatograms for the nonphosphopeptide and phosphopeptide, respectively. The area under the curve (AUC) was used for calculating the relative abundance of the “light” and “heavy” forms of a phosphopeptide. H/L, heavy to light ratio. Below the extracted ion chromatograms are Western-blot results using antibodies generated using the corresponding peptides.

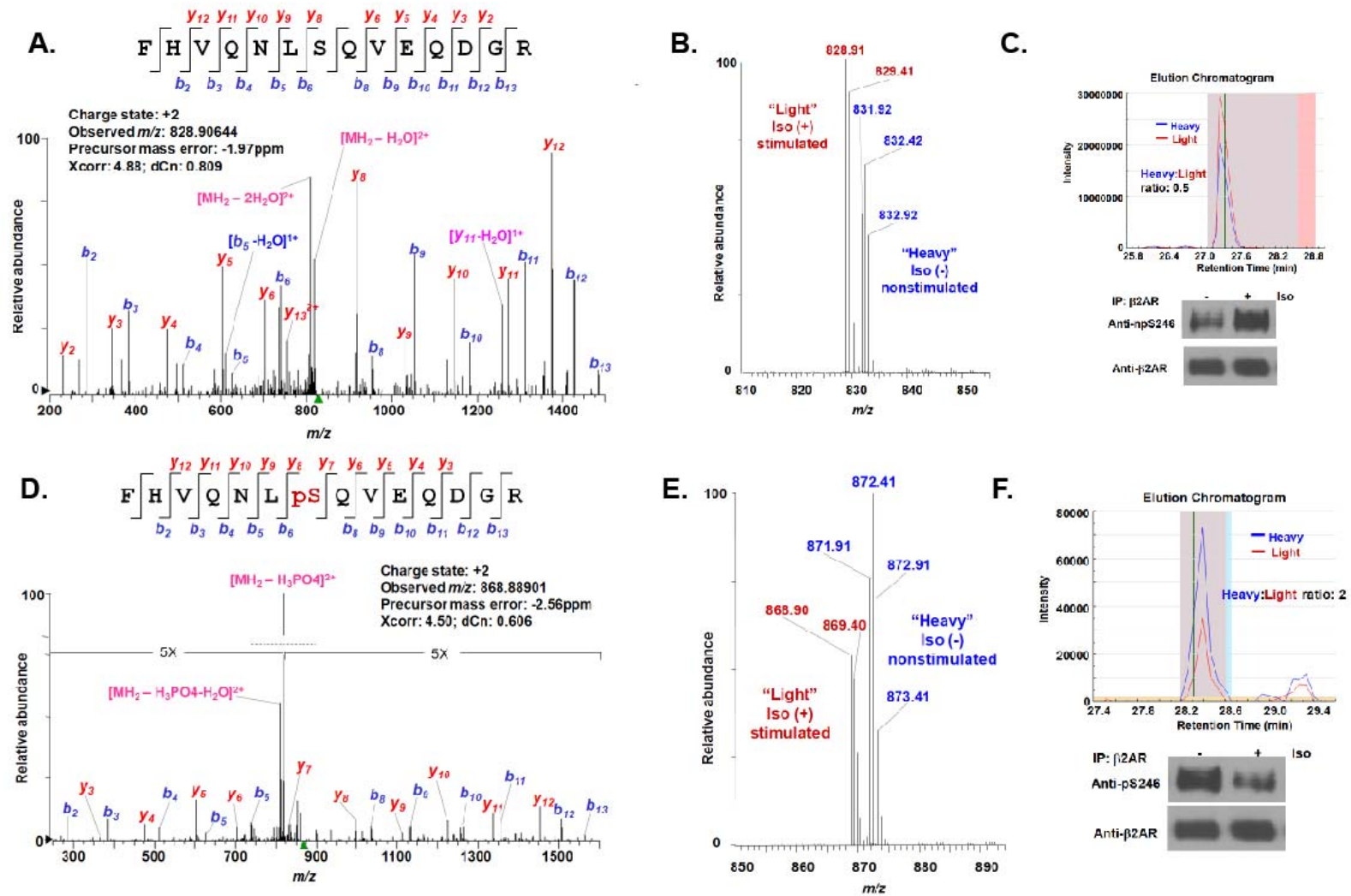
Figure 4-6: Dephosphorylation of β 2AR Ser246 by Isoproterenol Stimulation.

Figure 4-7: Quantitative mass spectrometry analysis of stimulated β_2 AR phosphorylation.

Profiling of phosphorylation changes in the β_2 AR upon isoproterenol or carvedilol treatment by LC/MS/MS in combination with SILAC. The 13 phosphorylation sites identified are presented as filled circles. The fold changes in phosphorylation are indicated for a phosphorylated residue or a cluster of residues (in the dashed line box). Carvedilol stimulation only induces significant changes in the phosphorylation levels at S355/S356. S246 is the only site whose phosphorylation decreased upon isoproterenol stimulation.

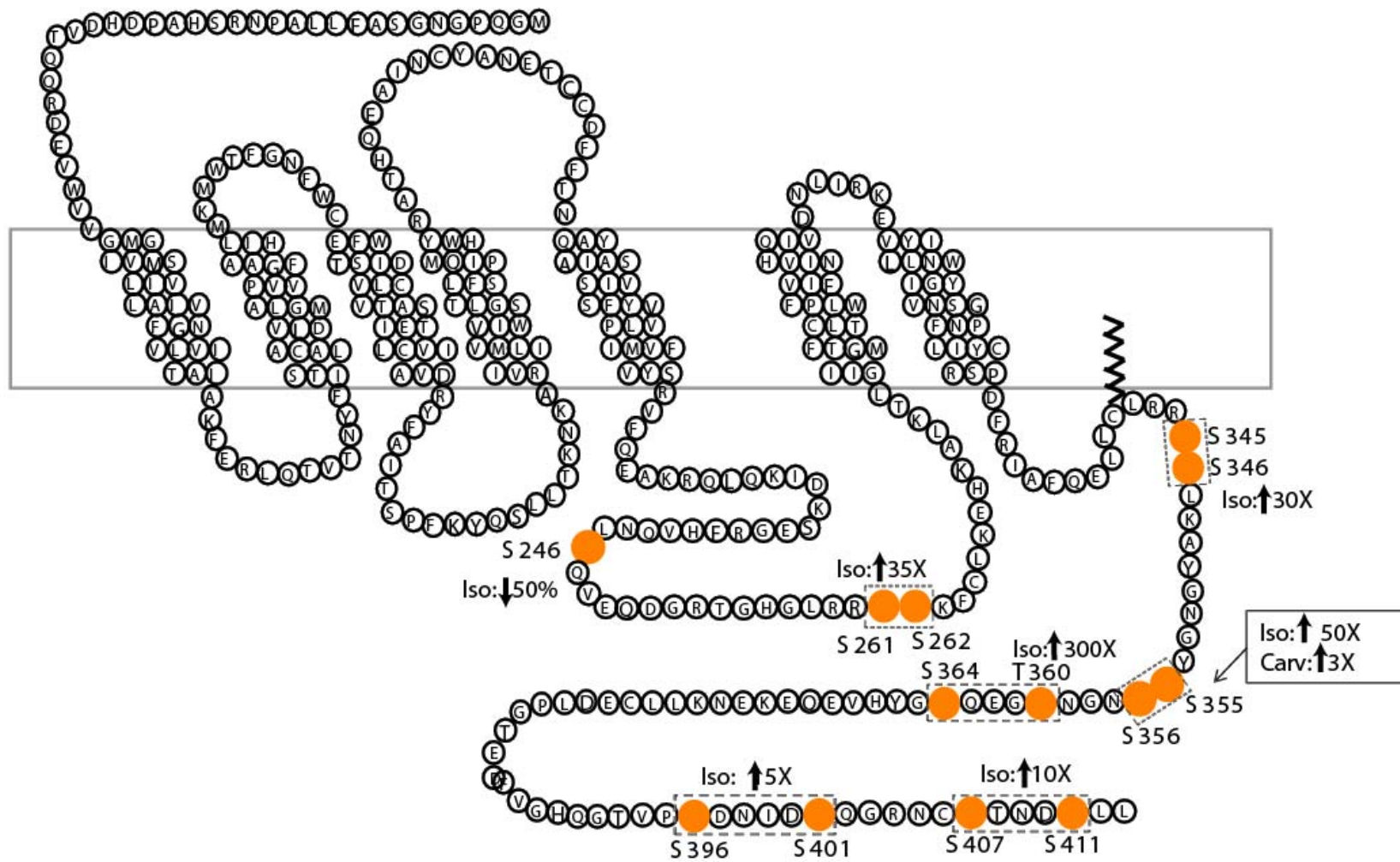


Figure 4-7: Quantitative MS Analysis of Stimulated β_2 AR Phosphorylation.

Mapping GRK2 and GRK6 phosphorylation sites on the β 2AR

Evidence from the literature suggests that 7TMRs use specific GRKs, or subsets thereof, and that this specificity is dictated not only by receptor type but also cell type [131]. Since our previous studies indicated that, in HEK293 cells, only GRK2 and 6 significantly regulate β -arrestin2 recruitment to the β 2AR (the preferred isoform for this receptor), we have focused this study on these two GRKs [131]. To determine the phosphorylation sites on the β 2AR for which GRK2 and 6 are responsible, we used RNAi technology to silence expression of these kinases individually from cells and then used SILAC to quantitatively measure the extent of phosphorylation of each site on the β 2AR when GRK2 or 6 was depleted.

We found that depletion of GRK6 specifically reduced isoproterenol-promoted phosphorylation of S355 and S356 five-fold (Figure 4-8). Depletion of GRK2 reduced the phosphorylation of T360, S364, S396, S401, S407 and S411 by 2- to 3-fold (Figure 4-8). The extents of phosphorylation of S261, S262, S345 and S346 did not significantly change when either GRK2 or 6 was depleted from cells. Based on these findings, we conclude that GRK2 is mainly responsible for phosphorylation of T360, S364, S396, S401, S407 and S411 and GRK6 is responsible for phosphorylation of S355 and S356 upon agonist stimulation (Figure 4-8). Also as shown in Figure 4-8, S261/S262 and S345/S346 are previously reported consensus sites for PKA. S246 is a consensus site for ATM phosphorylation and has been previously identified.

GRK 2 and 6 expression levels alter phosphorylation of the β 2AR serines 355 and 356

Panels A and B in figure 4-9 show the raw MS/MS data for the peptide containing phospho-S355 and -S356 and demonstrates that silencing of either GRK influences

Figure 4-8: GRK2 and 6 phosphorylate different sites on β_2 AR. GRK2 and GRK6 phosphorylation sites **were mapped** on the β_2 AR using both RNAi technology and a quantitative MS-based proteomic approach. GRKs responsible for phosphorylation of individual residues were determined by knocking down their expression by siRNA treatment and determining effects on the extent of phosphorylation analyzed by mass spectrometry. Significant fold changes of the phosphorylated residue clusters (in the dashed line box) are shown in solid boxes. Residues whose phosphorylation levels decreased upon GRK2 or GRK6 siRNA are indicated as red or blue filled circles, respectively. PKA consensus sites are shown. S246 is a consensus site for ATM phosphorylation and has been previously identified.

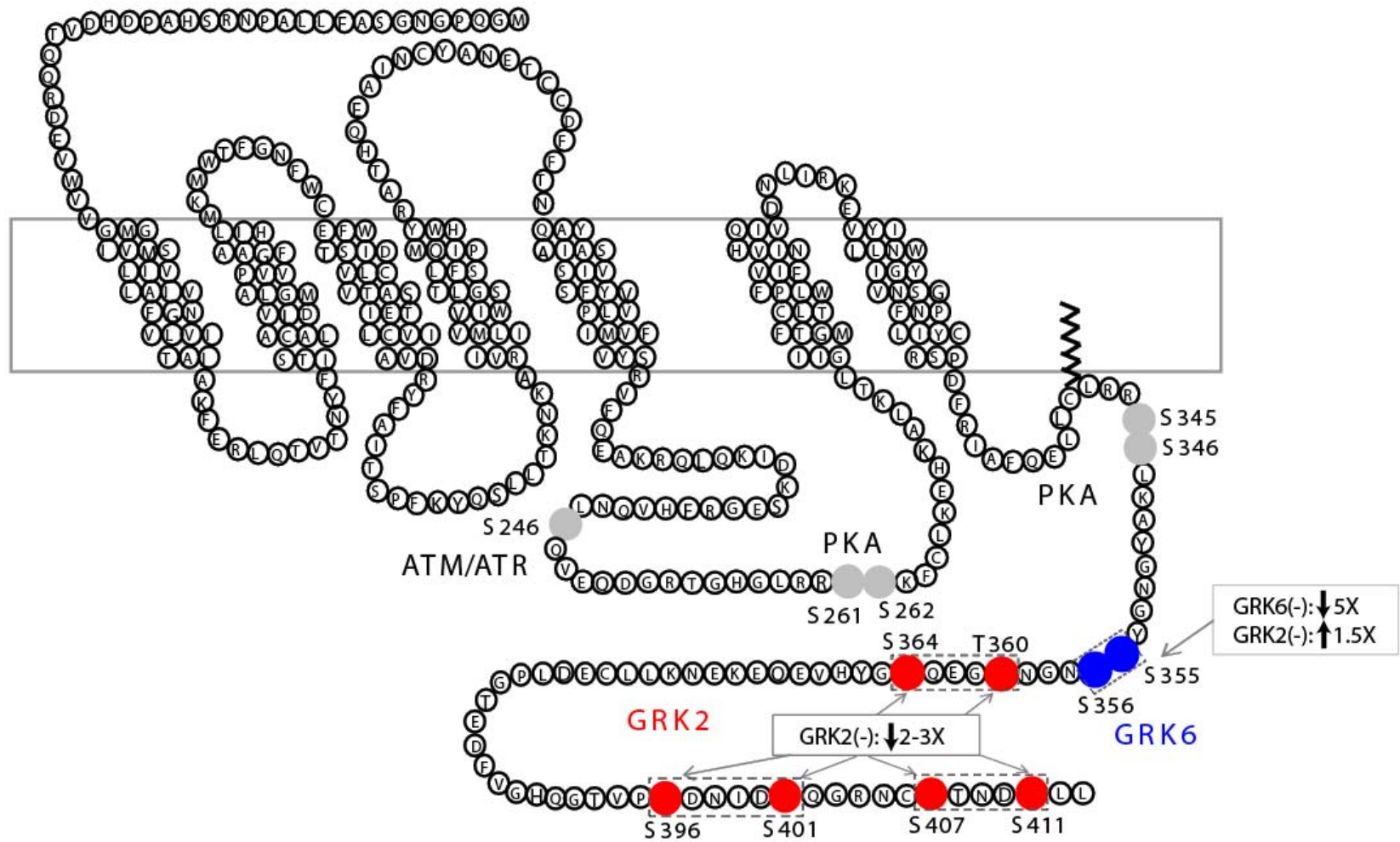


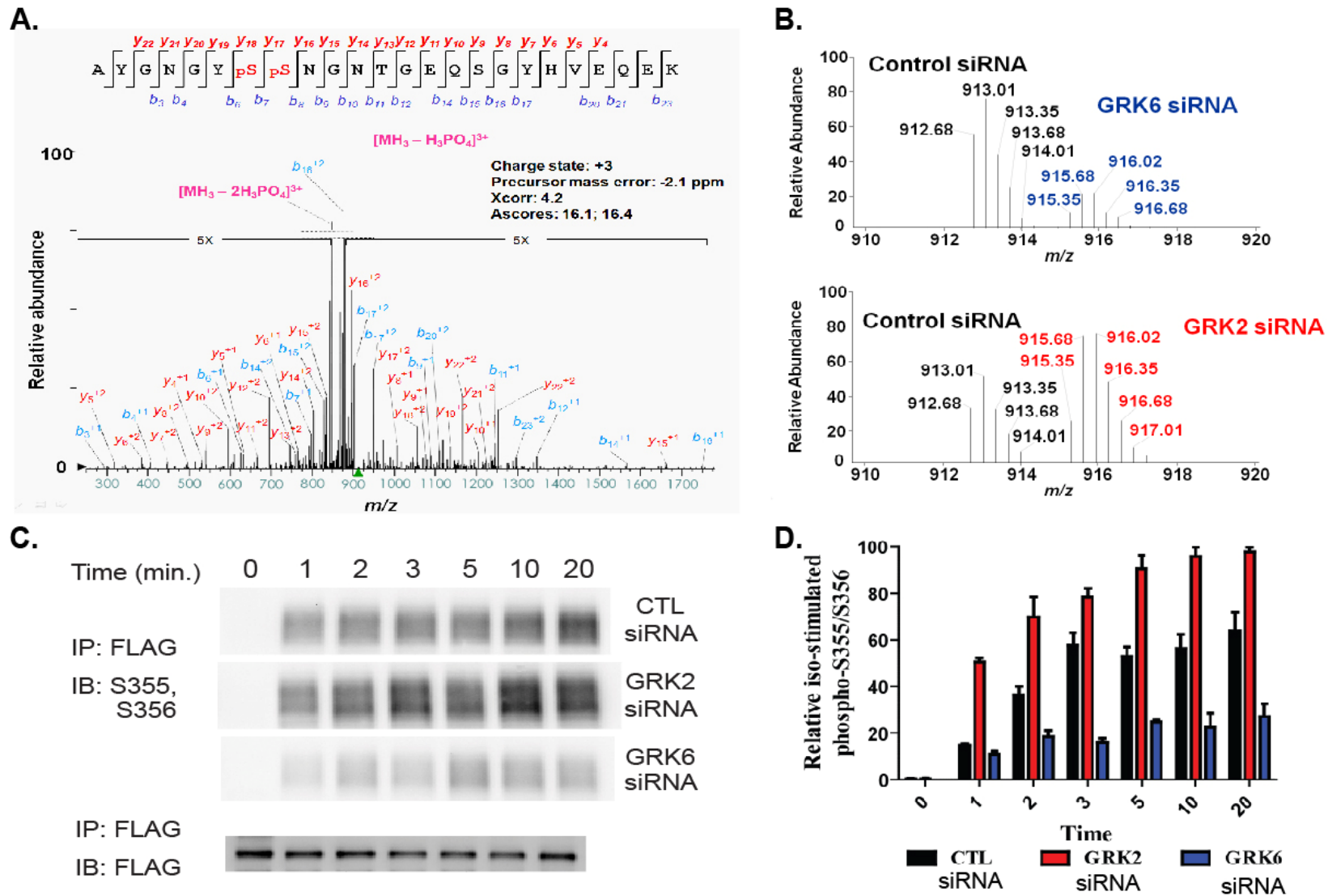
Figure 4-8: GRK2 and 6 Phosphorylate Different Sites on the β_2 AR.

phosphorylation levels at these sites, respectively. These results demonstrate that GRK2 appears to inhibit GRK6 phosphorylation of S355/S356. We verified phosphorylation at S355 and S356 by probing the immunoprecipitated, FLAG-tagged β 2AR from HEK293 cells stably expressing the receptors with a phospho-specific antibody directed at these sites. Treatment with a control siRNA and stimulation with isoproterenol led to a rapid, sustained and robust increase in phosphorylation of S355/S356 (Fig. 4-9 C and D). Treatment with GRK2 siRNA resulted in increased phosphorylation at these sites over the entire time course of stimulation with isoproterenol. The largest differences, in comparison to control siRNA, occurred at the earliest time points measured (Figure 4-9D; red bars). Conversely, GRK6 siRNA treatment led to a marked decrease in phosphorylation of S355/S356 at time points after two minutes (Figure 4-9D; blue bars).

β 2AR phosphorylation Induced by β -arrestin Biased Ligand Carvedilol

Carvedilol is a β -adrenergic antagonist which has recently been shown to selectively activate β -arrestin-mediated signaling even while blocking G-protein signaling [82, 129]. To determine the phosphorylation pattern of the β 2AR induced by carvedilol we quantitatively characterized the phosphorylation state of the β 2AR upon 10 μ M carvedilol stimulation for five minutes using the SILAC-based proteomic approach described above. As shown in figure 4-7, we found that carvedilol stimulation only induced increased phosphorylation at S355 and S356, the sites phosphorylated by GRK6.

Figure 4-9: Phosphorylation of S355/S356 on β 2AR. (A) is the annotated MS/MS fragmentation spectra for the “light” phosphopeptide AYGNGYpSpSNGNTGEQSGYHVEQEK from the sample which was treated with control siRNA. The peptide sequence is shown at the top of the MS/MS spectrum with phosphorylated residues highlighted in red. The identified fragmentation *y* (red color) and *b* (blue color) ions are indicated. (B) is the expanded MS spectrum section showing two isotope envelopes (peaks) corresponding to “light” and “heavy” forms of the unfragmented phosphopeptides. The “light” peak (black color) represents the peptide from the control siRNA-treated sample, whereas “heavy” peak represents those from the GRK6 (blue color, upper panel) or GRK2 (red color, lower panel) siRNA-treated sample. The relative abundance of the “heavy” and “light” forms of a phosphopeptide was calculated by the ratio of AUC (Area Under the Curve) for “heavy” to “light” peaks in the extracted ion chromatogram. In this case there is an 80% reduction in phosphorylation of S355/S356 when GRK6 is depleted. When GRK2 is depleted, the phosphorylation of S355/S356 increased 2.1-fold. (C) The top three panels are Western blot analyses with a phospho-specific antibody recognizing pSer355/pSer356 on β 2AR immunoprecipitated from stably expressing HEK293 cells (2pmols/mg) that have been transfected with either control (CTL), GRK2 or GRK6 siRNA, respectively. The bottom panel is a FLAG Western blot to show equal loading of immunoprecipitated β 2AR. (D) Quantitation of three independent experiments as described in A. The largest signal in each experiment was normalized to 100% subsequent to normalization via FLAG Western blots. Data shown are the mean \pm SEM for three independent experiments. The pS355/pS356 data for control (CTL)-siRNA transfected cells is shown in black; for GRK2-siRNA transfected cells is shown in red; for GRK6-siRNA transfected cells is shown in blue.

Figure 4-9: Phosphorylation of S355 and S356 on β 2AR.

4.3 Discussion

In this study, we have used MS-based quantitative proteomic approaches to map phosphorylation sites on the β 2AR, determined the GRKs responsible for phosphorylation of the sites and delineated the functional capabilities imparted to β -arrestin by these specific phosphorylation events. We have found that, in HEK293 cells, GRK2 sites are primarily responsible for β 2AR internalization while GRK6 sites are responsible for β -arrestin mediated ERK activation whereas both GRKs contribute to desensitization. We have also demonstrated that a β -arrestin biased ligand, carvedilol, induces a phosphorylation pattern distinct from that of an unbiased, full agonist, isoproterenol. Finally, we have shown that different phosphorylation patterns on the β 2AR elicited by either GRK2 or GRK6 induce distinct β -arrestin conformations. Our data thus provide direct support for the receptor phosphorylation “bar code” hypothesis (Figure 4-10), the idea that distinct patterns of multisite phosphorylation on a receptor by different GRKs differentially enable β -arrestin functions by inducing distinct β -arrestin conformations.

Several lines of evidence from the literature are also compatible with this notion. For example, it has been shown for several 7TMRs, including the V2R, CXCR4 and AT1AR that GRK6 and 5 support β -arrestin mediated ERK activation whereas GRK2 and 3 opposes it [84, 85, 134]. However, the molecular basis for this finding has not been previously established. Using a system of ligand bias for the CCR7 chemokine receptor in HEK293 cells, Kohout et al. have demonstrated that although both endogenous ligands, CCL19 and CCL21, induce G protein activation and subsequent calcium mobilization as well as G protein and β -arrestin dependent

Figure 4-10: Phosphorylation Bar Codes. GRKs 2 and 6 differentially phosphorylate an agonist-occupied 7TMR which instructs β -arrestin's conformation (white ribbon diagram). In turn, β -arrestin functions such as desensitization and signaling are determined by these different "active" conformations which are imparted to the β -arrestin by differential GRK phosphorylation.

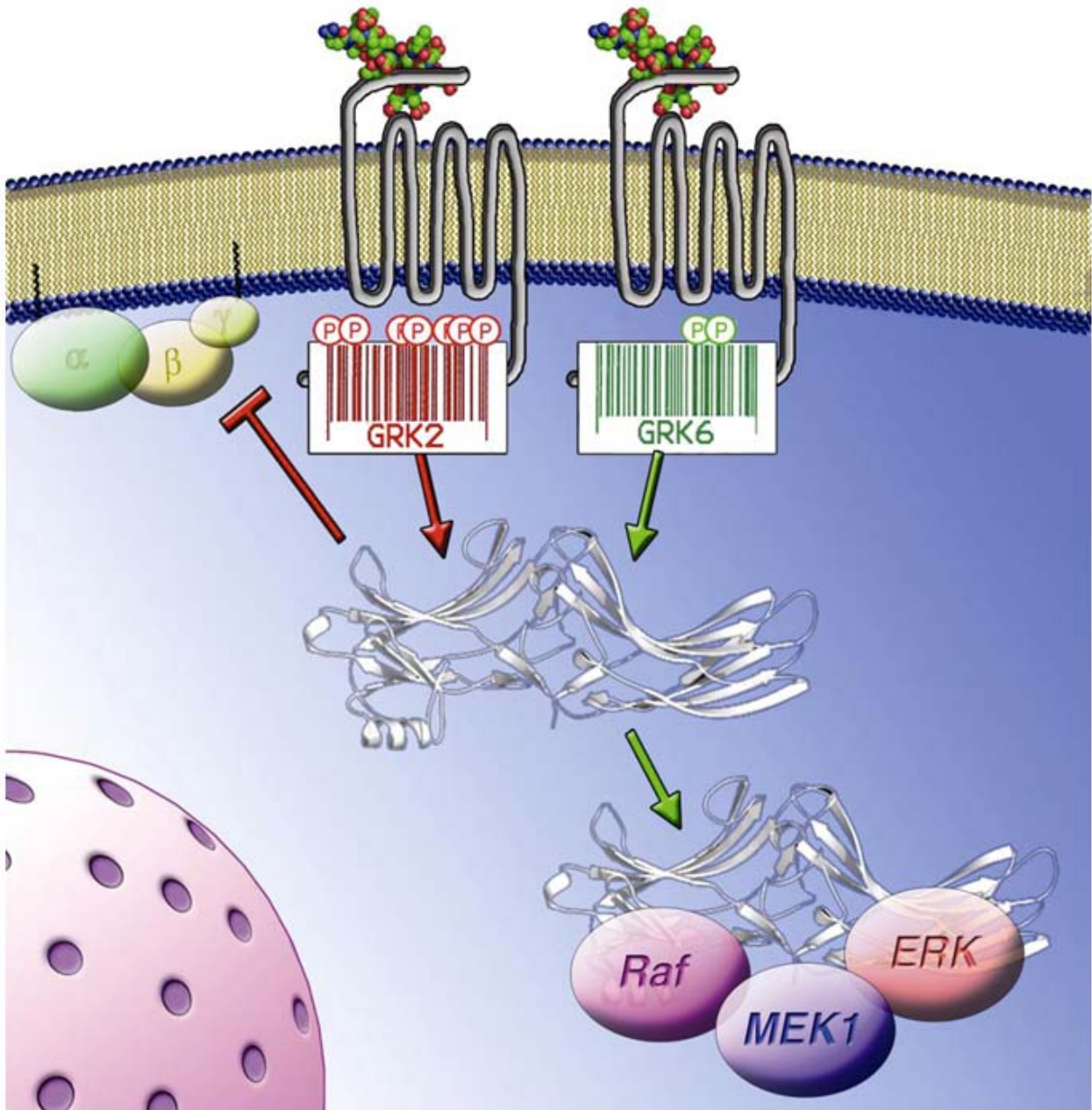


Figure 4-10: β2AR Phosphorylation Bar Codes.

ERK activation with equal potency, only activation by CCL19, not CCL21, promotes robust desensitization [135]. Zidar et al. have further shown that CCL19 leads to robust CCR7 phosphorylation and β -arrestin2 recruitment catalyzed by both GRK3 and GRK6 whereas CCL21 activates GRK6 alone and leads to weaker β -arrestin recruitment [136]. These data have suggested a strong correlation between CCR7 phosphorylation and β -arrestin-dependent activities; however, the relevant sites phosphorylated by different GRKs have not been determined.

A recent study on the chemokine receptor CXCR4 used mass spectrometry in conjunction with phospho-specific antibodies to map phosphorylation sites upon SDF1 stimulation in HEK293 cells [134]. Of the eighteen potential serine/threonine phosphorylation sites on the CXCR4's C-terminus, Busillo et al. were able to map three sites via mass spectrometry and to localize an additional four with phospho-specific antibodies. GRK6 accounted for the majority of the phosphorylation sites identified while no GRK2/3 sites were found; however, they demonstrated that multiple GRKs regulate CXCR4 signaling including GRK2. Silencing of either GRK2 or 6 by siRNA increased calcium mobilization while knock down of GRK3 or 6 led to decreased ERK1/2 activation. Interestingly, GRK2 knock down led to enhanced ERK1/2 activation, suggesting coordination among the GRKs in terms of signaling, though no mechanistic explanation could be deduced in the absence of identified GRK2 phosphorylation sites.

Synthetic phosphopeptides corresponding to the carboxy terminal sequences of two 7TMRs have been shown to bind to and induce conformational changes in β -arrestins [83, 137]. Moreover, phosphopeptides derived from the sequence of the V2R tail (a so called "class B"

receptor which binds β -arrestins tightly) have been shown to induce distinct conformational changes in β -arrestin from those observed with phosphopeptides from the “class A” β 2AR (a family of receptors which binds β -arrestin much less tightly)[73]. β -arrestins in these distinct conformations also interact differently with E3 ubiquitin ligases and de-ubiquitinases in a way which may explain the differences in endocytic behavior of class A receptors (which recycle rapidly after dissociation from β -arrestins) versus class B receptors (which recycle much more slowly and remain tightly bound to β -arrestins). Furthermore, in this context, Shenoy et al. were able to convert the β 2AR from a class A receptor to a class B receptor simply by over expression of GRK5 or 6, but not GRK2 which suggests that the sites phosphorylated by GRK6 promote a more stable interaction between β -arrestin and the β 2AR [73].

We have previously demonstrated, with several 7TMRs, that biased ligands which activate β -arrestin signaling in the absence of G-protein activation in fact induce distinct conformations of β -arrestin2 from those induced by unbiased ligands, as assessed by an intramolecular β -arrestin2 BRET Biosensor [93]. Our finding in the present study that a biased ligand such as carvedilol provokes a pattern of receptor site phosphorylation distinct from that obtained with the unbiased agonist isoproterenol is consistent with these findings. Carvedilol is a β -blocker which has proven particularly effective in the treatment of heart failure and which has been demonstrated to selectively stimulate β -arrestin-mediated signaling [82, 129]. This signaling may contribute to the unique clinical efficacy of carvedilol in the treatment of heart failure. Therefore, carvedilol may serve as a prototype for a new generation of therapeutic β 2AR ligands. One hypothesis to explain the selectivity of carvedilol for β -arrestin-mediated β 2AR signaling is that it induces a specific conformation of the receptor, leading to receptor

phosphorylation by specific GRK subtype(s). We determined that stimulation of the β 2AR with carvedilol induced phosphorylation only of Ser355/Ser356 by GRK6. This result suggests that while isoproterenol stimulation recruits both GRK2 and GRK6 to the receptor, carvedilol stimulation only recruits GRK6. This fits the notion that membrane association and activation of GRK2 occur through its interaction with G $\beta\gamma$ subunits [138, 139]. Without activation of G proteins during carvedilol stimulation, it is likely that GRK2 is not targeted to the membrane. These data further suggest that biased ligands, by inducing distinct receptor conformations, are able to recruit distinct GRKs.

We tested the hypothesis that distinct receptor phosphorylation patterns established by the different GRKs induce structurally and functionally distinct conformations of the bound β -arrestins. Using an intramolecular β -arrestin2 BRET biosensor we found that GRK2 siRNA treatment (resulting in phosphorylation by GRK6 on only S355 and S356, the phosphorylation pattern of carvedilol), produced the same directionally negative change in the BRET ratio as we previously demonstrated with several β -arrestin biased ligands in multiple 7TMR systems [93]. In addition, GRK6-siRNA treatment led to yet a third distinct β -arrestin conformation. These data provide the first direct evidence that distinct phosphorylation patterns on a 7TMR result in unique β -arrestin conformations.

Several published studies, however, do not seem to support the universality of such a “bar code” mechanism. Mutants of the AT1AR in which all potential C-terminal phosphorylation sites are removed by truncation or substitution with alanine still recruit β -arrestins, albeit in a weaker class A pattern than its wild type counterpart that induces a strong class B pattern [56]. The mutant receptors activate ERK to the same extent as wild type AT1AR.

However, in the absence of receptor phosphorylation, β -arrestin mediated desensitization and endocytosis of AT1ARs are largely abrogated. In contrast, when all of the phosphorylation sites on the β 2AR are mutated to alanine the receptor neither binds β -arrestin nor stimulates ERK in a β -arrestin-dependent manner [56]. These data clearly support the idea that β 2AR phosphorylation is a prerequisite for β -arrestin recruitment and β -arrestin-mediated signaling while the picture for AT1AR is less clear.

An interesting study by Terrillon et al. using a synthetic small molecule dimerizing agent demonstrated that when β -arrestin was linked to a cell membrane bound anchor protein, ERK activation occurred in the complete absence of 7TMR stimulation [140]. However, the kinetics of ERK1/2 activation by the heterodimeriser were significantly slower than that observed with stimulation of a 7TMR in a physiological context. In this study it appeared that membrane translocation of β -arrestin was sufficient to activate β -arrestin mediated signaling to ERK. This may suggest that in some cases 7TMRs may primarily serve as simply a means to translocate β -arrestin to the plasma membrane and not act as an integral part of a β -arrestin signaling scaffold. β -arrestins have been shown to adopt different conformations and are usually in a dynamic equilibrium of conformers with multiple driving forces (e.g. receptor conformation and phosphorylation) contributing to β -arrestin activation [83, 93, 137]. Thus, it is possible that in some cases receptor conformation alone is sufficient to determine β -arrestin conformation. However, it should be emphasized that the studies with artificial dimerizers and heavily mutated receptors present the cell with highly unnatural circumstances which may have limited relevance to cellular physiology.

An interesting finding in our study was the inhibitory effect of GRK2 on GRK6 phosphorylation of S355/356. This likely explains the elevated ERK activation that we observed in GRK2 siRNA transfected cells and which we previously observed for the AT1AR and the V2R [84, 85]. Recently, as noted above, Benovic et al. have made similar observations for the CXCR4 receptor [134]. For the AT1A and V2 receptors, GRK2 over-expression has also been shown to decrease β -arrestin2-dependent ERK activation. The negative regulation of GRK6/ β -arrestin-mediated ERK activation by GRK2 phosphorylation might be due to either of two potential regulatory mechanisms. First, it is known that activation of the β 2AR by a full agonist promotes activation of *Gas* and dissociation of the $G\beta\gamma$ subunits which target GRK2 to the membrane. It is possible that translocation of GRK2 to the β 2AR sterically hinders GRK6's ability to quickly and robustly phosphorylate Ser 355/Ser356. Alternatively, phosphorylation by GRK2 might alter the conformation of the β 2AR in a way that negatively regulates phosphorylation by GRK6. The two mechanisms are not mutually exclusive.

While several previous studies have been directed at the determination of phosphorylation sites on the β 2AR and other 7TMRs, these have generally relied on *in vitro* and mutagenesis approaches and virtually none have attempted to specifically assign these sites by MS analysis, much less to determine the kinases responsible. In the only previously published attempt to map phosphorylation sites on the β 2AR by mass spectrometry, Trester-Zedlitz et al. reported that a peptide, 339-369, contained multiple sites and determined that the net phosphorylation of this peptide increased with agonist stimulation [141]. However, they were unable to assign specific phosphorylation sites or to detect any of the distal C-terminal sites. An early study by Fredericks et al. used purified, recombinant human β 2AR in conjunction with

GRK2 and 5 to delineate overlapping patterns of phosphorylation sites with these two GRKs [142]. However, the relevance of these studies to the actual events occurring in cells is somewhat uncertain due to the high concentrations of receptors and GRKs utilized in these *in vitro* experiments. Mutagenesis studies have shown that mutation of all serine and threonine residues in the C-terminus of the β 2AR to alanines and/or glycines prevents agonist stimulated phosphorylation [143], receptor/ β -arrestin interaction [144], β -arrestin-mediated desensitization [145], internalization [144] and ERK activation [56]. However, more recent studies have shown that not all phosphorylation sites are required for each of the β -arrestin-mediated activities, consistent with our results.

A number of studies targeting various combinations of four phosphorylation sites (S355, S356, T360 and S364) on the β 2AR have shown that this region is important for β -arrestin binding and that loss of these sites impairs, to varying extents, receptor desensitization and internalization [144-148]. Krasel et al. have shown that while phosphorylation of these proximal sites (two of which are assigned as GRK6 sites in our study) can promote β -arrestin2 interaction with the β 2AR, it is phosphorylation at the distal (GRK2) sites that is required for high affinity receptor: β -arrestin2 interaction [144]. A L381 β 2AR truncation mutant demonstrated strong interaction with β -arrestin2, but failed to internalize which suggests that β -arrestin binding in and of itself is not sufficient for receptor internalization. In fact, deletion of only the last eight residues of the β 2AR C-terminus (Δ ASN405) also resulted in the failure of receptor internalization. These data suggest that while both the distal and proximal phosphorylation residues of the β 2AR are important for β -arrestin binding, it is the distal residues (assigned as GRK2 sites in our study) that confer high affinity binding and also coordinate protein:protein

interactions that facilitate internalization. These data are also consistent with our finding that silencing of GRK2 leads to more marked impairment of β 2AR internalization than that of GRK6.

A long-acting β 2AR agonist, salmeterol, which is commonly used in the treatment of asthma and chronic obstructive pulmonary disease (COPD), also displays unique properties [149]. Moore et al. demonstrated that salmeterol stimulation of β 2AR promotes GRK-mediated phosphorylation of serines 355 and 356 in HEK293 cells but fails to induce significant internalization or degradation of the receptor and is also incapable of stimulating translocation of β -arrestin2 [149]. The GRKs responsible were not determined. The data suggest that salmeterol may stimulate the phosphorylation of distinct sites when compared with other agonists. However, it is unclear from that study if salmeterol stimulation is at all capable of promoting GRK-mediated phosphorylation of the distal sites, which are important for β 2AR internalization and β -arrestin recruitment.

In summary we have quantitatively mapped sites on the β 2AR phosphorylated in response to stimulation with an unbiased agonist, isoproterenol, and a β -arrestin biased ligand, carvedilol. We demonstrate that the sites phosphorylated in response to the two types of ligand are distinct and mediated by different GRKs (2 and 6). Moreover, phosphorylation of the different sets of sites by the two GRKs engenders distinct functionality of the recruited β -arrestin by inducing different conformations of the bound β -arrestin. Antagonism of GRK6 phosphorylation by GRK2 mediated phosphorylation provides a mechanistic basis for antagonism between the two kinases at the level of β -arrestin mediated ERK activation previously observed for several 7TMRs. The findings are consistent with a model where the patterning of receptor phosphorylation sites by different GRKs establishes a “bar code” which

determines the conformation of the bound β -arrestins and subsequently its functional capabilities. Understanding such “bar codes” for various receptors may be useful in screening for potentially novel therapeutic agents.

5. Future Directions

A number of questions have arisen from this work and remain unanswered. *How do conformational changes in β -arrestin contribute to its endocytic and cellular functions?* We have demonstrated, *in vitro* and in cultured cells, that β -arrestin adopts multiple conformations in response to different phosphorylation patterns, the bar code hypothesis (Figure 4-9), which suggests the existence of multiple active states. This notion of a multistate model may help explain how only two ubiquitously expressed isoforms of β -arrestin can regulate such a large number of 7TMRs and interact with an ever-growing list of non-receptor partners to carry out diverse cellular functions (i.e. desensitization, internalization and the formation and activation of multi-component signaling complexes).

To date, no active structure of any arrestin family member exists. Co-crystallization of a β -arrestin ternary complex containing β -arrestin, a 7TMR (or activating phospho-peptide) and one of its interacting protein partners would provide insight into the “activated” structure of β -arrestin and β -arrestin’s protein-protein interface that is able to interact with a diverse array of non-receptor partners. The C-terminus of β -arrestin1 is not “visible” in any of the published crystal structures because it is either disordered or the β -arrestin1 construct used for structural determination is truncated (reviewed in [105]). Conformational changes observed in this study with β -arrestin1 and V₂Rpp suggest that upon 7TMR binding the C-terminus of β -arrestin1 is released. Thus it may be necessary to stabilize β -arrestin1’s C-terminus with a binding partner, such as clathrin, in order to gain a structural understanding of β -arrestin’s scaffolding functions. Alternatively, the four-phospho peptide used in this study (V₂R4p), which mimics 7TMR binding to the N-domain without releasing β -arrestin1’s C-terminus, may be more amenable to

crystallographic studies and would provide insight into how 7TMR binding to β -arrestin1 occurs.

What specific 7TMR factors determine if GRK phosphorylation is necessary for β -arrestin mediated ERK activation? Several published studies do not seem to support the universality of a bar code mechanism. Studies with a mutant AT1_AR that lacks all GRK phosphorylation sites is able to recruit β -arrestin and signal through ERK; however, the desensitization and internalization of this receptor are largely abrogated [56]. This observation may be due to β -arrestin binding to this mutant AT1_AR in a way that its C-terminus remains buried even after receptor binding thus precluding clathrin and AP2 binding. It is possible, in some cases, that the agonist-occupied 7TMR conformation alone is able to bind to and alter the conformation of β -arrestin thereby empowering a signaling competent β -arrestin conformation. Another theory is that recruitment of β -arrestin to the plasma membrane, even in transient Class A pattern, is sufficient to induce β -arrestin mediated signaling to ERK. A study using an artificial system of β -arrestin translocation showed that β -arrestin can activate ERK even in the absence of 7TMR stimulation [140].

What is the mechanism of the inhibitory effect of GRK2 on GRK6 phosphorylation? In this study, silencing of GRK2 with siRNA enhanced phosphorylation of β 2AR by GRK6. This increased GRK6 phosphorylation provides a possible explanation for the elevated ERK activation in GRK2 siRNA-transfected cells that has been observed in multiple 7TMR systems [84, 85]. Multiple possibilities exist to explain this phenomenon. First, it is possible that translocation of GRK2 to the 7TMR sterically hinders GRK6's ability to phosphorylate the

receptor. Second, GRK2 phosphorylation may alter the 7TMR conformation in a way that negatively regulates GRK6 phosphorylation.

Is there a universal mechanism by which β -arrestin biased ligands induce different phosphorylation patterns on 7TMRs? Carvedilol, a β 2AR antagonist, has recently been shown to selectively activate β -arrestin mediated signaling even while blocking G-protein dependent signaling [82]. In this study, we have shown that stimulation of β 2AR with carvedilol only induced an increase in phosphorylation levels at S355 and S356, the GRK6 phosphorylation sites. A recent study by Zidar et al., using a system of ligand bias for the chemokine CCR7, suggests a strong correlation between CCR7 phosphorylation and β -arrestin-dependent activities; however, the relevant sites phosphorylated by different GRKs have not been determined [136]. β -arrestin signaling represents a new paradigm in receptor biology and may offer a new host of therapeutic targets. However, the molecular basis of this ligand bias is unclear at this time. In order to determine if biased ligands instruct specific GRKs to phosphorylate 7TMRs as a general mechanism, quantitative mass spectrometry analyses will have to be performed in multiple 7TMR systems. Of particular interest is the AT1AR system since the role of GRK phosphorylation in β -arrestin mediated signaling is unclear. In summary, β -arrestin signaling represents a relatively new paradigm in 7TMR biology and remains an untapped resource for the development of novel therapeutics.

References

1. Venter, J.C., et al., *The sequence of the human genome*. Science, 2001. **291**(5507): p. 1304-51.
2. Ma, P. and R. Zimmell, *Value of novelty?* Nat Rev Drug Discov, 2002. **1**(8): p. 571-2.
3. Rosenbaum, D.M., S.G. Rasmussen, and B.K. Kobilka, *The structure and function of G-protein-coupled receptors*. Nature, 2009. **459**(7245): p. 356-63.
4. Wu, B., et al., *Structures of the CXCR4 Chemokine GPCR with Small-Molecule and Cyclic Peptide Antagonists*. Science, 2010.
5. Rasmussen, S.G., et al., *Crystal structure of the human beta2 adrenergic G-protein-coupled receptor*. Nature, 2007. **450**(7168): p. 383-7.
6. Rosenbaum, D.M., et al., *GPCR engineering yields high-resolution structural insights into beta2-adrenergic receptor function*. Science, 2007. **318**(5854): p. 1266-73.
7. Cherezov, V., et al., *High-resolution crystal structure of an engineered human beta2-adrenergic G protein-coupled receptor*. Science, 2007. **318**(5854): p. 1258-65.
8. Hanson, M.A., et al., *A specific cholesterol binding site is established by the 2.8 Å structure of the human beta2-adrenergic receptor*. Structure, 2008. **16**(6): p. 897-905.
9. Warne, T., et al., *Structure of a beta1-adrenergic G-protein-coupled receptor*. Nature, 2008. **454**(7203): p. 486-91.
10. Jaakola, V.P., et al., *The 2.6 angstrom crystal structure of a human A2A adenosine receptor bound to an antagonist*. Science, 2008. **322**(5905): p. 1211-7.
11. Palczewski, K., et al., *Crystal structure of rhodopsin: A G protein-coupled receptor*. Science, 2000. **289**(5480): p. 739-45.
12. Okada, T., et al., *X-Ray diffraction analysis of three-dimensional crystals of bovine rhodopsin obtained from mixed micelles*. J Struct Biol, 2000. **130**(1): p. 73-80.

13. Li, J., et al., *Structure of bovine rhodopsin in a trigonal crystal form*. J Mol Biol, 2004. **343**(5): p. 1409-38.
14. Farrens, D.L., et al., *Requirement of rigid-body motion of transmembrane helices for light activation of rhodopsin*. Science, 1996. **274**(5288): p. 768-70.
15. Altenbach, C., et al., *Structural features and light-dependent changes in the cytoplasmic interhelical E-F loop region of rhodopsin: a site-directed spin-labeling study*. Biochemistry, 1996. **35**(38): p. 12470-8.
16. Casey, P.J. and A.G. Gilman, *G protein involvement in receptor-effector coupling*. J Biol Chem, 1988. **263**(6): p. 2577-80.
17. Oldham, W.M., et al., *Mechanism of the receptor-catalyzed activation of heterotrimeric G proteins*. Nat Struct Mol Biol, 2006. **13**(9): p. 772-7.
18. Milligan, G. and E. Kostenis, *Heterotrimeric G-proteins: a short history*. Br J Pharmacol, 2006. **147 Suppl 1**: p. S46-55.
19. Lambright, D.G., et al., *The 2.0 Å crystal structure of a heterotrimeric G protein*. Nature, 1996. **379**(6563): p. 311-9.
20. Clapham, D.E. and E.J. Neer, *G protein beta gamma subunits*. Annu Rev Pharmacol Toxicol, 1997. **37**: p. 167-203.
21. Wilkie, T.M., et al., *Evolution of the mammalian G protein alpha subunit multigene family*. Nat Genet, 1992. **1**(2): p. 85-91.
22. Gilman, A.G., *G proteins and dual control of adenylate cyclase*. Cell, 1984. **36**(3): p. 577-9.
23. Taylor, S.J., J.A. Smith, and J.H. Exton, *Purification from bovine liver membranes of a guanine nucleotide-dependent activator of phosphoinositide-specific phospholipase C. Immunologic identification as a novel G-protein alpha subunit*. J Biol Chem, 1990. **265**(28): p. 17150-6.
24. Strathmann, M. and M.I. Simon, *G protein diversity: a distinct class of alpha subunits is present in vertebrates and invertebrates*. Proc Natl Acad Sci U S A, 1990. **87**(23): p. 9113-7.

25. Newton, A.C., *Regulation of protein kinase C*. *Curr Opin Cell Biol*, 1997. **9**(2): p. 161-7.
26. Toker, A., *Signaling through protein kinase C*. *Front Biosci*, 1998. **3**: p. D1134-47.
27. Kozasa, T., et al., *p115 RhoGEF, a GTPase activating protein for Galpha12 and Galpha13*. *Science*, 1998. **280**(5372): p. 2109-11.
28. Hart, M.J., et al., *Direct stimulation of the guanine nucleotide exchange activity of p115 RhoGEF by Galpha13*. *Science*, 1998. **280**(5372): p. 2112-4.
29. Hamm, H.E., *The many faces of G protein signaling*. *J Biol Chem*, 1998. **273**(2): p. 669-72.
30. Pierce, K.L., R.T. Premont, and R.J. Lefkowitz, *Seven-transmembrane receptors*. *Nat Rev Mol Cell Biol*, 2002. **3**(9): p. 639-50.
31. Marinissen, M.J. and J.S. Gutkind, *G-protein-coupled receptors and signaling networks: emerging paradigms*. *Trends Pharmacol Sci*, 2001. **22**(7): p. 368-76.
32. Rockman, H.A., W.J. Koch, and R.J. Lefkowitz, *Seven-transmembrane-spanning receptors and heart function*. *Nature*, 2002. **415**(6868): p. 206-12.
33. Petrofski, J.A. and W.J. Koch, *The beta-adrenergic receptor kinase in heart failure*. *J Mol Cell Cardiol*, 2003. **35**(10): p. 1167-74.
34. Berman, D.M., T.M. Wilkie, and A.G. Gilman, *GAIP and RGS4 are GTPase-activating proteins for the Gi subfamily of G protein alpha subunits*. *Cell*, 1996. **86**(3): p. 445-52.
35. Hunt, T.W., et al., *RGS10 is a selective activator of G alpha i GTPase activity*. *Nature*, 1996. **383**(6596): p. 175-7.
36. Grant, S.L., et al., *Specific regulation of RGS2 messenger RNA by angiotensin II in cultured vascular smooth muscle cells*. *Mol Pharmacol*, 2000. **57**(3): p. 460-7.
37. Song, L., P. De Sarno, and R.S. Jope, *Muscarinic receptor stimulation increases regulators of G-protein signaling 2 mRNA levels through a protein kinase C-dependent mechanism*. *J Biol Chem*, 1999. **274**(42): p. 29689-93.

38. Lefkowitz, R.J., *G protein-coupled receptors. III. New roles for receptor kinases and beta-arrestins in receptor signaling and desensitization.* J Biol Chem, 1998. **273**(30): p. 18677-80.
39. Freedman, N.J. and R.J. Lefkowitz, *Desensitization of G protein-coupled receptors.* Recent Prog Horm Res, 1996. **51**: p. 319-51; discussion 352-3.
40. Benovic, J.L., et al., *Phosphorylation of the mammalian beta-adrenergic receptor by cyclic AMP-dependent protein kinase. Regulation of the rate of receptor phosphorylation and dephosphorylation by agonist occupancy and effects on coupling of the receptor to the stimulatory guanine nucleotide regulatory protein.* J Biol Chem, 1985. **260**(11): p. 7094-101.
41. Pitcher, J., et al., *Desensitization of the isolated beta 2-adrenergic receptor by beta-adrenergic receptor kinase, cAMP-dependent protein kinase, and protein kinase C occurs via distinct molecular mechanisms.* Biochemistry, 1992. **31**(12): p. 3193-7.
42. Kunapuli, P., et al., *Expression, purification, and characterization of the G protein-coupled receptor kinase GRK5.* J Biol Chem, 1994. **269**(2): p. 1099-105.
43. Kim, C.M., S.B. Dion, and J.L. Benovic, *Mechanism of beta-adrenergic receptor kinase activation by G proteins.* J Biol Chem, 1993. **268**(21): p. 15412-8.
44. Benovic, J.L., et al., *Functional desensitization of the isolated beta-adrenergic receptor by the beta-adrenergic receptor kinase: potential role of an analog of the retinal protein arrestin (48-kDa protein).* Proc Natl Acad Sci U S A, 1987. **84**(24): p. 8879-82.
45. Richardson, R.M., et al., *Phosphorylation and desensitization of human m2 muscarinic cholinergic receptors by two isoforms of the beta-adrenergic receptor kinase.* J Biol Chem, 1993. **268**(18): p. 13650-6.
46. Ramkumar, V., et al., *Functional consequences of A1 adenosine-receptor phosphorylation by the beta-adrenergic receptor kinase.* Biochim Biophys Acta, 1993. **1179**(1): p. 89-97.
47. Lohse, M.J., et al., *beta-Arrestin: a protein that regulates beta-adrenergic receptor function.* Science, 1990. **248**(4962): p. 1547-50.

48. Lohse, M.J., et al., *Receptor-specific desensitization with purified proteins. Kinase dependence and receptor specificity of beta-arrestin and arrestin in the beta 2-adrenergic receptor and rhodopsin systems.* J Biol Chem, 1992. **267**(12): p. 8558-64.
49. Pitcher, J.A., N.J. Freedman, and R.J. Lefkowitz, *G protein-coupled receptor kinases.* Annu Rev Biochem, 1998. **67**: p. 653-92.
50. Penela, P., C. Ribas, and F. Mayor, Jr., *Mechanisms of regulation of the expression and function of G protein-coupled receptor kinases.* Cell Signal, 2003. **15**(11): p. 973-81.
51. Premont, R.T., J. Inglese, and R.J. Lefkowitz, *Protein kinases that phosphorylate activated G protein-coupled receptors.* FASEB J, 1995. **9**(2): p. 175-82.
52. Luttrell, L.M. and R.J. Lefkowitz, *The role of beta-arrestins in the termination and transduction of G-protein-coupled receptor signals.* J Cell Sci, 2002. **115**(Pt 3): p. 455-65.
53. Han, M., et al., *Crystal structure of beta-arrestin at 1.9 A: possible mechanism of receptor binding and membrane Translocation.* Structure, 2001. **9**(9): p. 869-80.
54. Oakley, R.H., et al., *Differential affinities of visual arrestin, beta arrestin1, and beta arrestin2 for G protein-coupled receptors delineate two major classes of receptors.* J Biol Chem, 2000. **275**(22): p. 17201-10.
55. Claing, A., et al., *beta-Arrestin-mediated ADP-ribosylation factor 6 activation and beta 2-adrenergic receptor endocytosis.* J Biol Chem, 2001. **276**(45): p. 42509-13.
56. DeWire, S.M., et al., *Beta-arrestins and cell signaling.* Annu Rev Physiol, 2007. **69**: p. 483-510.
57. Xiao, K., et al., *Global phosphorylation analysis of beta-arrestin-mediated signaling downstream of a seven transmembrane receptor (7TMR).* Proc Natl Acad Sci U S A, 2010. **107**(34): p. 15299-304.
58. Xiao, K., et al., *Functional specialization of beta-arrestin interactions revealed by proteomic analysis.* Proc Natl Acad Sci U S A, 2007. **104**(29): p. 12011-6.

59. Moore, C.A., S.K. Milano, and J.L. Benovic, *Regulation of receptor trafficking by GRKs and arrestins*. *Annu Rev Physiol*, 2007. **69**: p. 451-82.
60. Laporte, S.A., et al., *The interaction of beta-arrestin with the AP-2 adaptor is required for the clustering of beta 2-adrenergic receptor into clathrin-coated pits*. *J Biol Chem*, 2000. **275**(30): p. 23120-6.
61. Krupnick, J.G., et al., *Arrestin/clathrin interaction. Localization of the clathrin binding domain of nonvisual arrestins to the carboxy terminus*. *J Biol Chem*, 1997. **272**(23): p. 15011-6.
62. Goodman, O.B., Jr., et al., *Beta-arrestin acts as a clathrin adaptor in endocytosis of the beta2-adrenergic receptor*. *Nature*, 1996. **383**(6599): p. 447-50.
63. Krupnick, J.G., et al., *Modulation of the arrestin-clathrin interaction in cells. Characterization of beta-arrestin dominant-negative mutants*. *J Biol Chem*, 1997. **272**(51): p. 32507-12.
64. Luttrell, L.M., et al., *Beta-arrestin-dependent formation of beta2 adrenergic receptor-Src protein kinase complexes*. *Science*, 1999. **283**(5402): p. 655-61.
65. Ahn, S., et al., *Src-dependent tyrosine phosphorylation regulates dynamin self-assembly and ligand-induced endocytosis of the epidermal growth factor receptor*. *J Biol Chem*, 2002. **277**(29): p. 26642-51.
66. Ahn, S., et al., *Src-mediated tyrosine phosphorylation of dynamin is required for beta2-adrenergic receptor internalization and mitogen-activated protein kinase signaling*. *J Biol Chem*, 1999. **274**(3): p. 1185-8.
67. Mukherjee, S., J.E. Casanova, and M. Hunzicker-Dunn, *Desensitization of the luteinizing hormone/choriogonadotropin receptor in ovarian follicular membranes is inhibited by catalytically inactive ARNO(+)*. *J Biol Chem*, 2001. **276**(9): p. 6524-8.
68. Shenoy, S.K., et al., *Regulation of receptor fate by ubiquitination of activated beta 2-adrenergic receptor and beta-arrestin*. *Science*, 2001. **294**(5545): p. 1307-13.
69. Martin, N.P., R.J. Lefkowitz, and S.K. Shenoy, *Regulation of V2 vasopressin receptor degradation by agonist-promoted ubiquitination*. *J Biol Chem*, 2003. **278**(46): p. 45954-9.

70. Shenoy, S.K. and R.J. Lefkowitz, *Receptor-specific ubiquitination of beta-arrestin directs assembly and targeting of seven-transmembrane receptor signalosomes*. J Biol Chem, 2005. **280**(15): p. 15315-24.
71. Shenoy, S.K. and R.J. Lefkowitz, *Trafficking patterns of beta-arrestin and G protein-coupled receptors determined by the kinetics of beta-arrestin deubiquitination*. J Biol Chem, 2003. **278**(16): p. 14498-506.
72. Perroy, J., et al., *Real-time monitoring of ubiquitination in living cells by BRET*. Nat Methods, 2004. **1**(3): p. 203-8.
73. Shenoy, S.K., et al., *Beta-arrestin-dependent signaling and trafficking of 7-transmembrane receptors is reciprocally regulated by the deubiquitinase USP33 and the E3 ligase Mdm2*. Proc Natl Acad Sci U S A, 2009. **106**(16): p. 6650-5.
74. DeFea, K.A., et al., *The proliferative and antiapoptotic effects of substance P are facilitated by formation of a beta -arrestin-dependent scaffolding complex*. Proc Natl Acad Sci U S A, 2000. **97**(20): p. 11086-91.
75. McDonald, P.H., et al., *Beta-arrestin 2: a receptor-regulated MAPK scaffold for the activation of JNK3*. Science, 2000. **290**(5496): p. 1574-7.
76. Tohgo, A., et al., *beta-Arrestin scaffolding of the ERK cascade enhances cytosolic ERK activity but inhibits ERK-mediated transcription following angiotensin AT1a receptor stimulation*. J Biol Chem, 2002. **277**(11): p. 9429-36.
77. Ahn, S., et al., *Differential kinetic and spatial patterns of beta-arrestin and G protein-mediated ERK activation by the angiotensin II receptor*. J Biol Chem, 2004. **279**(34): p. 35518-25.
78. Shenoy, S.K., et al., *beta-arrestin-dependent, G protein-independent ERK1/2 activation by the beta2 adrenergic receptor*. J Biol Chem, 2006. **281**(2): p. 1261-73.
79. Gaborik, Z., et al., *The role of a conserved region of the second intracellular loop in AT1 angiotensin receptor activation and signaling*. Endocrinology, 2003. **144**(6): p. 2220-8.

80. Wei, H., et al., *Independent beta-arrestin 2 and G protein-mediated pathways for angiotensin II activation of extracellular signal-regulated kinases 1 and 2*. Proc Natl Acad Sci U S A, 2003. **100**(19): p. 10782-7.
81. Violin, J.D. and R.J. Lefkowitz, *Beta-arrestin-biased ligands at seven-transmembrane receptors*. Trends Pharmacol Sci, 2007. **28**(8): p. 416-22.
82. Wisler, J.W., et al., *A unique mechanism of beta-blocker action: carvedilol stimulates beta-arrestin signaling*. Proc Natl Acad Sci U S A, 2007. **104**(42): p. 16657-62.
83. Xiao, K., et al., *Activation-dependent conformational changes in {beta}-arrestin 2*. J Biol Chem, 2004. **279**(53): p. 55744-53.
84. Kim, J., et al., *Functional antagonism of different G protein-coupled receptor kinases for beta-arrestin-mediated angiotensin II receptor signaling*. Proc Natl Acad Sci U S A, 2005. **102**(5): p. 1442-7.
85. Ren, X.R., et al., *Different G protein-coupled receptor kinases govern G protein and beta-arrestin-mediated signaling of V2 vasopressin receptor*. Proc Natl Acad Sci U S A, 2005. **102**(5): p. 1448-53.
86. Charest, P.G., S. Terrillon, and M. Bouvier, *Monitoring agonist-promoted conformational changes of beta-arrestin in living cells by intramolecular BRET*. EMBO Rep, 2005. **6**(4): p. 334-40.
87. Caron, M.G., et al., *Affinity chromatography of the beta-adrenergic receptor*. J Biol Chem, 1979. **254**(8): p. 2923-7.
88. Rappsilber, J., Y. Ishihama, and M. Mann, *Stop and go extraction tips for matrix-assisted laser desorption/ionization, nanoelectrospray, and LC/MS sample pretreatment in proteomics*. Anal Chem, 2003. **75**(3): p. 663-70.
89. Haas, W., et al., *Optimization and use of peptide mass measurement accuracy in shotgun proteomics*. Mol Cell Proteomics, 2006. **5**(7): p. 1326-37.
90. Beausoleil, S.A., et al., *A probability-based approach for high-throughput protein phosphorylation analysis and site localization*. Nat Biotechnol, 2006. **24**(10): p. 1285-92.

91. Bakalarski, C.E., et al., *The impact of peptide abundance and dynamic range on stable-isotope-based quantitative proteomic analyses*. J Proteome Res, 2008. **7**(11): p. 4756-65.
92. Leff, P., *Potential errors in agonist dissociation constant estimation caused by desensitization*. J Theor Biol, 1986. **121**(2): p. 221-32.
93. Shukla, A.K., et al., *Distinct conformational changes in beta-arrestin report biased agonism at seven-transmembrane receptors*. Proc Natl Acad Sci U S A, 2008. **105**(29): p. 9988-93.
94. Sutton, R.B., et al., *Crystal structure of cone arrestin at 2.3A: evolution of receptor specificity*. J Mol Biol, 2005. **354**(5): p. 1069-80.
95. Carter, J.M., et al., *Conformational differences between arrestin2 and pre-activated mutants as revealed by hydrogen exchange mass spectrometry*. J Mol Biol, 2005. **351**(4): p. 865-78.
96. Celver, J., et al., *Conservation of the phosphate-sensitive elements in the arrestin family of proteins*. J Biol Chem, 2002. **277**(11): p. 9043-8.
97. Milano, S.K., et al., *Scaffolding functions of arrestin-2 revealed by crystal structure and mutagenesis*. Biochemistry, 2002. **41**(10): p. 3321-8.
98. Shilton, B.H., et al., *The solution structure and activation of visual arrestin studied by small-angle X-ray scattering*. Eur J Biochem, 2002. **269**(15): p. 3801-9.
99. Granzin, J., et al., *X-ray crystal structure of arrestin from bovine rod outer segments*. Nature, 1998. **391**(6670): p. 918-21.
100. Gray-Keller, M.P., et al., *Arrestin with a single amino acid substitution quenches light-activated rhodopsin in a phosphorylation-independent fashion*. Biochemistry, 1997. **36**(23): p. 7058-63.
101. Gurevich, V.V. and J.L. Benovic, *Visual arrestin binding to rhodopsin. Diverse functional roles of positively charged residues within the phosphorylation-recognition region of arrestin*. J Biol Chem, 1995. **270**(11): p. 6010-6.

102. Gurevich, V.V., et al., *Arrestin interactions with G protein-coupled receptors. Direct binding studies of wild type and mutant arrestins with rhodopsin, beta 2-adrenergic, and m2 muscarinic cholinergic receptors.* J Biol Chem, 1995. **270**(2): p. 720-31.
103. Gurevich, V.V., et al., *Visual arrestin binding to rhodopsin. Intramolecular interaction between the basic N terminus and acidic C terminus of arrestin may regulate binding selectivity.* J Biol Chem, 1994. **269**(12): p. 8721-7.
104. Gurevich, V.V. and J.L. Benovic, *Mechanism of phosphorylation-recognition by visual arrestin and the transition of arrestin into a high affinity binding state.* Mol Pharmacol, 1997. **51**(1): p. 161-9.
105. Gurevich, V.V. and E.V. Gurevich, *The molecular acrobatics of arrestin activation.* Trends Pharmacol Sci, 2004. **25**(2): p. 105-11.
106. Hanson, S.M., et al., *Visual arrestin binding to microtubules involves a distinct conformational change.* J Biol Chem, 2006. **281**(14): p. 9765-72.
107. Hirsch, J.A., et al., *The 2.8 Å crystal structure of visual arrestin: a model for arrestin's regulation.* Cell, 1999. **97**(2): p. 257-69.
108. Kovoor, A., et al., *Targeted construction of phosphorylation-independent beta-arrestin mutants with constitutive activity in cells.* J Biol Chem, 1999. **274**(11): p. 6831-4.
109. McDowell, J.H., et al., *Activation of arrestin: requirement of phosphorylation as the negative charge on residues in synthetic peptides from the carboxyl-terminal region of rhodopsin.* Invest Ophthalmol Vis Sci, 2001. **42**(7): p. 1439-43.
110. Puig, J., et al., *Synthetic phosphopeptide from rhodopsin sequence induces retinal arrestin binding to photoactivated unphosphorylated rhodopsin.* FEBS Lett, 1995. **362**(2): p. 185-8.
111. Song, X., et al., *Visual and both non-visual arrestins in their "inactive" conformation bind JNK3 and Mdm2 and relocalize them from the nucleus to the cytoplasm.* J Biol Chem, 2006. **281**(30): p. 21491-9.
112. Vishnivetskiy, S.A., et al., *Transition of arrestin into the active receptor-binding state requires an extended interdomain hinge.* J Biol Chem, 2002. **277**(46): p. 43961-7.

113. Vishnivetskiy, S.A., et al., *How does arrestin respond to the phosphorylated state of rhodopsin?* J Biol Chem, 1999. **274**(17): p. 11451-4.
114. Vishnivetskiy, S.A., et al., *An additional phosphate-binding element in arrestin molecule. Implications for the mechanism of arrestin activation.* J Biol Chem, 2000. **275**(52): p. 41049-57.
115. Gurevich, E.V. and V.V. Gurevich, *Arrestins: ubiquitous regulators of cellular signaling pathways.* Genome Biol, 2006. **7**(9): p. 236.
116. Barnes, W.G., et al., *beta-Arrestin 1 and Galphaq/11 coordinately activate RhoA and stress fiber formation following receptor stimulation.* J Biol Chem, 2005. **280**(9): p. 8041-50.
117. Povsic, T.J., T.A. Kohout, and R.J. Lefkowitz, *Beta-arrestin1 mediates insulin-like growth factor 1 (IGF-1) activation of phosphatidylinositol 3-kinase (PI3K) and anti-apoptosis.* J Biol Chem, 2003. **278**(51): p. 51334-9.
118. Ahn, S., et al., *Reciprocal regulation of angiotensin receptor-activated extracellular signal-regulated kinases by beta-arrestins 1 and 2.* J Biol Chem, 2004. **279**(9): p. 7807-11.
119. Gesty-Palmer, D., et al., *Distinct beta-arrestin- and G protein-dependent pathways for parathyroid hormone receptor-stimulated ERK1/2 activation.* J Biol Chem, 2006. **281**(16): p. 10856-64.
120. Lefkowitz, R.J. and S.K. Shenoy, *Transduction of receptor signals by beta-arrestins.* Science, 2005. **308**(5721): p. 512-7.
121. Luttrell, L.M., et al., *Activation and targeting of extracellular signal-regulated kinases by beta-arrestin scaffolds.* Proc Natl Acad Sci U S A, 2001. **98**(5): p. 2449-54.
122. Miller, W.E., et al., *Identification of a motif in the carboxyl terminus of beta -arrestin2 responsible for activation of JNK3.* J Biol Chem, 2001. **276**(30): p. 27770-7.
123. Gurevich, V.V. and E.V. Gurevich, *The structural basis of arrestin-mediated regulation of G-protein-coupled receptors.* Pharmacol Ther, 2006. **110**(3): p. 465-502.

124. Raman, D., et al., *The interaction with the cytoplasmic loops of rhodopsin plays a crucial role in arrestin activation and binding.* J Neurochem, 2003. **84**(5): p. 1040-50.
125. Vishnivetskiy, S.A., et al., *Mapping the arrestin-receptor interface. Structural elements responsible for receptor specificity of arrestin proteins.* J Biol Chem, 2004. **279**(2): p. 1262-8.
126. Gurevich, V.V. and E.V. Gurevich, *The new face of active receptor bound arrestin attracts new partners.* Structure, 2003. **11**(9): p. 1037-42.
127. Miller, W.E., et al., *G-protein-coupled receptor (GPCR) kinase phosphorylation and beta-arrestin recruitment regulate the constitutive signaling activity of the human cytomegalovirus US28 GPCR.* J Biol Chem, 2003. **278**(24): p. 21663-71.
128. Bruchas, M.R., et al., *Kappa opioid receptor activation of p38 MAPK is GRK3- and arrestin-dependent in neurons and astrocytes.* J Biol Chem, 2006. **281**(26): p. 18081-9.
129. Kim, I.M., et al., *Beta-blockers alprenolol and carvedilol stimulate beta-arrestin-mediated EGFR transactivation.* Proc Natl Acad Sci U S A, 2008. **105**(38): p. 14555-60.
130. Binkowski, B., F. Fan, and K. Wood, *Engineered luciferases for molecular sensing in living cells.* Curr Opin Biotechnol, 2009. **20**(1): p. 14-8.
131. Violin, J.D., X.R. Ren, and R.J. Lefkowitz, *G-protein-coupled receptor kinase specificity for beta-arrestin recruitment to the beta2-adrenergic receptor revealed by fluorescence resonance energy transfer.* J Biol Chem, 2006. **281**(29): p. 20577-88.
132. Ong, S.E., et al., *Stable isotope labeling by amino acids in cell culture, SILAC, as a simple and accurate approach to expression proteomics.* Mol Cell Proteomics, 2002. **1**(5): p. 376-86.
133. Sun, X., J.F. Chiu, and Q.Y. He, *Application of immobilized metal affinity chromatography in proteomics.* Expert Rev Proteomics, 2005. **2**(5): p. 649-57.
134. Busillo, J.M., et al., *Site-specific phosphorylation of CXCR4 is dynamically regulated by multiple kinases and results in differential modulation of CXCR4 signaling.* J Biol Chem, 2010. **285**(10): p. 7805-17.

135. Kohout, T.A., et al., *Differential desensitization, receptor phosphorylation, beta-arrestin recruitment, and ERK1/2 activation by the two endogenous ligands for the CC chemokine receptor 7*. J Biol Chem, 2004. **279**(22): p. 23214-22.
136. Zidar, D.A., et al., *Selective engagement of G protein coupled receptor kinases (GRKs) encodes distinct functions of biased ligands*. Proc Natl Acad Sci U S A, 2009. **106**(24): p. 9649-54.
137. Nobles, K.N., et al., *The active conformation of beta-arrestin1: direct evidence for the phosphate sensor in the N-domain and conformational differences in the active states of beta-arrestins1 and -2*. J Biol Chem, 2007. **282**(29): p. 21370-81.
138. Lefkowitz, R.J., et al., *G-protein-coupled receptors: regulatory role of receptor kinases and arrestin proteins*. Cold Spring Harb Symp Quant Biol, 1992. **57**: p. 127-33.
139. Pitcher, J.A., et al., *Role of beta gamma subunits of G proteins in targeting the beta-adrenergic receptor kinase to membrane-bound receptors*. Science, 1992. **257**(5074): p. 1264-7.
140. Terrillon, S. and M. Bouvier, *Receptor activity-independent recruitment of betaarrestin2 reveals specific signalling modes*. EMBO J, 2004. **23**(20): p. 3950-61.
141. Trester-Zedlitz, M., et al., *Mass spectrometric analysis of agonist effects on posttranslational modifications of the beta-2 adrenoceptor in mammalian cells*. Biochemistry, 2005. **44**(16): p. 6133-43.
142. Fredericks, Z.L., J.A. Pitcher, and R.J. Lefkowitz, *Identification of the G protein-coupled receptor kinase phosphorylation sites in the human beta2-adrenergic receptor*. J Biol Chem, 1996. **271**(23): p. 13796-803.
143. Bouvier, M., et al., *Removal of phosphorylation sites from the beta 2-adrenergic receptor delays onset of agonist-promoted desensitization*. Nature, 1988. **333**(6171): p. 370-3.
144. Krasel, C., et al., *Dual role of the beta2-adrenergic receptor C terminus for the binding of beta-arrestin and receptor internalization*. J Biol Chem, 2008. **283**(46): p. 31840-8.
145. Hausdorff, W.P., et al., *Phosphorylation sites on two domains of the beta 2-adrenergic receptor are involved in distinct pathways of receptor desensitization*. J Biol Chem, 1989. **264**(21): p. 12657-65.

146. Seibold, A., et al., *Desensitization of beta2-adrenergic receptors with mutations of the proposed G protein-coupled receptor kinase phosphorylation sites*. J Biol Chem, 1998. **273**(13): p. 7637-42.
147. Seibold, A., et al., *Localization of the sites mediating desensitization of the beta(2)-adrenergic receptor by the GRK pathway*. Mol Pharmacol, 2000. **58**(5): p. 1162-73.
148. Vaughan, D.J., et al., *Role of the G protein-coupled receptor kinase site serine cluster in beta2-adrenergic receptor internalization, desensitization, and beta-arrestin translocation*. J Biol Chem, 2006. **281**(11): p. 7684-92.
149. Moore, R.H., et al., *Salmeterol stimulation dissociates beta2-adrenergic receptor phosphorylation and internalization*. Am J Respir Cell Mol Biol, 2007. **36**(2): p. 254-61.

Biography

I was born in Richmond, Virginia on November 21, 1978, the second child of Earl and Donna Nobles and moved to North Carolina at age eight. I grew up in the Triangle area with one older brother, Christopher Nobles, one of the kindest and smartest people I have ever known. I matriculated to the North Carolina State University in 1997, where I met the most amazing friends who have influenced my life greatly. During my time at North Carolina State University, I worked as a research assistant in the laboratory of Dr. Paul F. Agris who fostered creativity in the laboratory and influenced me to pursue graduate studies in Biochemistry. I graduated in May 2001 with a B.S. degree in Biochemistry and a B.A. degree in Chemistry. In the fall of 2001, I entered the Department of Biochemistry at Duke University as a graduate student. I joined the laboratory of Dr. Robert J. Lefkowitz in 2002 where this thesis work was done. I plan to graduate in December 2010 with a Ph.D. degree in Biochemistry and to continue my research in receptor biology. I would like to thank the many teachers and mentors who have helped me become the scientist and person that I am today, and to thank my friends, family and dogs who have so greatly enriched my life.

Publications

1. **Nobles KN**, Xiao K, Ahn S, Shukla AK, Lam CM, Rajagopal S, Bressler EA, Hara M, Gygi SP, Lefkowitz RJ. Distinct GRK Phosphorylation Sites on the β_2 -adrenergic Receptor: A Bar Code Which Differentially Encodes β -arrestin Functions. *Submitted*.
2. Nelson CD, Kovacs JJ, **Nobles KN**, Whalen EJ, Lefkowitz RJ. β -arrestin Scaffolding of Phosphatidylinositol-4-phosphate 5-kinase I α Promotes Agonist-stimulated Sequestration of the β_2 -adrenergic Receptor. *J Biol Chem*, 283(30): 29093-101, 2008.
3. **Nobles KN**, Guan Z, Xiao K, Oas TG, Lefkowitz RJ. The Active conformation of β -arrestin1: Direct Evidence for the Phosphate Sensor in the N-domain and Conformational Differences in the Active States of β -arrestins1 and -2. *J Biol Chem*, 282(29): 21370-81, 2007.
4. Xiao K, Shenoy SK, **Nobles KN**, Lefkowitz RJ. Activation-Dependent Conformational Changes in β -arrestin2. *J Biol Chem*, 279(53): 55744-53, 2004.
5. **Nobles KN**, Yarian CS, Liu G, Guenther RH, Agris PF. Highly Conserved Modified Nucleosides Influence Mg^{2+} -dependent tRNA Folding. *Nucleic Acids Res*, 30(21): 4751-60, 2002.